UNIVERSITÄT OSNABRÜCK

Characterization of the essential role of Ynl152/Inn1 in cell division in *Saccharomyces cerevisiae*

Dissertation

zur Erlangung des akademischen Grades

Doctor rerum naturalium

(Dr. rer. nat.)

Fachbereich Biologie/Chemie der Universität Osnabrück

vorgelegt von

Arne Jendretzki

Osnabrück, März 2010

Table of contents

1 Introduction **4**
1.1 The cell division cycle 4
1.2 Cytokinesis 6
1.2.1 Cytokinesis in *Saccharomyces cerevisiae* 6
1.2.2 Septum formation and cell separation 9
1.2.3 Coordination of cell cycle and cytokinesis 11
1.2.4 CAR-independent cytokinesis 13
1.3 Aims of the thesis 16

2 Material and Methods **18**
2.1 Material 18
2.1.1 Chemicals and material 18
2.1.2 Kits and reagents 18
2.1.3 Enzymes 18
2.1.4 Antisera 19
2.1.5 Strains and media 19
2.1.5.1 *Saccharomyces cerevisiae* strains 19
2.1.5.2 Yeast media 23
2.1.5.3 Storage of yeast strains 24
2.1.5.4 *E. coli* strains 24
2.1.5.5 *E. coli* culture conditions 24
2.1.6 Plasmids 25
2.1.7 Oligonucleotides 29
2.2 Methods 34
2.2.1 Transformation 34
2.2.1.1 Transformation of *E. coli* 34
2.2.1.2 Transformation of *S. cerevisiae* 34
2.2.2 Sporulation, tetrad analysis and determination of the mating type 34
2.2.3 Growth analysis by serial drop dilution assays 35
2.2.4 Cell cycle arrest and synchronization 35
2.2.5 Analysis of DNA 35
2.2.5.1 Preparation of plasmid DNA by alkaline lysis 35
2.2.5.2 Preparation of plasmid DNA from *E. coli* 36
2.2.5.3 Preparation of plasmid DNA from *S. cerevisiae* 36
2.2.5.4 Preparation of chromosomal DNA from *S. cerevisiae* 36
2.2.5.5 Separation of DNA fragments by gel electrophoresis 37
2.2.5.6 Isolation of DNA fragments from agarose gels 37
2.2.5.7 Purification of PCR products 37
2.2.5.8 Restriction, dephosphorylation and ligation of DNA 37
2.2.5.9 Sequencing of plasmid DNA 38
2.2.5.10 Polymerase chain reaction (PCR) 38
2.2.6 Analysis of proteins 38
2.2.6.1 Preparation of whole cell extracts from *S. cerevisiae* 38
2.2.6.2 Determination of specific β-galactosidase activities 38
2.2.6.3 Co-immunoprecipitation 39
2.2.6.4 Subcellular fractionation 39
2.2.6.5 Quantification of protein concentrations 40
2.2.6.6 Separation of proteins via SDS-PAGE 40

2.2.6.7 Silver staining of proteins 41
2.2.6.8 Immunoblotting 41
2.2.6.9 Preparation of proteins from *E. coli* 41
2.2.6.10 Affinity-chromatography for the purification of GST fusion proteins 41
2.2.6.11 *In vitro* lipid binding assay 42
2.2.7 Cell imaging and microscopy 42
2.2.7.1 Microscopical setting 42
2.2.7.2 Image acquisition and processing 42
2.2.7.3 Time-lapse microscopy and the creation of kymographs 42
2.2.7.4 Actin and chitin staining 43

3 Results **44**
3.1 Phenotypes of *inn1* mutants 44
3.1.1 *INN1* is an essential gene 44
3.1.2 Downregulation of *INN1* gene expression leads to cell division defects 45
3.1.3 Depletion of Inn1 by induced protein degradation leads to cytokinesis defects 47
3.2 Subcellular localization of Inn1 49
3.2.1 Inn1 resides in the high speed pellet fraction 49
3.2.2 Inn1 localizes at the bud neck during cytokinesis 50
3.2.3 Inn1 is not a target of the anaphase-promoting complex 52
3.2.4 Inn1 is phosphorylated in mitosis 55
3.3 Interactions of Inn1 with other cytokinesis regulators 56
3.3.1 Inn1 interacts with Hof1 in a yeast two-hybrid assay 56
3.3.2 Inn1 physically interacts with Hof1 57
3.3.3 Inn1 co-localizes with Hof1 59
3.3.4 Identification of novel interaction partners for Inn1 by a yeast two-hybrid approach 59
3.3.5 Inn1 interacts with Cyk3 in a yeast two-hybrid assay 59
3.3.6 Inn1 co-localizes with Cyk3 61
3.3.7 Inn1, Hof1 and Cyk3 are recruited to the bud neck in a specific temporal order 61
3.4 Genetic interactions of *INN1*, *HOF1* and *CYK3* 63
3.4.1 *INN1* and *CYK3* are multicopy suppressors of a *hof1* deletion 64
3.4.2 The SH3 domains of either Cyk3 or Hof1 are required for viability 65
3.5 Regulation of Inn1 recruitment to the bud neck 67
3.5.1 Deletion of either *HOF1* or *CYK3* does not prevent Inn1 recruitment to the bud neck 67
3.5.2 Overproduction of either Hof1 or Cyk3 provokes an aberrant localization of Inn1 68
3.5.3 Inn1 redistributes upon simultaneous depletion of *HOF1* and *CYK3* 69
3.5.4 Overproduction of *CYK3* bypasses the requirement for a functional CAR 71
3.6 Function of Vrp1 in cytokinesis 73
3.6.1 Genetic interactions of *VRP1* with other cytokinesis regulators 73
3.6.2 Kinetics of Vrp1 appearance at the bud neck 73
3.6.3 Effect of Vrp1 on Inn1 dynamics 74
3.7 Investigation of the role of the Inn1-C2 domain in lipid binding 75
3.7.1 Purification of GST-tagged Inn1 from *E. coli* 75
3.7.2 Inn1 binds to phosphatidic acid 76

4 Discussion **78**
4.1 *INN1* is an essential gene encoding a novel regulator of cytokinesis 79
4.2 Inn1 is not a target of the anaphase-promoting complex 81
4.3 Inn1 interacts with the cytokinetic regulators Hof1 and Cyk3 82
4.4 Inn1 is recruited to the bud neck by the concerted action of Hof1 and Cyk3 84
4.5 Cyk3 acts in CAR-independent cytokinesis by recruiting Inn1 86
4.6 The molecular function of Inn1 87
4.7 The role of Vrp1 in cytokinesis 90

5 Summary **92**

6 References **93**

7 List of abbreviations **102**

8 Acknowledgements **103**

9 Statutory declaration **104**

1 Introduction

Cell division and the concomitant ability to propagate is a basic feature of all biological systems. In eukaryotes, this process is highly organized and can be divided into two major events: i) the duplication and separation of the genetic material in the nucleus (karyokinesis) and ii) the separation of the cytoplasm (cytokinesis). Progression through these events is coordinated by the cell division cycle and usually occurs only once per cycle.

1.1 The cell division cycle

The eukaryotic cell cycle can be divided into two microscopically and physiologically distinct phases. Cells spend most of their lifetime in the interphase between two cell divisions. This phase is dedicated to cell growth and DNA replication. It has been proposed that the length of this phase is controlled by the relationship of the nucleus to the cytoplasm. At a specific point during cell growth, the volumes of the cytoplasm and the nucleus reach an optimal ratio at which metabolism can be efficiently regulated. Further growth leads to suboptimal physiological conditions which then results in the activation of the cell division machinery (Johnston *et al*., 1977). Of course, cell division in higher eukaryotes is initiated hierarchically by growth factors, the so-called mitogens.

The interphase can be further divided into three different phases. During S-phase (DNA-**S**ynthesis), the chromosomes are duplicated. A complex mechanism ensures that the genetic material is replicated only once per cell cycle, since replication is an energy-consuming step and requires the concerted action of many proteins. Thus, a new round of the cell cycle and of DNA-synthesis is only initiated, if there is a sufficient supply of nutrients. Transcription and translation in the preceeding G1-phase (**G**ap 1) ensures that all necessary components for DNA replication are provided. Completion of DNA replication is followed by the G2-phase (**G**ap 2), in which cell growth continues and the DNA checkpoint controls whether replication has been completed and triggers the repair of DNA lesions, if necessary.

In M-phase (**M**itosis), the chromosomes are properly distributed and cytokinesis is completed. Mitosis can be divided into different phases based on the degree of chromosome condensation. During the interphase of the cell cycle, the DNA is more or less evenly distributed in the nucleoplasm, allowing for an efficient transcription of

the genes and for replication. In the beginning of the mitotic prophase, the DNA is condensed into its transportable state, with tightly packed chromosomes appearing at the transit to metaphase. The duplicated DNA in the form of the two chromatids for each chromosome is still connected at the centrosome. Furthermore, the spindle apparatus has been assembled, and the nuclear membrane is dissipated during metaphase in higher eukaryotes, but not in yeasts (Hawker, 1965). At the onset of anaphase, the cohesion of the two sister-chromatids is dissolved, and the spindles attach to the released kinetochors, a specialized organelle for the distribution of the chromatids. The spindle filaments pull the chromatids to the spindle poles, where a new nuclear membrane is assembled in telophase and chromatid condensation is reversed.

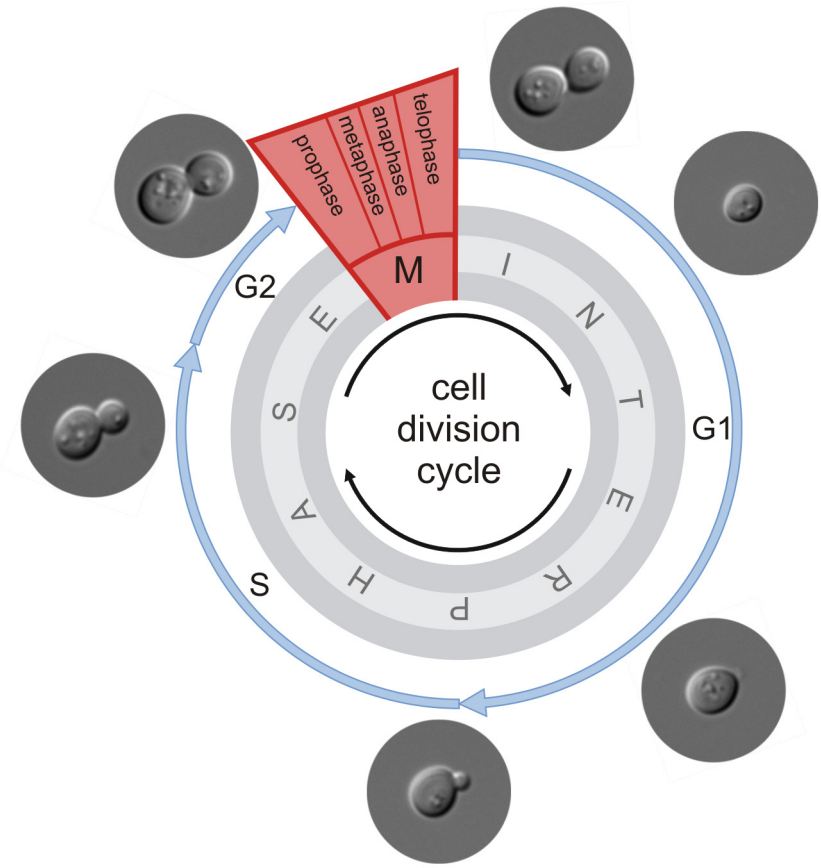

Fig. 1.1: Schematic drawing of the cell division cycle. The cell cycle is divided into interphase and mitosis (M). Interphase is further divided into G1-, S- and G2- phases (blue arrows). Mitosis is subdivided into pro-, meta-, ana-, and telophase (highlighted in red). The micrographs of *Saccharomyces cerevisiae* show cells in the indicated phases of the cell division cycle.

Many of the genes involved in the control of the cell division cycle were identified in the budding yeast *Saccharomyces cerevisiae*. Cell cycle progression in this yeast is accompanied by the constant growth of an initially small daughter cell at the beginning of G1-phase. Thus, the approximate position of a cell in the division cycle

can be estimated from the size ratio of mother to daughter cell. The basic mechanisms related to proliferation are highly conserved between all eukaryotes, but some significant differences occur during mitosis in *Saccharomyces cerevisiae*: The chromosomes do not condense to allow a microscopically visible detection (Gordon, 1977; Vas *et al*., 2007) and the nuclear membrane, which is dissolved at the onset of metaphase in higher eukaryotes, remains intact throughout mitosis in budding yeast (Hawker, 1965). Moreover, the spindle pole body, which is the microtubule-organizing centre that creates the spindle apparatus, is located within the nuclear membrane to ensure both chromatid separation and nuclear division at the end of mitosis and before cytokinesis.

1.2 Cytokinesis

Cytokinesis is a final event in the propagation cycle. It describes the separation of the cytoplasm of a mother cell from that of a newly formed daughter. This separation requires the coordination of different cellular processes: A large scaffold is assembled at the prospective division site, which provides the pulling force needed for the invagination of the plasma membrane. Additionally, new membrane material is delivered to the cleavage furrow, which further facilitates the invagination process and the final abscission for complete separation of the cytoplasmata. In *Saccharomyces cerevisiae*, these events have to be coordinated with the formation of a septum and the concomitant cell wall remodeling. In turn, these processes need to be regulated with regard to the ordered distribution of other cellular compartments and nuclear division.

1.2.1 Cytokinesis in *Saccharomyces cerevisiae*

One of the first events that mark a new cell cycle is the selection of the new bud position. The future division site is determined by cortical cues. Thus, bud site selection markers like Bud3, Bud4, and Axl2 (Chant *et al*., 1995) remain at the former mother-bud neck from the previous cell cycle, during which they were deposited from either side of the mother and daughter cells. When a new cell cycle is initiated, these markers recruit the small GTPase Cdc42, which determines cell polarity and triggers new bud emergence and the assembly of the cytokinetic apparatus (Zheng *et al*., 1995; Ziman *et al*., 1993).

The bud neck region constitutes a microcompartment during the entire division process. This compartment is defined by the septin proteins Cdc3, Cdc10, Cdc11, Cdc12, and Shs1. Depending on the activity of Cdc42, these GTP-binding proteins form heterooligomeric complexes, assembled into filaments with a width of 10 nm, which in turn can form a ring at the mother-bud neck (Field and Kellogg, 1999); reviewed in Kinoshita, 2006). This septin ring provides an essential scaffold for the assembly of the myosin ring and the recruitment of additional factors which regulate this process (Longtine and Bi, 2003). Later on in the cell cycle, at the onset of cytokinesis, the septins appear as a double-ring structure. Thus, the septin ring has been shown to split in order to form hourglass-shaped structures, which act as a diffusion barrier to maintain certain proteins at the bud neck (Dobbelaere and Barral, 2004).

The next key step in cytokinesis is the formation of the myosin ring on the septin scaffold. The only type II myosin in *Saccharomyces cerevisiae* which is encoded by the *MYO1* gene, was expressed as a GFP fusion and shown to localize to the prospective bud site during G1 phase at the initiation of bud formation, shortly after the formation of the septin ring. It remains there at a constant diameter in the first instance (Bi *et al*., 1998; Lippincott and Li, 1998b) and is thought to facilitate polar growth of the daughter cell by pulling actin cables through the bud neck (Huckaba *et al*., 2006). Actin cable formation for polarized secretion of membrane and cell wall materials is guided by the two formin proteins Bni1 and Bnr1 (Imamura *et al*., 1997). During this stage of the cell cycle Bni1 mediates the assembly of actin cables towards the bud tip, whereas Bnr1 assembles actin cables at the bud neck. During the mitotic anaphase, the formin Bni1 joins the second yeast formin Bnr1 at the myosin ring. It is assumed, that they not only regulate actin cable dynamics at the bud neck, but also polymerize the cytokinetic actin ring (CAR) (Tolliday *et al*., 2002). Formins have been shown to possess actin-nucleating activity in cytokinesis, but also in polarized growth. Their auto-inhibited state is loosened by the binding of small GTPases (Wallar and Alberts, 2003). Cdc42 and others have been shown to exert this function during polarized growth (Dong *et al*., 2003), but Rho1 seems to be the major activator of the formins for actin ring synthesis (Tolliday *et al*., 2002; Yoshida *et al*., 2009). The incorporation of actin into the myosin ring marks the onset of cytokinesis and is thought to initiate the subsequent ring constriction.

The function and regulation of Myo1 activity during cytokinesis is still a matter of debate. All functional myosins are composed of heavy and light chains. The motor activity of the myosin heavy chains (e.g. Myo1) is thought to be regulated by the association with the small polypeptides of the myosin light chains. The latter contain a calmodulin-like fold and bind to IQ motifs, which can be found in myosin heavy chains and some other proteins. This association is regulated both by calcium-binding and by phosphorylation of the light chains. Like all type II myosins, Myo1 can associate with an essential light chain (Mlc1) and a regulatory light chain (Mlc2) (Bi, 2001; Luo *et al*., 2004). Mlc2 apparently triggers the disassembly of the Myo1 ring, since an *mlc2* deletion causes a slight delay in this process and displays a mild cytokinesis defect (Luo *et al*., 2004). On the other hand, Mlc1 seems to be more important, since an *mlc1* deletion is lethal in all yeast strains tested so far (Bi, 2001). Mlc1 also localizes at the bud neck independent of Myo1 and interacts with at least two other proteins involved in cytokinesis: The first interaction partner is the type V myosin Myo2, which is involved in the transport of secretory vesicles to the bud neck, a key step in septum formation (Stevens and Davis, 1998; Wagner *et al*., 2002). Yet, direct experimental evidence for a regulation of either Myo1 or Myo2 motor activity by Mlc1 is still lacking. The second interaction partner of Mlc1 is Iqg1, which shares an essential function in cytokinesis (Shannon and Li, 2000). Iqg1 is a member of the IQGAP family, which has been extensively studied in mammalian cells. Thus, IQGAPs were shown to bundle actin filaments in a process dependent on GTP-activated Cdc42 (Fukata *et al*., 1997). Although Iqg1 has been shown to bind to actin, a regulatory effect or the ability to trigger bundle formation have not been demonstrated in yeast (Epp and Chant, 1997; Shannon and Li, 1999). The physiological significance of its interaction with Mlc1 also remains to be elucidated.

A preliminary model for cytokinesis in *Saccharomyces cerevisiae*, which summarizes the events described above, is presented in Fig.1.2. Depending on the polarity axis determined by the bud site selection markers, Cdc42 initiates the assembly of the septin collar. The myosin ring is assembled dependent on this scaffold structure during bud growth. At a specific point in the cell cycle, the cell polarity is shifted towards the bud neck. The formins redirect actin cables and trigger filamentous actin formation at the contractile ring. The actin filaments are bundled by Iqg1 and incorporated into the myosin ring. The mature cytokinetic actin ring constricts,

mediated by the activity of Myo1, and pulls in the plasma membrane. It is not yet clear, if active membrane scission occurs in *Saccharomyces cerevisiae*.

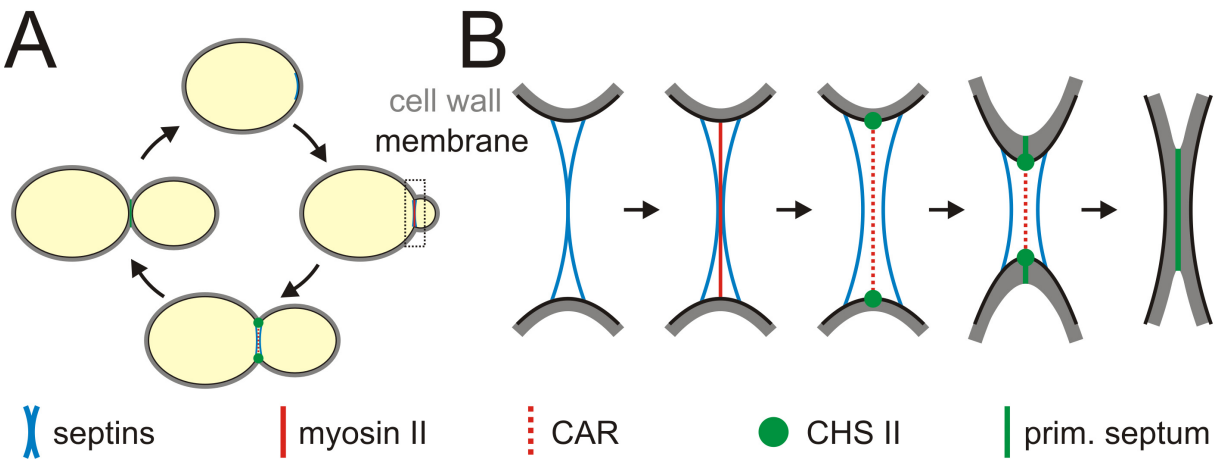

Fig. 1.2: Schematic drawing of cytokinesis in *Saccharomyces cerevisiae*. A. Localization of the cytokinetic apparatus throughout the cell cycle. Clockwise description starting at the top: 1. The septin collar (blue) is formed at the presumptive bud site. 2. With the initiation of bud formation a myosin II ring (red) assembles at the septin scaffold. 3. At the onset of cytokinesis, actin is incorporated into the myosin ring (red dotted line), and chitin synthase II (Chs2; green dots) is delivered to the bud neck. 4. After completion of CAR constriction the primary septum (green line) is formed. The dotted box marks the region depicted in B in greater detail. **B.** Ingression of the plasma membrane (represented by a black line) in the bud neck region during cytokinesis is shown as a cross-cut section. The cell wall is depicted as a grey layer. In the first step, the septin collar is assembled (blue). Next, myosin II (red) accumulates as a ring on the septin scaffold. Actin and other proteins are incorporated into the myosin ring to form the functional CAR. Additionally, chitin synthase II is delivered to the bud neck. In the fourth step, constriction of the CAR pulls in the plasma membrane, which is accompanied by the synthesis of the primary chitinous septum. Finally, abscission of the cytoplasmata completes cytokinesis and the primary septum is closed.

1.2.2 Septum formation and cell separation

To complete cell division, yeast cells not only require cytokinesis, but also the controlled separation of their cell walls. This is achieved by the formation of a specialized cell wall structure, the septum. The yeast septum is constructed in three stages: First, early during bud emergence, a chitin ring is deposited on the mother cell surface. As the cleavage furrow invaginates, chitin is concomitantly deposited. This centripetal chitin synthesis results in the separation of the two cells by a chitin disk - the so-called primary septum - when cytokinesis is completed. Once the primary septum has been established, mother and daughter cells deposit cell wall glucans at either sides of the disk to build up the final trilaminar septum. In the following, the molecular mechanisms involved in septum formation will be explained in detail.

Early in the process, the chitin ring is synthesized by the action of chitin synthase III. The catalytic subunit Chs3, a trans-membrane protein, is transported to the plasma

membrane in an inactive state. Its transport occurs through the secretory pathway, involves specialized transport vesicles (so-called chitosomes), and depends on the sequential action of the regulatory proteins Chs5-7 (Santos and Snyder, 1997; Trilla *et al*., 1999; Ziman *et al*., 1998) Chs3 is likely to be converted from its zymogenic to its catalytically active state by the action of Chs4. Since the latter may loosely associate with the septin collar at the bud neck, this would explain the specific activity of chitin synthase III in the formation of the chitin ring (DeMarini *et al*., 1997; Kozubowski *et al*., 2003).

Formation of the primary septum is mainly catalyzed by the chitin synthase II isozyme, with its catalytic subunit Chs2. Chs2 is also a transmembrane protein and is delivered to the bud neck through the secretory pathway in late mitosis. It is rapidly turned-over by endocytosis and degraded in the vacuole after establishment of the primary septum (Chuang and Schekman, 1996). Although direct experimental evidence for the delivery of Chs2 to the bud neck and its local activation is still missing, the exocyst complex is thought to play a crucial role in this process (VerPlank and Li, 2005). Transport of Chs2 from the endoplasmic reticulum to the plasma membrane at the bud neck is tightly controlled by the mitotic exit network (MEN). This control ensures that septum formation occurs only after the chromosomes have been separated (Zhang *et al*., 2006).

To complete cell wall formation during cytokinesis, the secondary septum is deposited from both sides onto the primary septum. This is achieved by the local activation of the cell wall synthetic machinery. The secondary septa are composed of the usual cell wall glucans and mannans. For this, the expression of several genes involved in cell wall biogenesis is induced, like that of *FKS1*, which encodes a catalytic subunit of the 1-3-β-glucan synthase (Igual *et al*., 1996). This process is coordinated with the cell cycle control and probably involves signaling through the cell wall integrity (CWI) pathway (Wilk *et al*., 2010). Moreover, many components of the cell wall synthetic machinery accumulate first at the tip of the growing bud and then at the bud neck during the time of secondary septum formation (reviewed in Bretscher, 2003).

Finally, cell separation is achieved by the action of hydrolytic enzymes. The primary septum between mother and daughter cell is digested by the endochitinase Cts1 (Kuranda and Robbins, 1991). The expression of *CTS1* is induced after mitosis in the daughter cells nucleus by the transcription factor Ace2 (Colman-Lerner *et al*., 2001;

O'Conallain *et al*., 1999), and the corresponding protein is secreted to digest the primary septum. The remaining parts of the chitin ring and the primary septum remain as a distinct bud scar on the mother cell and as a less prominent birth scar on the daughter cell. The endo-1,3-β-glucanase Dse4 is also expressed specifically in the daughter cell and is thought to contribute to the asymmetric degradation of the secondary septum on the side of the daughter to terminate cell separation (Baladron *et al*., 2002; Colman-Lerner *et al*., 2001).

1.2.3 Coordination of cell cycle and cytokinesis

To achieve a successful proliferation, cytokinesis has to be coordinated with other vital processes, such as the proper segregation of the genetic material. The regulatory pathway which governs the initiation of cell division is the mitotic exit network (MEN). This pathway is apparently directly activated by the partitioning of the sister chromatids into the daughter cell, i.e. it is initiated only after chromosome segregation. The peculiar localization of the small GTPase Tem1 seems to be crucial for the coordination of chromosome segregation and cytokinesis (Bardin *et al*., 2000; Shou *et al*., 1999). Tem1 localizes to the spindle pole bodies (SPBs) of mitotic cells, where it is kept in its inactive GDP-bound state by a dimeric GTPase activating protein (GAP), with the subunits Bub2 and Bfa1. When one Tem1-decorated SPB is segregated into the daughter cell together with the attached chromatids, the GTPase is placed into close proximity with a putative GDP/GTP-exchange factor (GEF) Lte1, positioned at the bud cortex. Whether Tem1 is indeed activated by Lte1 is not yet clear, since the latter does not display any GEF activity in *in vitro* assays. An alternative model suggests that Lte1 promotes the dissociation of Bfa1 from SPBs, which could trigger the activation of Tem1 (Geymonat *et al*., 2009). Tem1 then activates a variety of protein kinases and other regulators, which finally leads to the phosphorylation and nuclear export of Cdc14 (Lee *et al*., 2001; Mohl *et al*., 2009).

Cdc14 itself is a dual specificity phosphatase, which is strictly maintained in the nucleus until late anaphase. Upon its release into the cytoplasm, Cdc14 dephosphorylates Cdh1, an activator of the anaphase-promoting complex (APC) (Jaspersen *et al*., 1999). The APC is a multi-subunit ubiquitin ligase, which labels specific target proteins for proteosomal degradation. The complex contains more than a dozen subunits, which assemble into a large 1.5 MDa structure, constituting the most complex molecular machine known to catalyse protein ubiquitylation. For

APC-mediated ubiquitylation, at least one of two substrate recognition sequences has to be present in the target protein. The first motif, commonly known as the “destruction box” (DB), was identified in mitotic cyclins, whereas the second motif, the so-called KEN box, was first described in Cdc20, which itself activates the APC complex (Pfleger and Kirschner, 2000; Pfleger *et al*., 2001).

The specificity of the APC complex seems to be determined primarily through the binding of the activator subunits Cdc20 or Cdh1 (Zachariae and Nasmyth, 1999). These are able to detect the above mentioned recognition sequences and thereby directly bind to the substrate. Cdc20 activates the APC in the prophase of mitosis, when the activity of the main cell cycle regulator, the cyclin-dependent kinase Cdk1, is high. This triggers the ubiquitylation and degradation of the anaphase inhibitor securin (in yeast encoded by *PDS1*), allowing the separation of the sister chromatids. By this process the MEN is activated, finally culminating in the release of Cdc14 from the nucleus and the activation of Cdh1, which replaces Cdc20 as an APC activator (Jaspersen *et al*., 1999). At this stage, which by definition marks the exit from mitosis, Cdc20 and the mitotic cyclins are degraded.

The manner of regulation of cytokinesis by the APC or the MEN pathway is still a subject of extensive studies. Some of the MEN components, for example the kinase Dbf2, could be detected at the mother-bud neck after mitotic exit and at the onset of cytokinesis (Frenz *et al*., 2000; Lim and Surana, 2003). Accordingly, several cytokinetic regulators are phosphorylated after mitotic exit, but the kinases responsible have not yet been identified (Corbett *et al*., 2006; Vallen *et al*., 2000). Moreover, the cytokinetic regulators Hsl1 and Iqg1 localize to the bud neck and are targeted by the APC/Cdh1 complex for ubiquitylation and subsequent degradation (Burton and Solomon, 2000; Ko *et al*., 2007). Interestingly, the APC-activating protein Cdh1 was reported to shuttle between the nucleus and the bud neck and might escort cytoplasmic targets of the APC into the nucleus (Jaquenoud *et al*., 2002). Recently, a study on CAR-disassembly at the end of cytokinesis suggested an involvement of the APC in this process (Tully *et al*., 2009). However, experimental evidence is still rather circumstantial and the significance of the APC-dependent proteolysis on cytokinesis remains to be verified.

1.2.4 CAR-independent cytokinesis

Historically, the presence of a contractile cytokinetic actin ring (CAR) in *Saccharomyces cerevisiae* was dubious. Although an actin band was visualized by

the first specific staining methods, no contraction of this actin ring could be detected (Adams and Pringle, 1984; Kilmartin and Adams, 1984). This was partially due to the fact that the cells had to be chemically fixed prior to the actin staining. Moreover, the accumulation of actin patches at the division site masked the later stages of ring contraction. Since the bud neck region of *Saccharomyces cerevisiae* has a diameter of less than 1 µm, it was assumed that the targeted secretion of membrane and cell wall material would be sufficient to drive cell separation (Sanders and Field, 1994). Later on, the first *in vivo* studies on myosin II dynamics clearly showed the contraction of a myosin ring during cytokinesis (Bi *et al*., 1998; Lippincott and Li, 1998b).

Whether the motor function of Myo1 really creates the constricting force for the CAR has not yet been unequivocally demonstrated. On the one hand, Myo1 mutant proteins lacking the motor domain are still able to fulfill all functions of the wild-type protein during cytokinesis (Lord *et al*., 2005). On the other hand, mutations in the actin binding region of the Myo1 motor domain display cytokinesis defects (Huckaba *et al*., 2006). Some yeast strains are even viable and undergo cytokinesis in the absence of Myo1, but vary significantly in their phenotypes with respect to both cell and colony morphologies (Bi *et al*., 1998). Most likely, these phenotypic differences can be attributed to different genetic backgrounds of the yeast strains employed in these studies. Nevertheless, different mechanisms seem to promote cytokinesis in the absence of type II myosin. Thus, other myosins (e.g. Myo2, which also localizes to the mother-bud neck) could provide the motor activity necessary for CAR ring constriction. The most likely explanation for actomyosin ring-independent cytokinesis is based on the requirement for septum formation. In wild-type cells, the constriction of the actomyosin ring and the formation of the primary septum are thought to be interdependent processes (Schmidt *et al*., 2002). This conclusion was reached from the similar phenotypes of *chs2* and *myo1* mutants, which lacked synthetic phenotypes in the strains employed by the authors. The separation of cytoplasmata as the final goal of cytokinesis could be caused by an inward growth of the lateral cell wall, which normally forms the secondary septum. The observed formation of thick aberrant septa due to the less polarized deposition of cell wall material is consistent with this hypothesis (Schmidt *et al*., 2002).

The yeast IQGAP protein Iqg1 is a central player in the process of actomyosin ring-independent cytokinesis. Thus, overexpression of *IQG1* rescues a strain in which the

lack of *MYO1* is lethal, by partially restoring its ability to undergo cytokinesis (Ko *et al*., 2007). Besides its well established role in the formation of the actin ring (Shannon and Li, 2000), this result indicates an additional function for Iqg1 in septum formation. Since Iqg1 is also able to bundle actin cables, it might regulate the cytoskeleton dynamics and thus control the targeted transport of vesicles to the division site, which also governs the deposition of secondary septum materials.

Another protein involved in CAR-independent cytokinesis is Cyk3. The *CYK3* gene was initially identified as a multicopy suppressor of an *iqg1* deletion. It was shown to recover viability and cytokinesis of *iqg1* deletion mutants without restoring the cytokinetic actin ring (Korinek *et al*., 2000). Interestingly, the *cyk3* deletion only displays mild cytokinesis defects on its own, but is synthetically lethal with a *myo1* deletion. *CYK3* is also a very potent multicopy suppressor of a *myo1* deletion, which further supports a role in the process of actomyosin ring-independent cytokinesis (Ko *et al*., 2007). Cyk3 contains an amino-terminal SH3 domain, which mediates protein-protein interactions, and a transglutaminase-like domain, believed to be inactive. Albeit the exact role of Cyk3 in cytokinesis is not yet clear, phenotypic analyses suggest a regulatory role in septum deposition.

A further regulator involved in septum formation is the Hof1 protein. The protein belongs to the family of PSTPIP proteins and has been named Hof1 as **h**omologue **o**f cdc **f**ifteen from *Schizosaccharomyces pombe*. *Sp*Cdc15 seems to be a key regulator in the organization of actin during mitosis in this organism since the assembly of the actin ring and the recruitment of actin patches to the division site is affected in mutant strains (Balasubramanian *et al*., 1998; Fankhauser *et al*., 1995). Moreover, *Sp*Cdc15 could be involved in the formation of membrane domains at the cleavage site during cytokinesis, but this could rather be an indirect effect (Takeda *et al*., 2004).

Due to its peculiar localization (see Fig. 1.3), Hof1 most likely serves different functions in cytokinesis in *Saccharomyces cerevisiae*. It is recruited to the septin collar of the mother-bud neck early in the cell cycle, in a process independent from the myosin ring. At this time, Hof1 can be detected as a double ring structure. The two rings fuse at the onset of cytokinesis and partially constrict together with the CAR. Directly after completion of cytokinesis, Hof1 splits again and localizes as diffuse double rings to both the mother and the daughter side of the bud neck. It is then degraded after the septum has formed (Lippincott and Li, 1998a). Hof1 seems

to affect septin distribution, but also interacts with the formin Bnr1 and might be involved in CAR constriction (Kamei *et al*., 1998; Lippincott and Li, 1998a). Furthermore, *HOF1* shows similar genetic interactions as *CYK3*. Thus, the overexpression of *HOF1* can rescue the lethality of an *iqg1* deletion and the respective *hof1* deletion is synthetically lethal with a *myo1* deletion (Korinek *et al*., 2000; Vallen *et al*., 2000). Moreover, Hof1 has been shown to be phosphorylated in a MEN-dependent manner and to affect both CAR-constriction and septum formation (Vallen *et al*., 2000). Thus, to date, a likely hypothesis is that Hof1 coordinates septum formation with the CAR-constriction.

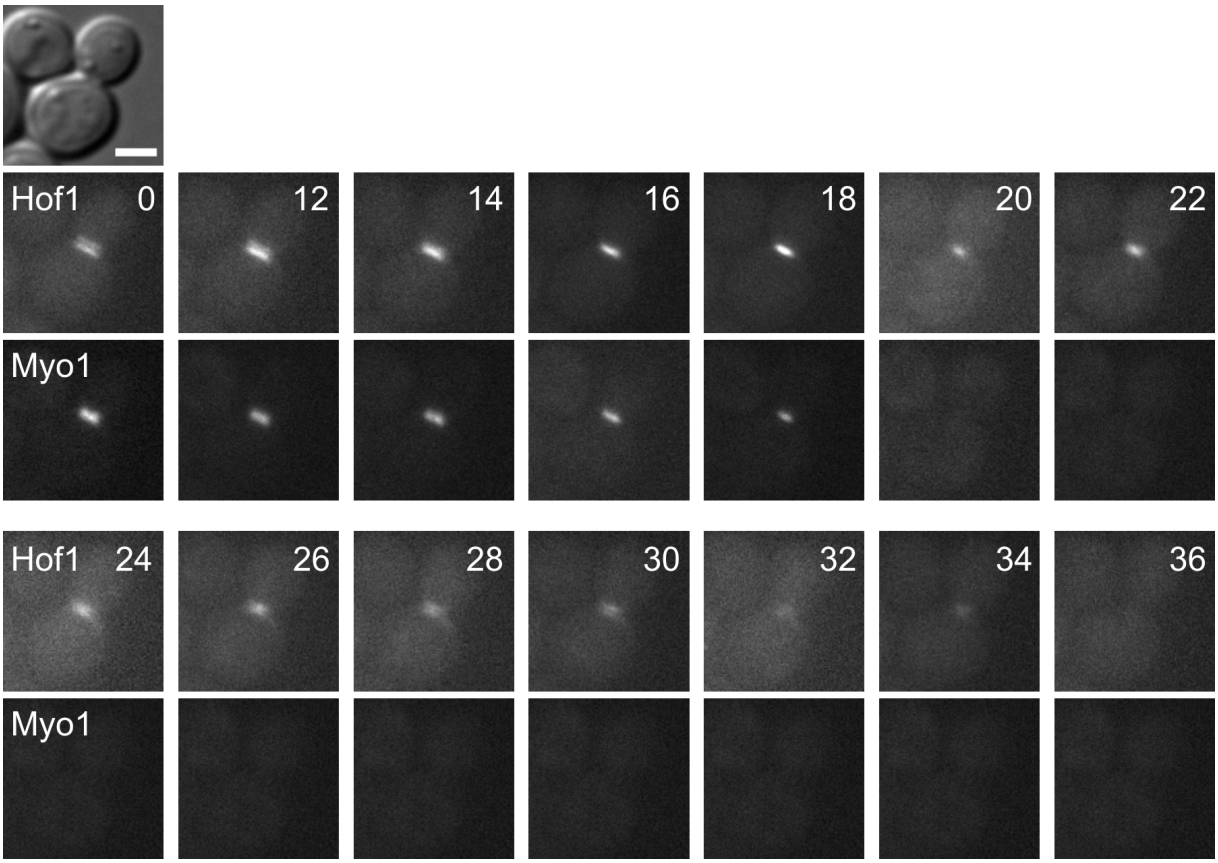

Fig. 1.3: Subcellular localization of Hof1 during cytokinesis. The micrographs depict the subcellular localization of GFP-tagged Hof1 during cytokinesis and septum formation in comparison with Myo1 fused to the red-fluorescent mCherry protein as a marker for cytokinesis. Numbers give the time in minutes after the first detection of Hof1-GFP at the bud neck. Initially, Hof1 localizes as double rings at the bud neck (0). Shortly before the onset of cytokinesis, the double rings merge (12-16). During cytokinesis, the Hof1 ring accompanies constriction of the CAR (18-20). After completion of CAR contraction, the Hof1 signal gets diffuse (22-24), divides again to double rings (26-30), and is degraded at the end of septum formation.

1.3 Aims of the thesis

As described above, the process of cytokinesis has been extensively studied in *Saccharomyces cerevisiae* in the past years. Many regulators were first identified and

subsequently characterized in detail. Nevertheless, many questions still remain unsolved, especially regarding the coordination of several key physiological steps. In the PhD thesis of Hans-Peter Schmitz (2001), a gene with the systematic name *YNL152w* was identified as encoding a novel putative negative regulator of the pathway governing cellular integrity. In another work in this laboratory, a role for Ynl152w in cell separation was suggested, yet a connection to cell wall integrity signaling could not be confirmed (Ciklic, 2007). It was shown, that a *ynl152w* deletion is lethal and that repression of *YNL152w* expression causes defects in cell separation.

When the thesis presented here was initiated, only little information about *YNL152w* could be gained from genome-wide studies published by then. Interestingly, genome-wide yeast two-hybrid approaches in *Saccharomyces cerevisiae* suggested the cytokinetic regulator Hof1 as a direct interaction partner of Ynl152w, supporting a function in cell division (Ito *et al*., 2001). Two independent global studies on the yeast proteome did not reveal a specific localization for the protein Ynl152w (Hazbun *et al*., 2003; Kumar *et al*., 2002).

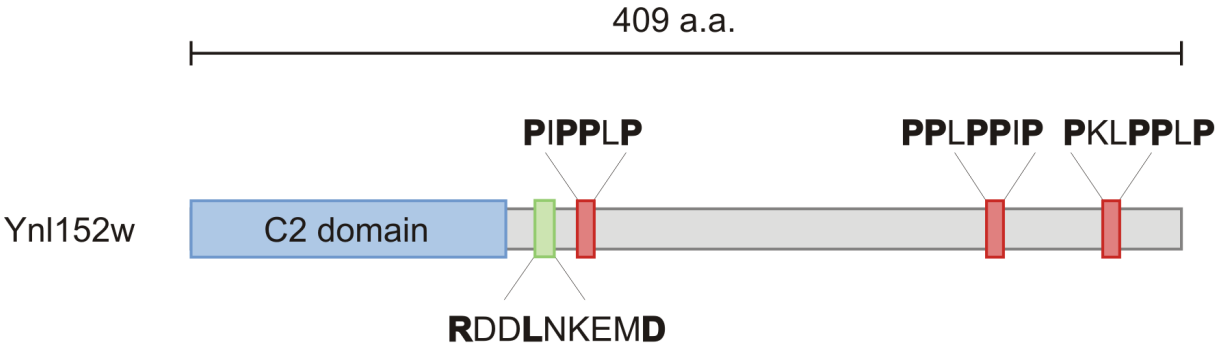

Fig. 1.4: Schematic drawing of the domain structure of Ynl152w. The 409 amino acid backbone of Ynl152w is depicted as grey box. The amino-terminal 130 amino acids represent the C2 domain and are highlighted in blue. Amino acids 142 to 150 represent the putative destruction box depicted in green. Three proline-rich motifs are highlighted in red in the carboxy-terminal part of the protein (amino acids 160-165, 329-335 and 377-383).

Ynl152w contains three remarkable features in its 409 amino acids long primary structure, which are depicted in Fig. 1.4. The amino-terminal 130 amino acids of Ynl152w encode a putative C2 domain. Such domains are either membrane-targeting modules, which mediate Ca^{2+}-dependent phospholipid association (Cho and Stahelin, 2006; Rizo and Sudhof, 1998) or they present interfaces for protein-protein interactions (Benes *et al*., 2005; Dai *et al*., 2007). The amino acids 142 to 150 match the recognition sequence of a destruction box (RXXLXXXXD) and render Ynl152 a putative target of the anaphase-promoting complex. Furthermore, three proline-rich

motifs (PRMs) are distributed in the carboxy-terminal part downstream of the putative destruction box. In other proteins, these motifs were shown to form poly-proline pockets that bind to SH3 domains (Ren *et al.*, 1993). The latter domains are present in multiple proteins, mostly involved in the organization of the actin cytoskeleton. The aim of this thesis was to characterize Ynl152w and its function in further detail and to investigate its suggested role in cytokinesis in *Saccharomyces cerevisiae.*

.

2 Material and Methods

2.1 Material

2.1.1 Chemicals and material

All chemicals were purchased from the companies Applichem (Darmstadt, Germany), BD (Franklin Lakes, USA), Boehringer Ingelheim (Ingelheim, Germany), Difco (Heidelberg, Germany), Merck (Darmstadt, Germany), Roth (Karlsruhe, Germany), Serva (Heidelberg, Germany) and Sigma-Aldrich (St. Louis, USA). Material was purchased from Eppendorf (Hamburg, Germany), Greiner BioOne (Frickenhausen, Germany), Omnilab (Bremen, Germany) and Roth (Karlsruhe, Germany).

2.1.2 Kits and reagents

All kits and reagents listed below were used in this study according to the instructions of the manufacturers.

“High Pure Plasmid Isolation Kit” (Roche, Mannheim), “High Pure PCR Product Purification Kit” (Roche, Mannheim), “µMACS GST Tagged Protein Isolation Kit” (Miltenyi Biotec, Bergisch-Gladbach), “GSTrap HP Columns" (GE Healthcare), “PIP strips” (Molecular Probes), “Rhodamine phalloidin” (Molecular Probes).

2.1.3 Enzymes

Restriction enzymes used in this work were purchased either from New England Biolabs (Ipswich, USA) or from Fermentas GmbH (St. Leon-Rot, Germany). For PCR product amplification either DreamTaq^{TM} DNA Polymerase or the “High Fidelity PCR Enzyme Mix” from Fermentas were used. The alkaline phosphatase and the T4 DNA-ligase were purchased from New England Biolabs, and Zymolyase 20 T from MP Biomedicals, Solon, Ohio, USA.

2.1.4 Antisera

Antisera used are listed in Table 1, stating the peptide/protein they were raised against (epitope) and the production organism, as well as the dilution applied on Western blots.

Tab. 1: Antibodies used in this work

Epitope	Organism	Dilution factor	Source
anti-GST	rabbit	2000	Sigma-Aldrich, G7781
anti-HA	mouse	10000	A. Lorberg, pers. communication
anti-GFP	mouse	2000	Roche, Mannheim
anti-Tkl1	rabbit	2000	Schaaff-Gerstenschlager and Zimmermann, 1993
anti-Vma6	rabbit	3000	C. Ungermann, pers. communication
anti-Actin	mouse	10000	anti-*Dictyostelium* actin; Boehringer (Mannheim)
anti-mouse	goat	5000	Li-Cor, 926-32210
anti-rabbit	donkey	10000	Rockland, 611-730-127

2.1.5 Strains and media

2.1.5.1 *Saccharomyces cerevisiae* strains

All strains used in this work isogenic to HD56-5A (Arvanitidis *et al*., 1993) and the diploid DHD5 (Kirchrath *et al*., 2000) derived from it by transient introduction of the *HO* gene are listed Tab. 2. Strains non-isogenic to the former ones are listed in Tab. 3.

Tab. 2: Isogenic *Saccharomyces cerevisiae* strains used in this work

Name	Genotype	Source
DHD5	*MAT a/α ura3-52/ura3-52 leu2-3,112/ leu2-3,112 his3-11,15/ his3-11,15*	Kirchrath *et al*., 2000
DAJ05	as DHD5 except *SpHIS5-GAL1p-INN1/INN1*	This study
DAJ24	as DHD5 except *⊿inn1::SpHIS5/INN1*	Jendretzki *et al*., 2009
DAJ25	as DHD5 except *SpHIS5-GAL1p-CYK3/ CYK3 KanMX-GAL1p-HOF1/HOF1*	Jendretzki *et al*., 2009
DAJ26	as DHD5 except *INN1-3HA::KanMX/ INN1-3HA::KanMX*	This study
DAJ27	as DAJ26 except *SpHIS5-GAL1p-CDH1/ CDH1*	This study
DAJ28	as DAJ26 except *SpHIS5-GAL1p-CDC20/ CDC20*	This study
DAJ34	as DHD5 except *CYK3⊿SH3-3HA::SpHIS5/CYK3 HOF1⊿SH3-3HA::KanMX/HOF1*	Jendretzki *et al*., 2009
DAJ83	as DHD5 except *SpHIS5-GAL1p-CDC20/ CDC20*	This study
DAJ84	as DHD5 except *SpHIS5-GAL1p-CDH1/ CDH1*	This study
DAJ85	as DHD5 except *⊿hof1::SpHIS5/HOF1*	This study
DAJ98	as DHD5 except *⊿vrp1::KanMX/VRP1*	This study
DAJ99	as DHD5 except *⊿myo1::KILEU2/MYO1*	This study
DAJ106	as DHD5 except *SpHIS5-GAL1p-CDC20-GFP::KanMX/CDC20*	This study
DAJ107	as DHD5 except *SpHIS5-GAL1p-CDH1-GFP::KanMX/CDH1*	This study
HAJ6-A	*MAT a ura3-52 leu2-3,112 his3-11,15*	Jendretzki *et al*., 2009
HAJ6-B	*MAT α ura3-52 leu2-3,112 his3-11,15*	Jendretzki *et al*., 2009
HAJ13-A	as HAJ6-A except *HOF1-yEGFP::SpHIS5*	This study
HAJ14-A	as HAJ6-A except *CYK3-yEGFP::SpHIS5*	This study

HAJ17-B	as HAJ6-B except *GAL1p-3HA-UBR1:: SpHIS5*	This study
HAJ22-A	as HAJ6-A except *INN1-3HA::KanMX*	This study
HAJ23-B	as HAJ6-B except *INN1-GST::SpHIS5*	This study
HAJ26-B	as HAJ6-B *INN1-GST::SpHIS5 CYK3-3HA::SpHIS5*	This study
HAJ27-B	as HAJ6-B *INN1-GST::SpHIS5 HOF1-3HA::SpHIS5*	This study
HAJ28-A	as HAJ6-A except *INN1-GFP(S65T)::KanMX*	This study
HAJ28-B	as HAJ6-B except *INN1-GFP(S65T)::KanMX*	This study
HAJ34-A	as HAJ6-A except *Δvrp1::KanMX*	This study
HAJ36-B	as HAJ6-B except *Δcyk3::KanMX*	This study
HAJ41-A	as HAJ6-A except *HOF1-3HA::SpHIS5*	This study
HAJ42-A	as HAJ6-A except *CYK3-3HA::SpHIS5*	This study
HAJ45-B	as HAJ6-B except *CYK3-GST::SpHIS5*	This study
HAJ46-B	as HAJ6-B except *HOF1-GST::SpHIS5*	This study
HAJ47-B	as HAJ6-B except *HOF1-mCherry::SpHIS5*	This study
HAJ48-A	as HAJ6-A except *MYO1-mCherry::SpHIS5*	This study
HAJ48-B	as HAJ6-B except *MYO1-mCherry::SpHIS5*	This study
HAJ49-B	as HAJ48-B except *HOF1-yEGFP::SpHIS5*	Jendretzki *et al*., 2009
HAJ50-A	as HAJ48-A except *CYK3-yEGFP::SpHIS5*	This study
HAJ50-B	as HAJ48-B except *CYK3-yEGFP::SpHIS5*	Jendretzki *et al*., 2009
HAJ51-B	as HAJ6-B except *CYK3-GST::SpHIS5 INN1-3HA::KanMX*	This study
HAJ52-A	as HAJ6-A except *HOF1-GST::SpHIS5 INN1-3HA::KanMX*	This study
HAJ54-B	as HAJ6-B except *CYK3-mCherry::SpHIS5*	This study
HAJ56-A	as HAJ6-A except *INN1-GFP(S65T)::KanMX HOF1-mCherry::SpHIS5*	This study
HAJ62-B	as HAJ6-B except *KanMX-CUP1p-UBI4-Myc-INN1 GAL1p-3HA-UBR1:: SpHIS5*	This study
HAJ64-B	as HAJ62-B except *CYK3-yEGFP::SpHIS5*	This study

	MYO1-mCherry::SpHIS5	
HAJ67-B	as HAJ6-B except *Δhof1::SpHIS5*	This study
HAJ75-A	as HAJ6-A except *SpHIS5-GAL1p-CYK3*	This study
HAJ76-A	as HAJ6-A except *KanMX-GAL1p-HOF1*	This study
HAJ77-B	as HAJ6-B except *KanMX-GAL1p-HOF1 INN1-GFP(S65T)::KanMX MYO1-mCherry::SpHIS5*	This study
HAJ91-A	as HAJ6-A except *SpHIS5-GAL1p-CYK3 KanMX-GAL1p-HOF1*	This study
HAJ92-B	as HAJ6-B except *VRP1-mCherry::SpHIS5*	This study
HAJ93-B	as HAJ6-B except *INN1-GFP(S65T)::SpHIS5 Δcyk3::KanMX*	Jendretzki *et al*., 2009
HAJ94-B	as HAJ6-B except *INN1-GFP(S65T)::KanMX Δhof1::SpHIS5*	Jendretzki *et al*., 2009
HAJ95-A	as HAJ6-A except *KanMX-GAL1p-HOF1 SpHIS5-GAL1p-CYK3 INN1-GFP(S65T):: KanMX MYO1-mCherry::SpHIS5*	Jendretzki *et al*., 2009
HAJ96-A	as HAJ48-A except *INN1-GFP(S65T)::KanMX*	This study
HAJ96-B	as HAJ48-B except *INN1-GFP(S65T)::KanMX*	Jendretzki *et al*., 2009
HAJ103-A	as HAJ13-A except *VRP1-mCherry::SpHIS5*	This study
HAJ104-A	as HAJ96-A except *Δvrp1::KanMX*	This study
HAJ106-B	as HAJ6-B except *SpHIS5-GAL1p-CYK3 INN1-GFP(S65T)::KanMX MYO1-mCherry::SpHIS5*	Jendretzki *et al*., 2009
HAJ109-A	as HAJ6-A except *CYK3-yEGFP-3HA::SpHIS5*	This study
HAJ111-A	as HAJ6-A except *CYK3ΔSH3-yEGFP-3HA::SpHIS5*	This study
HAJ119-A	as HAJ6-A except *INN1-GFP(S65T)::KanMX CYK3-mCherry::SpHIS5*	This study

HAJ125-A	as HAJ6-A except *CLB2-6HA::KanMX*	This study
HAJ129-B	as HAJ6-B except *⊿iqg1::KlLEU2 SpHIS5-GAL1p-CYK3 MYO1-mCherry::SpHIS5 INN1-GFP(S65T)::KanMX*	This study
HAJ138-A	as HAJ48-A except *CYK3-yEGFP-3HA::SpHIS5*	This study
HAJ139-B	as HAJ6-B except *⊿myo1::KlLEU2 SpHIS5-GAL1p-CYK3 INN1-GFP(S65T)::KanMX*	This study
HAJ140-A	as HAJ48-A except *CYK3⊿SH3-yEGFP-3HA::SpHIS5*	This study
HCB07	as HAJ6-A except *SpHIS5-GAL1p-INN1*	C. Broeker, pers. comm.

Tab. 3: Non-isogenic *Saccharomyces cerevisiae* strains used in this work

Name	Genotype	Source
LD3R-7B	*MAT a ⊿leu1*	S. Hohmann, pers. comm.
inn1-td	*MAT α ade2-1; ura3-1; his3-11,15; trp1-1; leu2-3,112; can1-1 SpHIS5-GAL1p-HA-UBR1 KanMX-CUP1p-UBI4-Myc-INN1*	Sanchez-Diaz *et al*., 2008
PJ69-4A	*MAT a trp1-901 leu2-3,112 ura3-52 his3-200 gal4Δ gal80Δ LYS::GAL1-HIS3 GAL2-ADE2 met2::GAL7-lacZ*	James *et al*., 1996
SMC-19A	*MAT α ⊿leu1*	F.K. Zimmermann, pers. comm.

2.1.5.2 Yeast media

Rich medium (YEP): 1% (w/v) yeast extract, 2% (w/v) peptone
Carbon sources: 2% (w/v) glucose, 2% (w/v) galactose or (w/v) 2% raffinose.

Synthetic medium: 0.67% (w/v) Yeast Nitrogen Base w/o amino acids (YNB)

Amino acids and nucleotide bases were added according to the concentrations listed in Zimmermann (1975).
Carbon sources: 2% (w/v) glucose, 2% (w/v) galactose or 2% (w/v) raffinose.
The pH was adjusted to 6.2, prior to sterilization.

Sporulation medium: 1% (w/v) potassium acetate, 3% agar.

For plates 1.5% (w/v) agar were added to the medium. Plates and liquid cultures were incubated at 30°C unless stated otherwise. Drugs and antibiotics were added after cooling the sterile media to 50°C. 200 mg/ml G418 were added for the selection of *KanMX*-expressing cells. 5-FOA plates were made from synthetic complete medium lacking uracil, by addition of 1 mg/l 5-fluoroorotic acid directly to the medium cooled to 50°C with constant stirring.

2.1.5.3 Storage of yeast strains

Yeast strains were stored on agar plates at 4°C and inoculated to fresh plates approximately every two months. For long term storage, strains were preserved in glycerol cultures. 0.5 ml of a fresh overnight culture were added to 1 ml of 33% (v/v) sterile glycerol solution and stored at -80°C.

2.1.5.4 *E. coli* strains

E. coli strain DH5α from Stratagene (*F´glnV44 thiA-1 ⊿(argF-lac) U169 deoR endA1 gyrA96 hsdR17 recA1 supE44 (Ø80lacZ⊿M15) NalR*) was used for cloning and strain BL21-DE3 (*fhuA2 [lon] ompT gal (λ DE3) [dcm] ∆hsdS λ DE3 = λ sBamHIo ∆EcoRI-B int::(lacI::PlacUV5::T7 gene1) i21 ∆nin5*) was used for heterologous expression in *E. coli*.

2.1.5.5 *E. coli* culture conditions

Rich medium (LB): 1% (w/v) tryptone, 0.5% (w/v) yeast extract, 0.5% (w/v) NaCl

Plates were made with the addition of 1.5% (w/v) agar. *E. coli* strains were cultivated at 37°C. For the preparation of selective media for plasmid maintenance, either

ampicillin was added to a final concentration of 50 µg/ml or kanamycin to 20 µg/ml. For blue/white screens, 100 µl of an IPTG/X-Gal solution (2.4 mg/ml IPTG, 10 mg/ml X-Gal dissolved in dimethylformamide) were spread onto the plates prior to plating of *E. coli*.

2.1.6 Plasmids

All vectors and plasmids from former studies used in this work are listed in Tab. 4, whereas the vectors and plasmids constructed in this thesis are listed in Tab. 5.

Tab. 4: Vectors and plasmids used in this work

Name	Description	Source
pAGT211	Amplification of C-terminal *mCherry*-tagging cassettes with the *NAT1* marker	Kaufmann and Philippsen, 2009
pFA6a-KanMX6	Amplification of *KanMX* deletion cassettes	Longtine *et al*. 1998
pFA6a-GFP(S65T)-KanMX6	Amplification of C-terminal *GFP*-tagging cassettes with the *KanMX* marker	Longtine *et al*. 1998
pFA6a-3HA-His3MX6	Amplification of C-terminal *3HA*-tagging cassettes with the *SpHIS5* marker	Longtine *et al*. 1998
pFA6a-3HA-KanMX6	Amplification of C-terminal *3HA*-tagging cassettes with the *KanMX* marker	Longtine *et al*. 1998
pFA6a-GST-His3MX6	Amplification of C-terminal *GST*-tagging cassettes with the *SpHIS5* marker	Longtine *et al*. 1998
pFA6a-KanMX6-PGAL1	Amplification of the *GAL1* promoter preceded by the *KanMX* marker	Longtine *et al*. 1998
pFA6a-His3MX6-PGAL1	Amplification of the *GAL1* promoter preceded by the *SpHIS5* marker	Longtine *et al*. 1998
pFA6a-His3MX6-PGAL1-3HA	Amplification of the *GAL1* promoter and N-terminal *3HA*-tag preceded by the *SpHIS5* marker	Longtine *et al*. 1998
pKT128	Amplification of C-terminal *yEGFP*-tagging cassettes preceded by the *SpHIS5* marker	Sheff and Thorn, 2004

pKT221	Amplification of C-terminal *yECFP-3HA*-tagging cassettes preceded by the *KanMX* marker	Sheff and Thorn, 2004
pUG73	Amplification of *KlLEU2* deletion cassettes	Gueldener *et al*., 2002
YEp352	*2 µm S. cerevisiae- E. coli* shuttle vector with a *URA3* marker and *lacZ'* for blue/white screening	Hill *et al*., 1986
pYM14	Amplification of C-terminal *6HA*-tagging cassettes with the *KanMX* marker	Janke *et al*., 2004
pGAD424A/B/C	Yeast two-hybrid cloning vector for Gal4 activation domain fusions with a *LEU2* marker	Bartel *et al*., 1993
pGBD-C1/2	Yeast two-hybrid cloning vector for Gal4 DNA-binding domain fusions with a *TRP1* marker	James *et al*., 1996
pSA15	*S. cerevisiae- K. lactis- E. coli* shuttle vector pCXs22 with *MYO1*, a pKD1 origin for *K. lactis*, a *CEN/ARS* and a *URA3* marker from *S. cerevisiae*	S. Albermann, pers. comm.; pCXs22 described in Heinisch *et al*., 2010
pSU19c	Cloning vector with low copy expression and *lacZ'* for blue/white screening	Martinez *et al*., 1988
pTM30c	Cloning vector for the overexpression of proteins in *E. coli*	Morrison and Parkinson, 1994
YCplac111	*CEN/ARS* vector with the *LEU2* marker and *lacZ'* for blue/white screening	Gietz and Sugino, 1988
YIplac211	Integrative vector with the *URA3* marker and *lacZ'* for blue/white screening	Gietz and Sugino, 1988

Tab. 5: Vectors and plasmids constructed in this work

Name	Insert	Backbone	Construction
pAJ001	*mCherry*	pKT128	*Hin*dIII and *Asc*I subcloning of *mCherry*

			from pAGT211 into pKT128
pAJ005	*SLA1*(1-500)	pGAD424B	Amplification with 06.125 and 06.126, cloned with *Bam*HI and *Sal*I
pAJ007	*MYO3*(1119-1183)	pGAD424B	Amplification with 06.128 and 06.129, cloned with *Eco*RI and *Pst*I
pAJ008	*BUD14*(1-350)	pGAD424B	Amplification with 07.099 and 07.100, cloned with *Bam*HI and *Pst*I
pAJ009	*HOF1*(1-601)	pGAD424B	Amplification with 07.044 and 07.157, cloned with *Bam*HI and *Pst*I
pAJ010	*CYK3*(1-80)	pGAD424B	Amplification with 07.044 and 07.043, cloned with *Bam*HI and *Pst*I
pAJ011	*BOI1*(1-100)	pGAD424B	Amplification with 07.095 and 07.096, cloned with *Bam*HI and *Pst*I
pAJ012	*BOI2*(1-150)	pGAD424B	Amplification with 07.093 and 07.094, cloned with *Bam*HI and *Pst*I
pAJ013	*CDC25*(1-150)	pGAD424B	Amplification with 07.128 and 07.129, cloned with *Bam*HI and *Pst*I
pAJ014	*BEM1*(1-250)	pGAD424B	Amplification with 07.097 and 07.098, cloned with *Bgl*II and *Pst*I
pAJ015	*HOF1*	pGAD424A	Amplification with 04.029 and 04.030, cloned with *Bam*HI and *Pst*I
pAJ016	*HOF1*(501-669)	pGAD424C	Amplification with 04.030 and 06.180, cloned with *Sal*I and *Pst*I
pAJ017	CYK3	pGAD424B	Amplification with 07.044 and 07.157, cloned with *Bam*HI and *Pst*I
pAJ018	*CYK3*(81-885)	pGAD424B	Amplification with 07.293 and 07.157, cloned with *Bam*HI and *Pst*I
pAJ022	*INN1*	YEp352	Amplification with 03.005 and 07.139, cloned with *Bam*HI and *Sph*I
pAJ023	*HOF1*	YEp352	Amplification with 04.030 and 08.064, cloned with *Sac*I and *Pst*I
pAJ024	*CYK3*	YEp352	Amplification with 07.214 and 08.065, cloned with *Eco*RI and *Sph*I

pAJ025	*INN1*	pGBD-C2	Amplification with 04.034 and 04.035, cloned with *Bam*HI and *Pst*I
pAJ027	*INN1*(1-367)	pGBD-C2	Amplification with 04.034 and 06.265, cloned with *Bam*HI and *Pst*I
pAJ029	*INN1*(1-259)	pGBD-C2	Amplification with 04.034 and 06.266, cloned with *Bam*HI and *Pst*I
pAJ030	*INN1*(1-161)	pGBD-C2	Amplification with 04.034 and 06.267, cloned with *Bam*HI and *Pst*I
pAJ032	*INN1-GST*	pTM30c	Amplification with 07.356 and 07.357 from HAJ23-B, cloned with *Hin*DIII and *Pst*I
pAJ036	*INN1*(160-409)-*GST*	pTM30c	Amplification with 08.162 and 07.357 from pAJ032, cloned with *Hin*dIII and *Pst*I
pAJ044	*IQG1*	YEp352	Amplification with 08.363 and 08.364, cloned with *Sac*I and *Sal*I
pAJ046	*IQG1*	pGAD424C	Amplification with 08.363 and 08.362, cloned with *Cfr*9I and *Sal*I
pAJ047	*VRP1*	YEp352	Amplification with 09.018 and 09.019, cloned with *Bam*HI and *Sph*I
pAJ048	*3HA*	pKT128	*Mun*I and *Bgl*II subcloning of *3HA* from pKT221 into pKT128
pAJ052	*INN1*	YCplac211	*Bam*HI and *Sph*I subcloning of *INN1* from pAJ022 into YCplac211
pAJ054	*INN1-GFP*	YCplac211	*In vivo* recombination of *GFP(S65T)::KanMX* into pAJ052
pAJ055	*MYO1*	YEp352	*Pst*I subcloning of *MYO1* from pSA15 into YEp352
pAJ056	*INN1-GFP*	YIplac211	*Kpn*I and *Pst*I subcloning of *INN1-GFP* from pAJ054 into YIplac211
pAJ057	*'INN1-GFP'*	pSU19c	*Bam*HI subcloning of an *INN1-GFP* fragment into pSU19c
pAJ058	*'INN1ΔDB-GFP'*	pSU19c	Amplification of pAJ057 with 09.204

			and 09.205; restriction with *Xho*I and self-ligation
pAJ059	*INN1ΔDB-GFP*	YIplac211	*Sex*AI and *Blp*I subcloning of *INN1ΔDB-GFP* from pAJ058
pAJ061	*LSB3*(351-451)	pGAD424B	Amplification with 07.188 and 07.189, cloned with *Bam*HI and *Sal*I
pAJ062	*YSC84*(368-468)	pGAD424B	Amplification with 07.185 and 07.186, cloned with *Bam*HI and *Sal*I
pAJ063	*INN1*(150-409)	pGBD-C1	Amplification with 04.035 and 06.127, cloned with *Bam*HI and *Pst*I
pAJ066	*INN1-GFP*	YEp352	*Kpn*I and *Pst*I subcloning of *INN1-GFP* from pAJ056 into YEp352
pAJ067	*INN1ΔDB-GFP*	YEp352	*Kpn*I and *Pst*I subcloning of *INN1ΔDB-GFP* from pAJ059 into YEp352

2.1.7 Oligonucleotides

All oligonucleotides used in this study were purchased from MWG Biotech AG (Ebersberg, Germany) or Metabion international AG (Martinsried, Germany) and are listed in Tab. 6.

Tab. 6: Oligonucleotides used in this work

Number	Name	Sequence 5'-3'
03.005	YNL152endSph	GGGCGCATGCGAAGAGGCCGCCTTTTAGTTG
03.007	YNL152del5' (Xba)	GGTCGCCCACCTTGTATTGCACGGG
03.042	152 vor	CAGGATCGCCTTCAGAGCATC
03.043	152 hinter	GGCGGATGATGATTTCGAAG
04.019	GALpEco	CTGCATAACCACTTTAACTAATAC
04.025	Prion3SacKpn	GTATGAGCTCGGTACCGGGTGACCCGGCGGGGACGAGG
04.029	HOF1thvor	GGCGGGATCCATATGAGCTACAGTTATGAAGCTTG
04.030	HOF1thnach	GGCGCTGCAGGAGAGGTGTCCTTCTCCCACGG
04.034	YNL152thnach	GGCGCTGCAGGTTTAGATCGGCGGTGAGGG
04.035	YNL152thBam	GGCGGGATCCATATGTCCGAAGAAGTATGGAATGG

04.113	ynlGFPF4	CTTCCTGTAAAATTGTATGAAAAGCCGCCTCTGCTG ATCATGAATGACGGAATTCGAGCTCGTTTAAAC
05.019	YNL152w5raus	GCTCGATGTAGAGTGTTGCTGG
05.077	ynlGALR2	GCTCACATATACGGAGAGGATTCCTTGGTTTCCATT CCATACTTCTTCGGACATTTTGAGATCCGGGTTTT
05.117	Hof1HAF4	GGATAGGATTAATTCCCTATAATTTCATTCAGCTACT GCATCAAGGTCTTCGGATCCCCGGGTTAATTAA
05.118	Hof1HAR1	CTTTTAGCCACTGCGCGGAAATATGTAGTATTCGTA ACAAGTGACTCGAATTCGAGCTCGTTTAAAC
05.133	YNL152endR1	GGTTTAGATCGGCGGTGAGGGCGCAACAGATTTAT GTATACATATTGAAAGAATTCGAGCTCGTTTAAAC
05.134	YNL152wF2	GATGTCTCCTACAAGAAAAAGACCACCTCCAAGGCT CAGCCGGATCCCCGGGTTAATTAA
06.125	SLA1thnach_1-500_SalI	GCGTCGTCGACCTATTACCATAGACGCGATTTTTTT G
06.126	SLA1thvor_BamHI	GCGTCGGATCCATGACTGTGTTTCTGGGCAT
06.127	YNL152wthvor_ 150-409_BamHI	GCGTCGGATCCAGGTTGGATTCATCTATGGC
06.128	MYO3thvor_ 1119-1183_EcoRI	GCGTCGAATTCCAAAGGATCCGAAATTCGA
06.129	MYO3thnach_ 1119-1183_PstI	GCGTCCTGCAGCTATTATCTTGTGTCTTTATAAGGA G
06.130	VRP1-5	ATCCGCACAGTCAGTAAATA
06.131	VRP1-3	GCGAAAAGGACGGGAAGCTA
06.132	HOF1delSH3-F1	TACCTTGCCTATTGTCACCAGTGAAGGTTTTCCAGT CATTTAGTAACGGATCCCCGGGTTAATTAA
06.133	HOF1delSH3-R2	TCTTTTATCAGAAAACTAGTAAAATTGATATACATCG AGAGAATTCGAGCTCGTTTAAAC
06.180	HOF1thvor_501-669_ SalI	GCGTGGTCGACTGCGCACAACCTCAATGA
06.252	TEFterm-3'out	TCGCCTCGACATCATCTGCCCAG
06.265	YNL152del42th_PstI	GCGTCCTGCAGCTATTATGAGTTAGGCGAAGAGGA ATC
06.266	YNL152del150th_PstI	GCGTCCTGCAGCTATTATAAATTGGCAAAATGGAAT TTTG
06.267	YNL152del250th_PstI	GCGTCCTGCAGCTATTACCTCATAGCCATAGATGAA TCC
07.028	HOF1-F4	GAGACTTGGAAAGTGTACTACTAATATTCAGAAAAA GGTGAAAGAGAATTCGAGCTCGTTTAAAC
07.029	HOF1-R2	ACCATTGTCGTTTGGGTCCCAAAAACAAGCTTCATA ACTGTAGCTCATTTTGAGATCCGGGTTTT
07.043	CYK3thnach_1-80_PstI	GCGTCCTGCAGCTATTACCTACCATTTTCAGTGCTC GAATTT
07.044	CYK3thvor_BamHI	GCGTCGGATCCGCCACTAACTTAACATCTTTGAAGC
07.045	CYK3-R1	GAATGATACAGATTATAGCGCTGTAAAAAAATTTGT GAAAAACGTGAATTCGAGCTCGTTTAAAC

07.046	CYK3-F2	GACTCTGGTATTGGGTGGTCCGTTTTTGCTGAATGG TTGTGCGTACGGATCCCCGGGTTAATTAA
07.060	CYK3-5'	ACCTCGTTTTCGGACTTGCC
07.089	YNL152w_N-Tag-5'	AGGTTTCACAACTGGAATTGGGTTAACTCGTTGAGT CACTGTCGAATGTGCAGGTCGACAACCCTTAAT
07.090	YNL152w_N-Tag-3'	ATATACGGAGAGGATTCCTTGGTTTCCATTCCATAC TTCTTCGGAGCGGCCGCATAGGCCACT
07.093	BOI2thvor_BamHI	GCGTCGGATCCAGTAATGACAGGGAAGTACCCACA C
07.094	BOI2thnach_1-150_PstI	GCGTCCTGCAGCTATTACGGGGTTGGCAGTTCACT GTTTGAA
07.095	BOI1thvor_BamHI	GCGTCGGATCCAGTCTCGAAGGAAATACCCTAGGC A
07.096	BOI1thnach_1-100_PstI	GCGTCCTGCAGCTATTAATTTCCATATTTAACACCA GAATTT
07.097	BEM1thvor_PstI	GCGTCCTGCAGCTGAAAAACTTCAAACTCTCAAAAA
07.098	BEM1thnach_1-250_ BglII	GCGTCAGATCTCTATTATTTGTATCTTGCAATGTTGC TTTTC
07.099	BUD14thvor_BamHI	GCGTCGGATCCAGTAATAAGGAAGAGCATGTTGAT G
07.100	BUD14thnach_1-350_PstI	GCGTCCTGCAGCTATTAAGAGCTGATGGAATCATCT TTCGAA
07.102	MYO1-R1	TAAATAAAGGATATAAAGTCTTCCAAATTTTTAAAAA AAAGTTCGGAATTCGAGCTCGTTTAAAC
07.103	MYO1-5’	CAGAGGATCCTTTGGAGATGTGG
07.126	UBR1-F4	TCCCTAATCTTTACAGGTCACACAAATTACATAGAAC ATTCCAATGAATTCGAGCTCGTTTAAAC
07.127	UBR1-R3	CCTAATGTGACCTTGTAAAGATCCTAAATCATCATCA GCAACGGAGCACTGAGCAGCGTAATCTG
07.128	CDC25th_BamHI	GCGTCGGATCCTCCGATACTAACACGTCTATTCCCA
07.129	CDC25th_1-150_PstI	GCGTCCTGCAGCTATTAGCACTATTGCCCAAGCTAT TTAAGC
07.139	YNL152wvor_BamHI	GCGCTGGATCCAATGGTCCTCTGTTAGTTTCTTGGC G
07.151	MYO1-F5	TCGAAAAATATTGATAGTAACAATGCACAGAGTAAA ATTTTCAGTGGTGACGGTGCTGGTTTA
07.152	CYK3-F5	GACTCTGGTATTGGGTGGTCCGTTTTTGCTGAATGG TTGTGCGTAGGTGACGGTGCTGGTTTA
07.153	HOF1-F5	GGATTAATTCCCTATAATTTCATTCAGCTACTGCATC AAGGTCTTGGTGACGGTGCTGGTTTA
07.157	CYK3thnach_PstIneu	GCGTCCTGCAGCACCTTCCTGAGTAGAATGTATG
07.176	HOF1-5_3	TCGAGTAGCCGAGGTATATG
07.177	HOF1-3_5	CACAGTAGAACTGTCATTAGAGC
07.178	CYK3-5_3	CTGTTTGCTATAAGCATACATTGC
07.184	YSC84thvor_BamHI	GCGTCGGATCCGGTATCAATAATCCAATTCCTCGAA GC
07.185	YSC84thnach_SalI	GCGTCGTCGACTTAAGAAACTCTAACGTAGTTTGCA GG

07.186	YSC84thvor_ 368-468_BamHI	GCGTCGGATCCAGAGAAAGGGGTTATAGCCTTGG
07.187	LSB3thvor_BamHI	GCGTCGGATCCGGTATTAACAATCCTATTCCAAGGAG
07.188	LSB3thnach_SalI	GCGTCGTCGACTTAAACTAGTTCAACGTAATTTGCTGG
07.189	LSB3thvor_351-451_ BamHI	GCGTCGGATCCGATAGGACAAAAGACCGTGAAG
07.214	CYK3-3_5	GCCAAATCTAACGCAAGC
07.228	YNL152w-F1	AGGTTTCACAACTGGAATTGGGTTAACTCGTTGAGTCACTGTCGACGGATCCCCGGGTTAATTAA
07.293	CYK3th_81-885_BamHI	GCGTCGGATCCCAACCTTCAAAAATAGTAGAAAG
07.356	YNL152w_vor_PstI	GCTCGCTGCAGTCCGAAGAAGTATGGAATG
07.357	YNL152w_nach_HindIII	CGTGCAAGCTTGAGGTGTGGTCAATAAGAGC
07.366	CYK3-F4	AACATTTAATTCCTGAATTTACCGTATTACATTTAAATTTGCATAGAATTCGAGCTCGTTTAAAC
07.367	CYK3-R2	GGCCTTCACCTTAAATGGTGGCTTCAAAGATGTTAAGTTAGTGGCCATTTTGAGATCCGGGTTTT
07.368	CYK3delSH3-for	ATTTAATTCCTGAATTTACCGTATTACATTTAAATTTGCATAATGTGCAGGTCGACAACCCTTAAT
07.369	CYK3delSH3-rev	AACTTTATTTGATTTTTCAAAACTTTCTACTATTTTTGAAGGTTGGCGGCCGCATAGGCCACT
08.064	HOF1vor_SacI	CGTCGAGCTCGAGTAGCCGAGGTATATG
08.065	CYK3vor	GATATCTTGCATGCTTGGACC
08.137	HOF1-F1	GAGACTTGGAAAGTGTACTACTAATATTCAGAAAAAGGTGAAAGACGGATCCCCGGGTTAATTAA
08.162	Ynl152w(160-409)vor_PstI	GCTGCCTGCAGCCGATACCACCATTGCCAAC
08.362	IQG1thvor_SmaI	GCTCGCCCGGGACAGCATATTCAGGCTCTCC
08.363	IQG1thnach_SalI	GCTGCGTCGACCCCAATATGCTCAAAACCGAG
08.364	IQG1vor_SacI	GTGTAGAGCTCGAACGAGAAC
08.366	IQG1del3'	AAATTTAGTAACAGCTTTTGCCCAATATGCTCAAAACCGAGTTATGCGGCCGCATAGGCCACT
08.367	IQG1del5'	TTATTGCACCAGTTCAATTATATGTAACAAGGTGGTGCAAAAACATGCAGGTCGACAACCCTTAAT
08.368	IQG1-5'	GCAGTTGTTTCGCGCTTAC
08.369	IQG1-3'	GAGCAGACGGAAGGAGAGC
08.417	VRP1-R1	TATTTTCTTGTTCTTCAGTGATTTATTGTAACCATGGAGAAATGCGAATTCGAGCTCGTTTAAAC
08.418	VRP1-F5	AGTGGAAAGGGTAGTAGTGTGCCATTGGACTTAACATTATTTACGGGTGACGGTGCTGGTTTA
09.017	HOF1delSH3-F2	TACCTTGCCTATTGTCACCAGTGAAGGTTTTCCAGTCATTCGGATCCCCGGGTTAATTAA

09.018	VRP1vor_BamHI	CGTGCGGATCCTGTTCGGATGTTAAGCAGGC
09.019	VRP1nach_SphI	CGTCGGCATGCGCAGCTGTGGACTGGCTATC
09.108	MYO1del5'	GGTTAGAAGATCATAACAAAGTTAGACAGGACAACA ACAGCAATATGCAGGTCGACAACCCTTAAT
09.109	MYO1del3'	AATGCATATTCTCATTCTGTATATACAAAACATCTCA TCATTATTGCGGCCGCATAGGCCACT
09.153	MYO1-3'out	GGAAATGGCCCAAGAAATTG
09.204	INN1delDB_5-3	CCGAGCTCGAGGTTGGATTCATCTATGGC
09.205	INN1delDB_3-5	GCTGGCTCGAGTTTAAACGAGGTACTTTGGG
09.335	CDC20-F2	TACAAGGAGGCCCTCTAGTACCAGCCAATATTTGAT CAGGCGGATCCCCGGGTTAATTAA
09.336	CDC20-R1	TTCATTATATGCCTTGACATGAACTTTTATTTTTTTTA TTGAATTCGAGCTCGTTTAAAC
09.337	CDC20_3-5	CCTTTTCTTGTGAATCCTGTG
09.338	CDH1-F2	GCCAAATTCGTTAATATTTGACGCATTTAATCAAATA CGTCGGATCCCCGGGTTAATTAA
09.339	CDH1-R1	TACAGAATTTTTGAGATGATATTACTACTATGAAAAC CCTGAATTCGAGCTCGTTTAAAC
09.340	CDH1_3-5	GCTTCTTTTGCCGATTTCTAG
09.341	CDC20-F4	GTGCAGAAATATCAAAAGACAAGTATTACAAAGAAG ACTAGAATTCGAGCTCGTTTAAAC
09.342	CDC20-R2	CGCTAATTGCTGCATTTCCCTTATCTCTAGAGCTTTC TGGCATTTTGAGATCCGGGTTTT
09.343	CDC20_5-3	CCAGAGTGAGGAAACGTTAG
09.344	CDH1-F4	TGTCACCCTTCCTTCTAGTCTTCATCCTAAATTTAGT TGCGAATTCGAGCTCGTTTAAAC
09.345	CDH1-R2	AGGAAGGCGTATTATTCATGAATGGGTTCAGGTTTG TGGACATTTTGAGATCCGGGTTTT
09.346	CDH1_5-3	GAAGCGCATAATCTGCCAAC
09.386	CLB2-S3	GGTTAGAAAAAACGGCTATGATATAATGACCTTGCA TGAACTTCGTACGCTGCAGGTCGAC
09.387	CLB2-R1	CGATTATCGTTTTAGATATTTTAAGCATCTGCCCCTC TTCGAATTCGAGCTCGTTTAAAC
09.388	CLB2_3-5	GAAACCAAGGTATGGCTCTG

2.2 Methods

2.2.1 Transformation

2.2.1.1 Transformation of *E. coli*

Transformation of *E. coli* was performed with the rubidium chloride method (Hanahan, 1983).

2.2.1.2 Transformation of *S. cerevisiae*

For the integration of DNA fragments into the genome, *S. cerevisiae* was transformed with the lithium-acetate method (Gietz *et al*., 1995). Plasmid DNA was introduced into *S. cerevisiae* with the freeze method (Klebe *et al*., 1983).

2.2.2 Sporulation, tetrad analysis and determination of the mating type

For sporulation of diploid yeast strains, 3 ml of stationary cells were collected in a table-top centrifuge at 3,000 rpm for 2 min. The supernatant was discarded, the cells were resuspended in the remaining drop of medium and transferred to a sporulation plate. After 2-3 days of incubation at 30°C, cells were examined under the microscope for the presence of tetrads. A toothpick tip of sporulating cells was resuspended in 100 µl distilled water and incubated 10 min at room temperature after the addition of 4 µl Zymolyase (10 mg/ml). Tetrads were dissected on agar plates using a micromanipulator (Singer MSM system series 300). After the spores germinated and grew to visible colonies, master plates were created and the segregants were checked for markers by replica-plating onto the respective media. The mating type was determined by crossing with two tester strains LD3R-7B (*MATa leu1*) and SMC-19A (*MAT*α *leu1*) and checked for complementation on synthetic minimal medium with 2% glucose.

2.2.3 Growth analysis by serial drop dilution assays

Cells were grown overnight in liquid media at the permissive temperatures. After determination of the OD_{600} (Shimadzu UV mini 1240 photometer), the overnight cultures were diluted to an OD_{600} of 0.25 and further incubated to reach an OD_{600} of approximately 1.0. Cultures were diluted again to an OD_{600} of 0.3, and serial dilutions of 10^{-1}, 10^{-2}, 10^{-3}, 10^{-4} were made. 3 µl of each dilution were dropped onto the different media. Plates were further incubated as indicated. For documentation the plates were scanned with a transmitted light scanner at 400 dpi and adjusted for contrast and further processing with Corel Photo Paint 12.

2.2.4 Cell cycle arrest and synchronization

For the cell cycle arrest in metaphase, cells were grown to early logarithmic phase in complete media and subsequently incubated for an additional 2 h in the presence of 5 µg/ml nocodazole. For the arrest in G1 phase, cells of mating type **a** were grown to early logarithmic phase in YEPD pH 3.8, before 2 µg/ml α-factor were added. After one hour of incubation an additional 1 µg/ml α-factor was added and further incubated until more than 95% were arrested as non-budded cells. For synchronization, cells were washed twice in ice cold water and once in YEPD, before further incubation in YEPD at 30°C.

2.2.5 Analysis of DNA

2.2.5.1 Preparation of plasmid DNA by alkaline lysis

The preparation of plasmid DNA was performed according to Sambrook *et al*. (1989) with some modifications. The instructions of Roche were followed up to the addition of 3 M potassium-acetate and the subsequent centrifugation step. From the resulting supernatant, nucleic acids were precipitated with 0.8 volumes of isopropanol, pelleted and resuspended in 50 µl of sterile water.

2.2.5.2 Preparation of plasmid DNA from *E. coli*

For sequencing, plasmid DNA from *E. coli* was isolated using the "High Pure Plasmid Isolation Kit" (Roche, Mannheim), according to the manufacturers' instructions.

2.2.5.3 Preparation of plasmid DNA from *S. cerevisiae*

To prepare plasmid DNA from yeast, cells from 2 ml of an overnight culture were pelleted in a table-top centrifuge at 3,000 rpm for 1 min. The pellet was resuspended in 250 µl suspension buffer from the "High Pure Plasmid Isolation Kit" (Roche, Mannheim). After the addition of 100 µg of glass beads, cells were broken by shaking for 10 min on an "IKA-Vibrax-VXR" at 4°C. The following steps were performed according to the manufacturers' instructions for the isolation of plasmid-DNA from *E. coli*. The plasmid DNA was eluted in 30 µl elution buffer from the columns and 10 µl were used to transform *E. coli* in order to amplify the DNA.

2.2.5.4 Preparation of chromosomal DNA from *S. cerevisiae*

Cells from a 3 ml overnight culture were harvested by centrifugation at 3,000 rpm for 1 min and resuspended in 300 µl spheroblast buffer (50 mM $NaPO_4$ buffer, 0.9 M sorbitol and 0.1 M EDTA, 1 mM β-mercapto-ethanol). Over a period of 1 hour, the cell wall was enzymatically digested at 37°C in the presence of 10 µl zymolyase (10 mg/ml). After the addition of 50 µl 0.5 M EDTA and 50 µl 10% (w/v) SDS solution, cells were lysed by an incubation for 30 min at 65°C , which also served to inactivate DNases. After 5 min of cooling to room temperature, the proteins were precipitated by the addition of 150 µl 5 M KAc (pH = 8.6) and a subsequent incubation on ice for 1h. The proteins were pelleted together with cell debris by centrifugation at 10,000 rpm for 10 min. To precipitate the DNA from the supernatant, 0.8 volumes of isopropanol were added and incubated for 5 min at room temperature, before another centrifugation step at 13,000 rpm for 15 min was performed. To remove RNA, the pellet was resuspended in 100 µl DNAse-free RNAse-solution (50 mM Tris-HCl, 10 mM EDTA, 0.2 mg/ml RNAse H and 150 mM sodium acetate) and incubated for 30 min at 37°C. The DNA was precipitated again by the addition of 10 µl 3 M sodium acetate and 250 µl ethanol followed by a centrifugation for 15 min at 13,000

rpm. The pellet was washed with 70% (v/v) ethanol and the DNA was dissolved in 50 µl of sterile water and stored at -20°C.

2.2.5.5 Separation of DNA fragments by gel electrophoresis

DNA fragments were analyzed by electrophoretic separation in agarose gels. Depending on the sizes of the DNA fragments, 0.7-2.0% (w/v) agarose-gels (dissolved in 1× TAE buffer) were used. As running buffer 1× TAE (40 mM Tris-HCl pH 8.3, 20 mM acetic acid, 1mM EDTA) was used. A current of 120 V was applied for 35 minutes, using a “Power Pack P25” from Biometra. The “2-Log DNA Ladder” or the “100 bp DNA Ladder” (New England Biolabs) were used as size markers for the DNA fragments. The DNA was stained by incubation of the agarose gels in an aqueous solution of 0.5 µg/ml ethidium bromide, and subsequently visualized by exposition to UV light (λ = 366 nm).

2.2.5.6 Isolation of DNA fragments from agarose gels

To isolate specific DNA fragments, they were separated by electrophoresis in an 0.7-1.0% (w/v) agarose gel as described above and then excised under a UV lamp (λ = 312 nm). The DNA fragments were purified from the agarose blocks using the “High Pure PCR Product Purification Kit” (Roche, Mannheim) following the instructions provided by the manufacturer.

2.2.5.7 Purification of PCR products

PCR products were purified using the “High Pure PCR Product Purification Kit” (Roche, Mannheim), according to the manufacturers’ instructions.

2.2.5.8 Restriction, dephosphorylation and ligation of DNA

Restriction, dephosphorylation and ligation of DNA were performed according to the instructions provided by the enzymes manufacturer.

2.2.5.9 Sequencing of plasmid DNA

Custom sequencing was provided by the Scientific Research and Development GmbH (Bad Homburg, Germany). Plasmid DNA was prepared with the “High Pure Plasmid Isolation Kit” (Roche, Mannheim). The DNA sample (150-300 ng in 6.5 µl) was pre-mixed with the required oligonucleotides at 10 pmol/ml.

2.2.5.10 Polymerase chain reaction (PCR)

For PCR product amplification either DreamTaqTM DNA Polymerase or the “High Fidelity PCR Enzyme Mix” from Fermentas GmbH (St. Leon-Rot, Germany) were used. All PCR reactions were performed as suggested by the instructions delivered with the corresponding DNA polymerases, in a “Personal Cycler” from Biometra. A standard setting employed 2min/95°C for a first denaturation, followed by 33 cycles between 30sec/95°C for denaturation, 30sec/58°C for annealing, and 1min/kb of desired product at either 72°C (up to 3 kb) or 68°C (> 3kb).

2.2.6 Analysis of proteins

2.2.6.1 Preparation of whole cell extracts from *S. cerevisiae*

For the fast detection of proteins in cells by immunoblotting, whole cell extracts were prepared. 1 OD_{600} unit of cells was resuspended in 500 µl Roedel mix (0.25 N NaOH, 140 mM β-mercaptoethanol, 3 mM PMSF and yeast specific protease inhibitor cocktail (TY, Serva)) and incubated on ice for 10 min. Proteins were precipitated with 13% (v/v) TCA for 10 min on ice and then pelleted by centrifugation at 4°C for 10 min at 14,000 rpm in a table-top centrifuge. The pellet was washed once with ice-cold acetone, before it was dried at 56°C and resuspended in Laemmli-buffer (125 mM Tris-HCl pH 6.8, 5% (w/v) sucrose, 2% (w/v) SDS, 2% (v/v) β-mercaptoethanol, 0.005% (w/v) bromphenol-blue).

2.2.6.2 Determination of specific β-galactosidase activities

After two initial washing steps with sterile water, 20-50 OD_{600} units of cells were resuspended in 0.5 ml 50 mM potassium phosphate buffer (pH 7.0) and 0.5 g of

glass beads were added. Cells were mechanically broken for 10 min on an “IKA-Vibrax-VXR” at 4°C. The broken cells were centrifuged at 4°C with 13,000 rpm for 10 min in a microfuge. The supernatant was transferred to a new tube and used as crude extract for further determinations.

To determine the specific β-galactosidase activities, 950 µl of preheated (30°C) LacZ buffer (60 mM Na_2HPO_4, 40 mM NaH_2PO_4, 10 mM KCl, 1 mM $MgSO_4$, 1 mg/ml ONPG, pH 7.0), were mixed with 50 µl of crude extract and incubated at 30°C until the colourless solution turned yellow. The reaction was stopped by the addition of 500 µl 1 M Na_2CO_3, and the absorbance of the samples was measured against a blank at 420 nm (Shimadzu UV mini 1240 photometer). The specific β-galactosidase activity was calculated from the measured absorption according to the equation.

2.2.6.3 Co-immunoprecipitation

The preparation of crude extracts for co-immunoprecipitation was basically as described in 2.2.6.2 besides the following differences: 100 OD_{600} units of cells were harvested to yield higher final protein concentrations. Cells were broken in 1 ml of a specific lysis buffer supplied with “µMACS GST Tagged Protein Isolation Kit” (Miltenyi Biotec, Bergisch-Gladbach). Broken cells were centrifuged at 4°C at 300g for 3 min. The supernatant represented the crude extract and was transferred to a new tube for the precipitation. Protein extracts were incubated for 1 hour on ice with the magnetic beads, which are coupled to an anti-GST antibody, to precipitate the fusion proteins. The magnetic beads with the precipitated proteins were separated from the residual crude extract with the help of “MACS Separation Columns” clamped into a magnetic “MACS Multi Stand”. Unspecifically bound proteins were removed by extensive washing with the supplied buffers before GST-fusion proteins were eluted from the beads with the supplied elution buffer pre-heated to 95°C.

2.2.6.4 Subcellular fractionation

60 OD_{600} units of cells were harvested and used to prepare spheroblasts. To this end, cells were resuspended in 1 ml DTT solution (0.1 M Tris-HCl pH 9.4, 10 mM DTT) and incubated at 30°C for 10 min to reduce disulfide bonds in cell wall proteins. The cells were then pelleted and resuspended in spheroblast buffer (16% (v/v) YEPD, 50 mM potassium-phosphate buffer pH 7.4, 0.6 M sorbitol) before the addition

of 100 µg Zymolyase and the subsequent incubation in a 30°C water bath for 20 min. After another centrifugation step for 3 min at 1.500 g, cells were lysed by the resuspension in lysis buffer (20 mM Hepes-KOH pH 6.8, 50 mM KAc, 0.2 M Sorbitol, 2 mM EDTA, 1 mM PMSF, 1 mM DTT and yeast specific protease inhibitor cocktail (TY, Serva)) and subsequent incubation steps on ice for 5 min followed by 2 min at 30°C. The crude extract was collected by pelleting cell debris and unlysed cells at 300 g for 3 min.

For the fractionation of cell components, one half of the crude extract was removed ("total") and the other half was subjected to differential centrifugation. The pellet of the first centrifugation step for 15 min at 13,000 g was designated as the P13 fraction, containing heavy membranes like those from vacuoles, the plasma membrane, and nuclei. The supernatant was again centrifuged at 100,000 g for 60 min. The resultant P100 pellet contained the light membranes including transport vesicles, in addition to large protein complexes. The supernatant formed the S100 fraction with the cytoplasmic content of the cell.

2.2.6.5 Quantification of protein concentrations

The protein concentration of the crude extracts was determined by the method of (Bradford, 1976). Therefore, the "Protein Assay" from Bio-Rad Laboratories (Munich, Germany) was used, according to the manufacturers' instructions. The absorbance was measured against a blank at 595 nm (Shimadzu UV mini 1240 photometer). Using a conversion factor (obtained with BSA as a standard) the absorbance values were converted to protein concentrations in mg/ml.

2.2.6.6 Separation of proteins via SDS-PAGE

The separation of proteins according to their molecular weight was performed as described previously (Shapiro *et al*., 1967). The stacking gels contained a 3% (v/v) acrylamide solution, the concentrations of the separation gels varied between 7.5 and 12.5% (v/v), depending on the sizes of the proteins of interest. Ready to use acrylamide solutions (37.5:1) were purchased from Roth (Karlsruhe).

2.2.6.7 Silver staining of proteins

Proteins in SDS gels were visualized by silver staining as described previously (Rabilloud *et al*., 1988).

2.2.6.8 Immunoblotting

The transfer of proteins from SDS gels to nitrocellulose membranes was performed with the “Trans-Blot SD Semi-Dry Electrophoretic Transfer Cell” (Bio-Rad Laboratories, Munich, Germany) according to the manufacturers’ instructions. After the transfer, membranes were blocked with TBST (50 mM Tris-HCl pH 8.0, 150 mM NaCl, 0.05% (v/v) Tween 20) supplemented with 3% (w/v) BSA. To visualize proteins on the membranes, specific antisera were employed. All antisera and secondary antibodies were used at the concentrations indicated in Tab. 1 in TBST with 3% (w/v) BSA. The incubation was performed for one hour at room temperature or at 4°C over night. Residual unbound antibodies were removed by five washing steps with TBST. The detection of the fluorescent secondary antibodies was performed after a final washing step with TBS with an “Odyssey Infrared Imaging System” (Li-Cor, Lincoln, USA).

2.2.6.9 Preparation of proteins from *E. coli*

For the preparation of proteins for subsequent purification from *E. coli*, 200 ml of logarithmically growing cells induced for 4 hours with 100 µM IPTG were pelleted by centrifugation and resuspended in 4 ml PBS (137 mM NaCl, 2.7 mM KCl, 10 mM Na_2HPO_4, and 2 mM KH_2PO_4) supplemented with 1 µM AEBSF. Cells were lysed by sonication in a “Branson Digital Sonifier 250D” in three 10 second long intervals interrupted by 10 seconds breaks. The crude extracts were cleared from cell debris and unbroken cells in three centrifugation steps at 14,000 rpm for 10 min at 4°C.

2.2.6.10 Affinity-chromatography for the purification of GST fusion proteins

The purification of GST-tagged proteins was performed on “GSTrap HP Columns" (GE Healthcare) with an “Äkta FPLC” system (Amersham Biosciences), following the manufacturers’ instructions.

2.2.6.11 *In vitro* lipid binding assay

The lipid binding properties of proteins were investigated by using “PIP strips” (Molecular Probes). Strips were treated as suggested in the manufacturers’ instruction and incubated with 50 ng/ml of protein at 4°C over night. Unbound protein was removed by extensive washing with TBST, before immunodetection was performed as described in 2.2.6.8.

2.2.7 Cell imaging and microscopy

2.2.7.1 Microscopical setting

For microscopical analyses, an “Axioplan2” microscope with “Plan-Apochromat 100x/1.45 NA Oil DIC” objectives (Carl Zeiss AG, Feldbach, Switzerland) and the appropriate filter sets (Chroma, Rockingham, USA) was used. The additional light source for fluorescent imaging was a 100 W HBO lamp (OSRAM AG, Augsburg, Germany). The camera shutter was controlled by a “MAC200” (LUDL, Hawthorne, USA) which was synchronized with the cooled charged-coupled device camera “CoolSNAP HQ” (Roper Scientific, Tucson, USA). The microscope was operated with “MetaMorph v6.2” software (Universal Imaging Corporation, Downington, USA).

2.2.7.2 Image acquisition and processing

For standard microscopic observation, cells were grown to early logarithmic phase in SC medium or in rich medium, which required an additional washing step with PBS prior to examination. Brightfield images were acquired as single planes using differential-interference-contrast (DIC). All fluorescence images were from single focal planes and scaled using MetaMorphs “Scale Image” command. For co-localization studies, the processed images were merged using MetaMorphs “Overlay” function.

2.2.7.3 Time-lapse microscopy and the creation of kymographs

To perform time-lapse microscopy, cells were spread on an agarose matrix (SC medium with 4% (w/v) glucose and 0.05% (w/v) agarose) contained on the cavity of a

special time-lapse microscope slide. The microscope was focused on a dividing cell or a group of dividing cells, and set to make brightfield followed by fluorescence images, when required. For the observation of cellular growth by bright field microscopy, pictures were taken every 30 min. For the observation of protein dynamics at the bud neck by detection of GFP- or mCherry- fluorescence signals, images were acquired every two minutes. Rectangles were placed over the bud neck regions and MetaMorphs “Create Kymograph” function was used to align the signals.

2.2.7.4 Actin and chitin staining

For the visualization of the actin and chitin distribution, 4 OD_{600} units of cells from an early logarithmic culture were fixed by the addition of 4% (v/v) formaldehyde and prolonged incubation for one hour. Cells were washed twice with PBS and resuspended in 50 µl PBS before 2.5 µl rhodamine-phalloidin (200 U/ml) and 2.5 µl 1% (v/v) Triton X-100 were added. Cells were incubated with the dye for 30 min on ice in the dark and washed three times with PBS. For the additional chitin staining, cells were incubated for 5 min with 1 µl Calcofluor white (200 µg/ml) and washed again three times prior to microscopic examination.

3 Results

3.1 Phenotypes of *inn1* mutants

Mutations in the open reading frame *INN1 (YNL152W)* were previously identified in this laboratory in a genetic screen designed to isolate negative regulators of the CWI pathway. To address the question of the molecular function of the protein encoded by the open reading frame, different mutants were employed, starting with the confirmation of the lethal phenotype assigned in a previous Ph.D. thesis (Ciklic, 2007) to the deletion in the yeast strain generally utilized in our group and in genome-wide analyses within a different genetic background (SGD database).

3.1.1 *INN1* is an essential gene

To delete the *INN1* gene from the genome of the diploid yeast strain DHD5, a PCR-based, one-step gene deletion method via homologous recombination was used (Longtine *et al*., 1998). For this purpose, a cassette containing the selectable *SpHIS5* gene was amplified from the vector pFA6a-His3MX6 using the oligonucleotides 05.133 and 07.228, which added homologous regions of *INN1* to either end of the deletion cassette. The resultant PCR product was transformed into the diploid yeast strain DHD5. Transformants were selected for histidine-prototrophy and strains carrying the expected substitution were confirmed by PCR with two different primer combinations to produce DNA fragments of the expected lengths (Fig. 3.1A).

The strain with the heterozygous *inn1* deletion was sporulated and subjected to tetrad analysis on YEPD. Only a maximum of two segregants out of 36 tetrads separated produced viable colonies and none of the viable segregants was prototrophic for histidine, as expected for the deletion of an essential gene (Fig. 3.1B). To test whether *INN1* is required for the initial germination of the spores or for later stages during colony formation, the microcolonies produced by the non-viable spores were examined by light microscopy. Clearly, all spores were able to germinate, but arrested growth after 5-10 cell cycles. Some tube-like structures could be observed in the microcolonies, indicating a failure of the daughter cells to separate from their mothers (Fig. 3.1C).

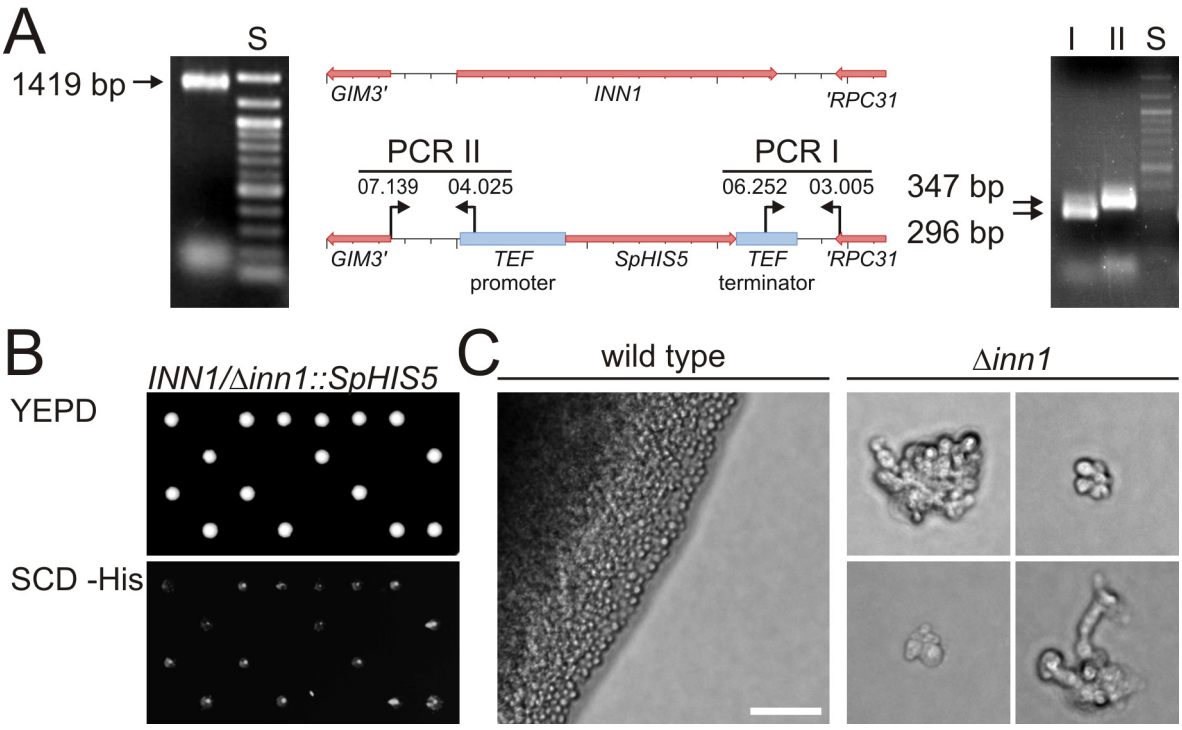

Fig. 3.1: *INN1* is an essential gene. A. The *inn1::SpHIS5* deletion cassette was amplified from pFA6a-His3MX6 with the oligonucleotides 05.133 and 07.228. The expected size of the PCR product was confirmed in a 1.5% agarose gel with the 100 bp DNA ladder from NEB as size marker (left picture). The PCR product was transformed into the diploid wild-type strain DHD5. The lower map in the middle schematically shows the substitution of the *INN1* locus by the deletion cassette. The arrows mark the binding sites of the two oligonucleotide pairs used to control the correct integration of the cassette. The agarose gel on the right shows the correct sizes of the PCR products together with the 100 bp DNA ladder from NEB as size marker. **B.** Tetrads of strain DAJ24 with the heterozygous *inn1* deletion were dissected on YEPD (upper panel) and replica-plated on media lacking histidine (lower panel). **C.** Micrographs of non-viable segregants of strain DAJ24 carrying the *inn1* deletion were obtained (right panels) and compared to a wild-type segregant (left panel). All micrographs were obtained with the same magnification and the scale bar represents 20 µm.

3.1.2 Downregulation of *INN1* gene expression leads to cell division defects

To investigate the effect of a lack of Inn1 on cell morphology, the native *INN1* promoter was replaced by the conditional *GAL1* promoter (Fig. 3.2A), again by using the PCR-based one-step gene replacement, as described above in the context of *inn1* deletions. For this experiment, the oligonucleotides 04.113 and 05.077 were used with pFA6a-His3MX6-PGAL1 as a template. Segregants with the *GAL1p-INN1* construct lacked the ability to produce colonies on media containing glucose. Since the *GAL1* promoter is repressed under these conditions, this finding confirms the essential cellular function of Inn1 suggested by the deletion phenotype. On the other hand, overexpression of *INN1*, provoked by growth on galactose as a sole carbon source, did not affect the colony-forming ability (Fig. 3.2B).

Next, a depletion experiment was performed. Haploid cells harbouring the *GAL1p-INN1* construct were initially grown to early logarithmic phase in rich medium containing galactose as carbon source. Under these inducing conditions, the *GAL1* promoter governs a high-level expression of *INN1*, allowing for normal cell growth. In order to repress *INN1* gene expression, cells were then harvested and resuspended in glucose medium. The following cell divisions were monitored microscopically at intervals of one hour. After approximately four hours of growth under such repressing conditions, clear morphological changes became apparent: Cells failed to separate and formed either large clusters and/or showed a tubular appearance. After 16 hours, representing about 10 consecutive cell cycles, substantial cell lysis could be observed (Fig. 3.2C).

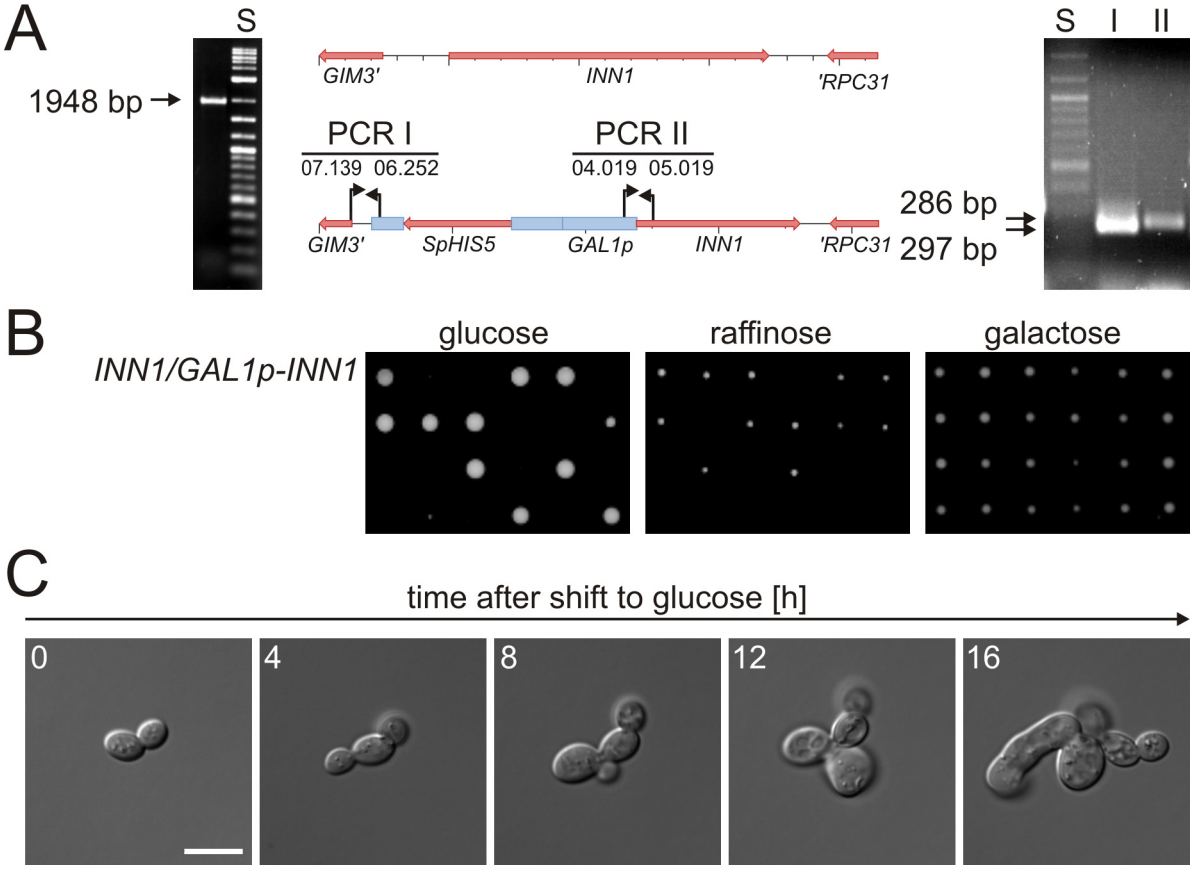

Fig. 3.2: Downregulation of INN1 gene expression leads to defects in cell division. A. The *SpHIS5-GAL1p* cassette was amplified from pFA6a-His3MX6-pGAL1 with the oligonucleotides 04.113 and 05.077. The expected size of the PCR product was confirmed in a 1.0% agarose gel with the 2 log DNA ladder from NEB as size marker (left picture). The PCR product was transformed into the diploid wild-type strain DHD5. The lower map in the middle schematically shows the integration of the promoter cassette at the *INN1* locus displayed above. The arrows mark the binding sites of the two oligonucleotide pairs used to control the correct integration of the cassette. The PCR products together with the 100 bp DNA ladder from NEB as size marker were separated in a 1.5% agarose gel to control correct sizes (upper right picture). **B.** Tetrads of strain DAJ23 with the heterozygous *GAL1p-INN1* construct were dissected on rich media supplemented with the three different carbon sources as indicated. **C.** Growth of a single cell of segregant HCB07 harbouring the *GAL1p-INN1* construct obtained from strain DAJ23 was followed under repressing conditions in the presence of glucose by live cell imaging for 16 hours. The scale bar represents 5 µm.

3.1.3 Depletion of Inn1 by induced protein degradation leads to cytokinesis defects

Studies like those described above with a conditional *GAL1* promoter may have some pitfalls: i) promoter leakage could allow a basal-level expression of the gene of interest and ii) the mRNAs and proteins formed under the non-repressed growth conditions could be quite stable and thus may obscure the observation of the immediate effects of protein depletion. Thus, in order to confirm the results obtained above by promoter regulation, the temperature-sensitive degron system was applied to more readily study the effects of protein depletion (Sanchez-Diaz *et al*., 2008). The principle is shown in Fig. 3.3A. A temperature sensitive allele encoding the dihydrofolate-reductase from mice was amplified from strain inn1-td with the oligonucleotides 03.007 and 03.043 and inserted by homologous recombination at the 5'-end of *INN1* to obtain strain HAJ62-B. At 25°C this fusion does not affect cell growth. However, a shift to the restrictive temperature of 37°C causes a conformational change in the dihydrofolate-reductase, which leads to the exposure of two lysine residues. These become accessible for ubiquitylation and subsequent degradation of the entire fusion protein by the proteasome. The expression of this *inn1-td* fusion gene is additionally controlled by the repressible *CUP1* promoter, whose expression is shut down at low medium copper concentrations. Moreover, the ubiquitin ligase Ubr1 is concomitantly overexpressed for efficient degradation of the DHFR-Inn1 fusion protein.

To confirm that the fusion protein in the *inn1-td* strain (HAJ62-B) is fully functional, it was first tested for its growth in a drop dilution assay. As expected, the *inn1-td* strain grows normally under permissive conditions and fails to grow under restrictive conditions, i.e. at 37°C upon overexpression of *UBR1* (Fig. 3.3B). A control strain, which only overexpresses *UBR1* (HAJ17-B), also shows slight growth impairment under restrictive conditions, but no apparent changes in cell morphology as compared to a wild-type strain (Fig. 3.3B and data not shown).

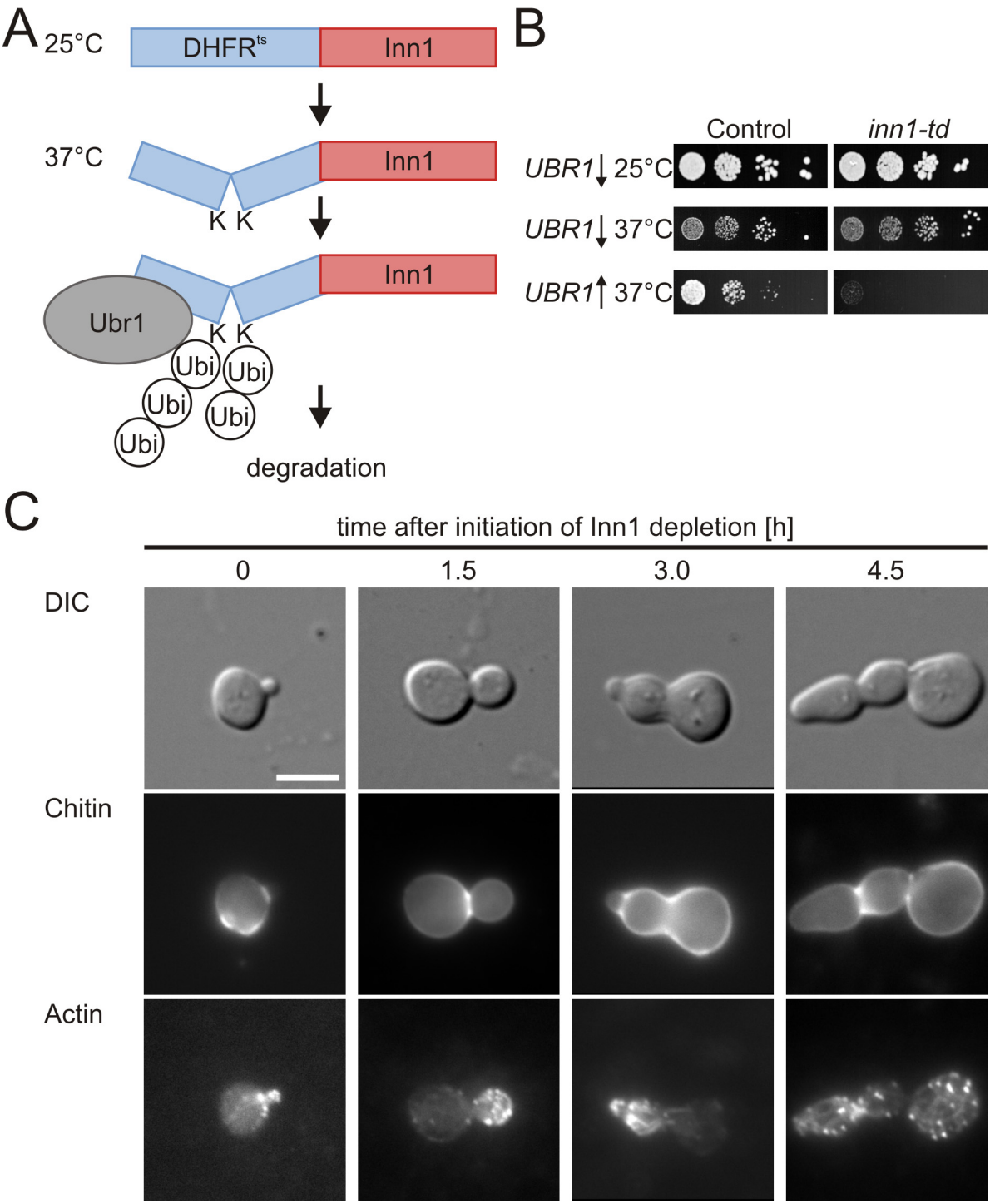

Fig. 3.3: Depletion of Inn1 causes defects in primary septum formation. A. Schematic representation of the temperature-sensitive degron system (see text for details). **B.** The *inn1-td* strain (HAJ62-B) was tested and compared to a control strain (HAJ17-B) in a drop dilution assay as described in section 2.2.3. The cells displayed in the upper panels were incubated at 25°C on rich medium in the presence of raffinose supplemented with 100 µM $CuSO_4$. Cells in the middle panels were incubated on the same medium but at 37°C, and the cells in the lower panel were incubated at 37°C on rich medium with galactose. **C.** Cells from the *inn1-td* strain HAJ62-B were incubated at 37°C with low copper concentrations to induce the depletion of Inn1 and fixed at the indicated time points. Fixed cells were stained for actin and chitin as described in section 2.2.7.4. The panels in the upper row show the DIC images of a single growing cell. The micrographs in the middle row display the corresponding chitin fluorescence picture obtained with the DAPI filter and the pictures in the lower row show the corresponding actin stain obtained with the DsRed filter after treatment of fixed cells with rhodamine-phalloidin. The scale bar represents 5 µm.

To investigate the morphological defects caused by a loss of Inn1 in further detail, cells were examined under the microscope using different staining techniques. The cell separation defects observed in 3.1.2 could be due to a failure in the organization of the actin cytoskeleton, which can be visualized with a rhodamine-phalloidin staining of cellular actin. Alternatively, there could be a defect in the formation of the chitinous primary septum, which can be visualized with the chitin-binding agent Calcofluor white. As shown in Fig. 3.3C, the actin distribution was not affected upon depletion of Inn1. The cell cycle-dependent polarization of the actin patches and cables, as well as the formation of the actin ring, were apparently normal in cells examined at different growth stages. In contrast, the chitin staining revealed a pronounced failure to close the primary septum between mother and daughter cell.

3.2 Subcellular localization of Inn1

The subcellular localization of an uncharacterized protein may provide valuable hints to its cellular function. In a first step, subcellular fractionations can be employed to investigate whether a protein is cytoplasmic or associated to membranes, organelles or large proteinaceous structures. In addition, its subcellular localization in living cells can be directly followed by fusion of the protein of interest to the green-fluorescent protein (GFP).

3.2.1 Inn1 resides in the high speed pellet fraction

Strain HAJ22-A which produces an Inn1-3HA fusion protein controlled by its native *INN1* promoter was obtained by *in vivo* recombination of a 3HA-tagging cassette (amplified from the vector pFA6a-3HA-KanMX6 with the oligonucleotides 05.133 and 05.134) at the *INN1* locus. For subcellular fractionation, crude extracts obtained from the resulting strain HAJ22-A were separated by differential centrifugation, to give rise to the heavy membrane and nuclei fraction (P13), the fraction containing lighter membranes and large protein complexes (P100), and the cytoplasmic fraction (S100). As a control for proper fractionation, all samples were tested in a Western blot analysis with antibodies against the pentose phosphate pathway enzyme transketolase (Tkl1) and the vacuolar ATPase subunit Vma6. As expected, Tkl1 mainly resides in the cytoplasmic S100 fraction, whereas Vma6 is primarily detected in the heavy membrane fraction P13. Interestingly, the Inn1-3HA fusion protein

resides almost exclusively in the P100 fraction. This indicates that it is associated either with a large protein complex or with light membranes, such as transport vesicles (Fig. 3.4A).

3.2.2 Inn1 localizes at the bud neck during cytokinesis

To further investigate its subcellular localization *in vivo*, a C-terminal Inn1-GFP fusion was obtained as described in 3.2.1 for the 3HA-tagged strain (pFA6a-GFP(S65T)-KanMX6 was used as template in conjunction with the oligonucleotide pair 05.133/05.134). Cells from strain HAJ28-A expressing this GFP-fusion protein from the *INN1* locus are viable and show wild-type cell morphologies. Thus, the fusion protein appears to be fully functional. Cells were grown to early logarithmic phase in synthetic complete media and examined by fluorescence microscopy. A prominent fluorescence signal could be detected for a short period at the bud neck between mother and large daughter cells. There, Inn1-GFP formed a ring-like structure with varying diameters in different cells (Fig. 3.4B).

Next, cell growth was synchronized in order to determine the exact timing of Inn1 recruitment to the bud neck. For this purpose, cells from strain HAJ28-A described above were arrested in the G1-phase of the cell cycle by the addition of the mating pheromone alpha-factor. After the arrest, cells were washed, incubated in fresh medium and quantified for the percentage of cells with Inn1-GFP at the bud neck under the fluorescence microscope every 10 minutes. The first specific Inn1-GFP signals could be observed 60 minutes after the release from alpha-factor arrest. The frequency of cells with Inn1-GFP signals peaked after 80 minutes of incubation, with a maximum of 26% of the total cell population. This comparatively low value indicates that the culture was not perfectly synchronous. Nevertheless, Inn1 localization to the bud neck is clearly cell cycle dependent.

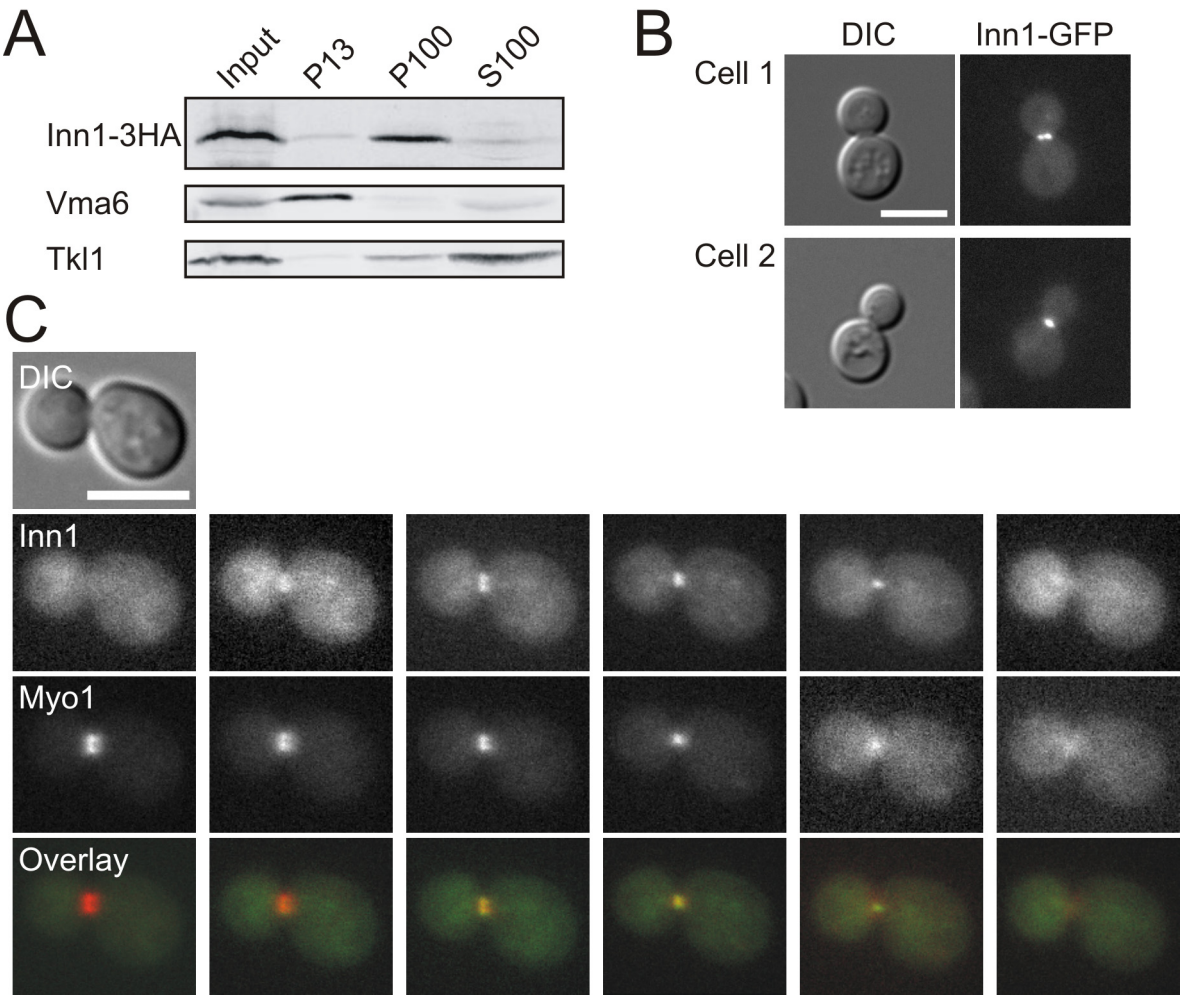

Fig. 3.4: Inn1 co-localizes with the contractile ring during cytokinesis A. Cells from strain HAJ22-A expressing Inn1-3HA were subjected to subcellular fractionation as described in 2.2.6.4. The upper panel represents the Inn1-3HA fusion protein, reacting with an anti-HA antiserum. As controls, the fractions were additionally probed with an anti-Vma6 (middle panel) and an anti-Tkl1 antiserum (bottom panel). **B.** Cells from strain HAJ28-A expressing Inn1-GFP were investigated under the fluorescence microscope. Micrographs of two different cells are shown with the DIC images in the left panels and the corresponding fluorescence pictures obtained with the FITC/GFP filter in the right panels. The scale bar represents 5 µm. **C.** A large budded cell from strain HAJ96-A expressing Inn1-GFP and Myo1-mCherry was observed in live cell imaging. The panels at the very left display from top to bottom the cell in DIC optics, the corresponding fluorescence picture representing Inn1-GFP obtained with the FITC/GFP filter, the micrograph representing Myo1-mCherry obtained with the DsRed filter, and an overlay of the two fluorescence images. The panels to the right display the corresponding pictures, which were acquired in two minutes time intervals. The scale bar represents 5 µm.

Since the localization of Inn1-GFP is strongly reminiscent of the localization of the cytokinetic actin ring (CAR), a red-fluorescent mCherry-protein was fused to the carboxy-terminal end of the CAR constituent protein Myo1 again by *in vivo* recombination (oligonucleotides 07.102 and 07.153 with pAJ001 as template). Myo1 belongs to the type II myosins and forms a contractile actomyosin ring together with actin during cytokinesis. Myo1 localizes to the division site early in the cell cycle and remains there as a ring with a constant diameter until actin is incorporated and the

CAR begins to constrict (Bi *et al*., 1998; Lippincott and Li, 1998b). At the completion of CAR constriction, the cytokinetic apparatus is disassembled and the Myo1 signal vanishes. Interestingly, Inn1-GFP co-localizes with Myo1 from the beginning of CAR constriction until the disassembly of the ring in a strain expressing both fusion proteins (HAJ96-A), indicating a role of Inn1 in cytokinesis confined to the late mitotic anaphase (Fig. 3.4C).

3.2.3 Inn1 is not a target of the anaphase-promoting complex

In the deduced amino acid sequence of Inn1, residues 142 to 150 display a high similarity to a putative destruction box (DB; Fig. 3.5A). The latter is thought to function as a recognition motif for the anaphase promoting complex (APC), which regulates cell cycle progression by specific degradation of target proteins at specific stages (Zachariae and Nasmyth, 1999). Therefore, the functional significance of the DB motif for the Inn1 protein was investigated.

For this purpose, an integrative plasmid encoding *INN-GFP* (pAJ056) was created. In order to delete the putative DB via inverted PCR, a corresponding fragment of *INN1* was subcloned into a smaller vector (pAJ057). The mutated gene fragment was introduced back into pAJ056 to express a complete Inn1-GFP fusion protein lacking the putative internal DB (pAJ059). Both plasmids were linearized in the *URA3* gene and integrated into the *ura3-52* locus of strain DAJ24, which also contains a heterozygous *INN1/inn1* deletion. The two strains with either one of the integrated plasmids were subjected to tetrad analysis and spores were dissected on complete media. Whereas the *INN1-GFP* fusion gene encoded on the integrated pAJ056 could fully complement the *inn1* deletion, the mutated *INN1ΔDB-GFP* fusion gene from pAJ059 did not complement at all (Fig. 3.5B).

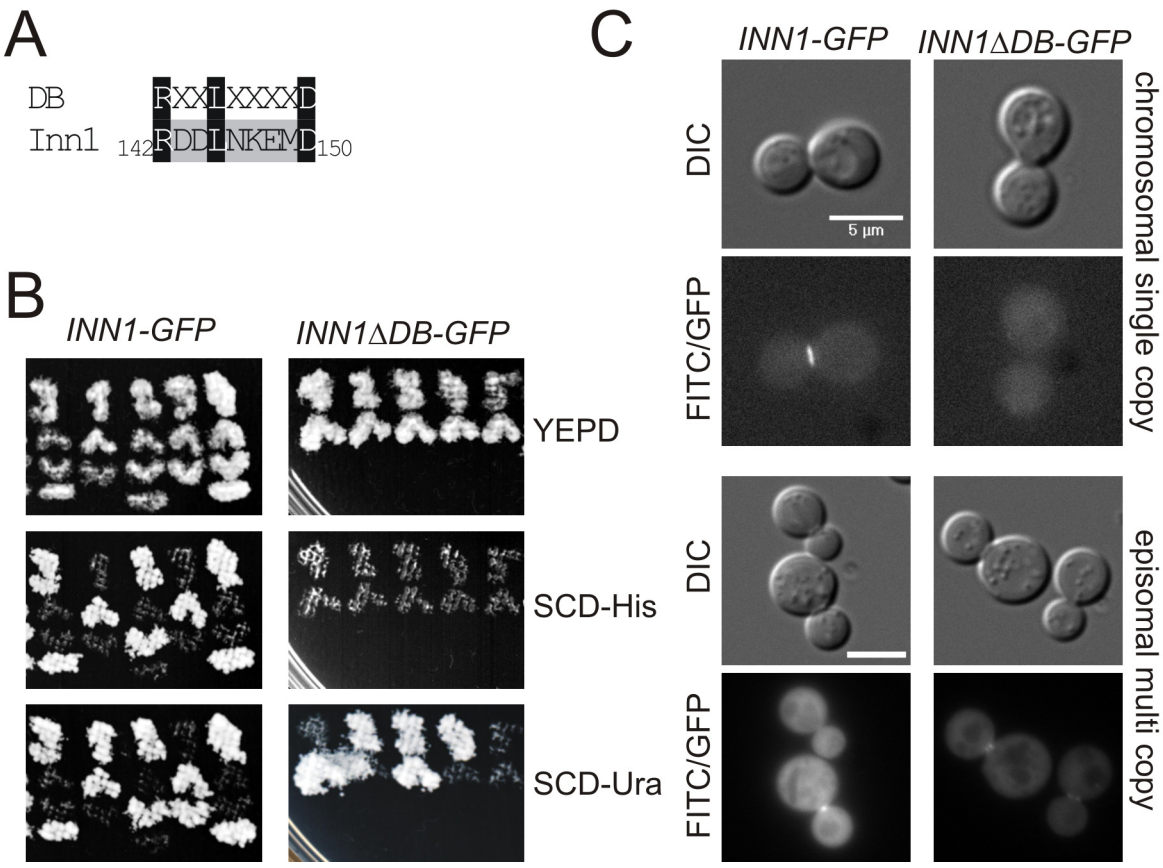

Fig. 3.5: Deletion of the putative destruction box of Inn1 influences protein stability. A. Alignment of amino acids 142 to 150 of Inn1 compared to the consensus sequence of a destruction box (DB). Amino acids matching the consensus sequence are highlighted in black, X represents any amino acid. **B.** Tetrads from strain DAJ24 with integrated copies of pAJ056 (*INN1-GFP*; left panels) or pAJ059 (*INN1ΔDB-GFP*; right panels) were dissected on YEPD. Masterplates were created and replica-plated onto media lacking either histidine or uracil, as indicated. **C.** Segregants expressing *INN1* from the native locus and additionally *INN1-GFP* or *INN1ΔDB-GFP* from the integrated plasmids obtained from (B) were investigated by fluorescence microscopy. The left panels in the upper half display DIC and FITC/GFP-fluorescence micrographs from a large-budded cell with Inn1-GFP at the bud neck. The panels on the right display the corresponding pictures of a cell with the same bud size, but without a fluorescence signal at the bud neck. Cells expressing *INN1* from the native locus and additionally *INN1-GFP* or *INN1ΔDB-GFP* from the multicopy plasmids pAJ066 or pAJ067 were also investigated by fluorescence microscopy as indicated. The scale bar represents 5 µm.

Segregants expressing wild-type *INN1* from the native locus and additionally the plasmid-born copies of *INN1-GFP* were investigated by fluorescence microscopy. Inn1-GFP could be detected at the mother-bud necks of large-budded cells as described in 3.2.2, but no signal for Inn1-GFP lacking the DB could be found in more than 200 cells observed from every cell cycle stage (Fig. 3.5C). In a next step, *INN-GFP* and the mutated *INNΔDB-GFP* were subcloned into an episomal multicopy vector to test whether the loss of function of the DB mutant could be suppressed by increasing the gene dosage. Interestingly, *INNΔDB-GFP* expressed from the multicopy plasmid could suppress the *inn1* deletion and could also be detected at the bud neck. Nevertheless, the fluorescence intensity of cells expressing the mutated

Inn1-GFP fusion protein was decreased in comparison to cells expressing the wild type fusion protein.

To assess the importance of the putative DB box for the stability of Inn1 in more detail, the suspected relation to the APC complex was further investigated. According to literature data, the overproduction of the two regulatory APC subunits - Cdc20 and Cdh1 - is lethal because of an increased complex activity. In order to test whether Inn1 is a target of the APC, one copy of either *CDC20* or *CDH1* were placed under the control of the *GAL1* promoter in a diploid strain, which also expressed Inn1-3HA from its native chromosomal locus. Overexpression of either of the two APC subunits was confirmed using GFP-fusions (Fig. 3.6C) and GFP-specific antibodies in a Western blot (Fig. 3.6B). Clearly, both Cdc20-GFP and Cdh1-GFP could be overproduced, resulting in different terminal phenotypes. With the non-tagged constructs, overproduction of Cdc20 caused a complete growth arrest, whereas the overproduction of Cdh1 resulted in a defect in cytokinesis and cell separation, forming long chains of cells (Fig. 3.6A). Nevertheless, the amounts of Inn1-3HA determined in a Western blot remained similar in either overexpression strain (DAJ83 and DAJ84) as compared to the wild-type (DAJ26; Fig. 3.6D). It should be noted, that the concentration of Inn1-3HA was considerably lower in all strains when cells were grown on galactose as a sole carbon source, as compared to glucose media.

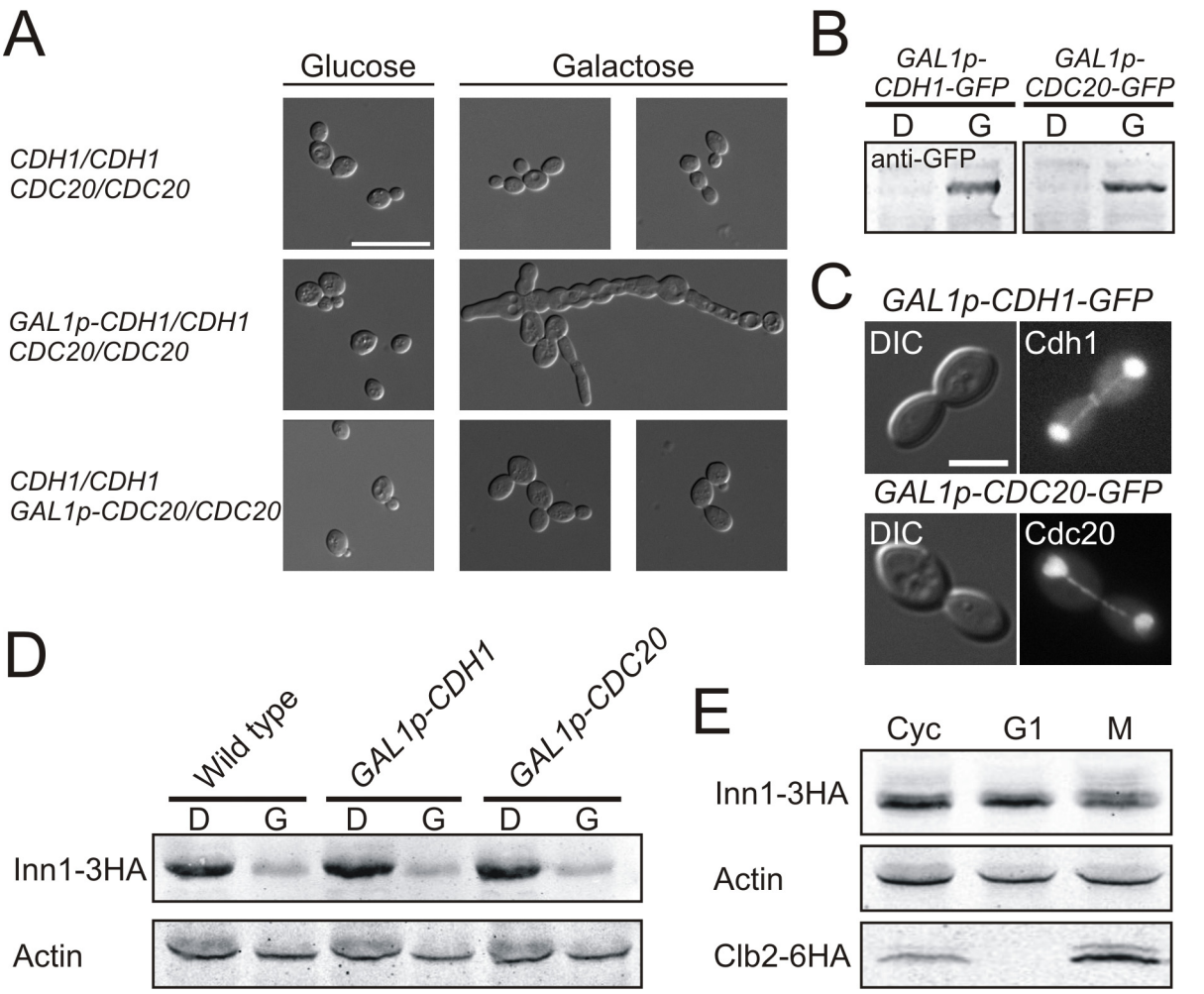

Fig. 3.6: Inn1 is not a target of the APC but post-translationally modified during mitosis. A. Cells from the diploid strain DAJ26 (homozygous for *INN-3HA*) and strains DAJ27 and DAJ28, which are additionally heterozygous for *GAL1p-CDH1* or *GAL1p-CDC20*, respectively, were grown overnight in media containing glucose or galactose. Micrographs of representative cells are shown. The scale bar represents 10 µm. **B.** Cells from strains DAJ106 and DAJ107 (heterozygous for GFP-tagged Cdc20 or Cdh1, respectively, each under the control of the *GAL1* promoter) were pregrown to early logarithmic phase in rich media containing glucose and then equally divided for further incubation in rich media with either glucose (D) or galactose (G) for four hours. Crude extracts from 1 OD_{600} unit each were prepared and treated with a GFP-specific antiserum. **C.** Cells from B. were incubated as described above and cells grown in galactose were examined by fluorescence microscopy. DIC and the corresponding fluorescence pictures obtained with the FITC/GFP filter are shown. The scale bar represents 5 µm. **D.** Cells from the strains described in A. were incubated as described in B. before crude extracts of 2 OD_{600} units each were prepared and probed with an HA antiserum. **E.** Cells from strain HAJ22-A (expressing Inn1-3HA) were grown in rich medium with glucose as a carbon source and arrested as described in section 2.2.4. Crude extracts of 2 OD_{600} units from untreated early logarithmic cells (Cyc) or cells arrested in G1- or M- phase were prepared and probed with an HA-specific antiserum (upper panel). An actin antiserum was used as a control for equal loading amounts shown in the middle panel. Strain HAJ125-A expressing Clb2-6HA was treated accordingly, to confirm the validity of the method (bottom panel).

3.2.4 Inn1 is phosphorylated in mitosis

Given that Inn1 displays a cell cycle-dependent intracellular localization but is not a target of the APC, its intracellular concentration throughout the yeast cell cycle was determined. For this purpose, strain HAJ22-A, expressing Inn1-3HA as described in

3.2.1, was arrested at different stages of the cell cycle: Cells were arrested in G1-phase by the addition of mating pheromone alpha-factor, and in mitosis by nocodazole treatment. Total extracts from cells of an untreated control and from the two cultures of arrested cells were analysed for their Inn1-3HA concentration by Western blotting, employing an HA-specific antiserum. As a control, a strain producing the mitotic cyclin Clb2 tagged with a 6HA epitope was tested in parallel. As expected, a signal for Clb2-6HA could be detected in the untreated cycling cells. Since Clb2 is a target of the APC, no signal could be detected in the G1-arrested sample, but a strong accumulation of Clb2-6HA was observed for the cells arrested in mitosis (M-phase). In contrast, the overall amount of Inn1-3HA did not vary between the samples from the different cell cycle stages. However, a more diffuse smear with a tendency to higher molecular weight bands was observed for the sample arrested in mitosis (Fig. 3.6E). These higher molecular bands have been suggested to be caused by a hyper-phosphorylation of Inn1 (Nishihama *et al*., 2009).

3.3 Interactions of Inn1 with other cytokinesis regulators

The identification of physical protein-protein interactions is a valuable tool to gain insight into the molecular pathway, in which a protein could be involved. Furthermore, it can indicate how a protein is recruited to its cellular site of action. Several genome-wide interaction studies have been performed to identify such molecular networks in *S. cerevisiae* (e.g. by (Ito *et al*., 2001). Interestingly, a yeast two-hybrid screen revealed an interaction between Inn1 and the cytokinesis regulator Hof1, as well as with Sla1, a component involved in endocytosis. Since genome-wide two-hybrid analyses frequently yield false positive results, these findings had to be confirmed first. Indeed, a two-hybrid interaction between Inn1 and Sla1 could not be reproduced in this laboratory.

3.3.1 Inn1 interacts with Hof1 in a yeast two-hybrid assay

The complete open reading frames encoding *INN1* and *HOF1* were cloned into suitable yeast two-hybrid vectors and used to express fusion proteins with either the Gal4 DNA-binding or the Gal4 transcriptional activation domain. Plasmids and standard control vectors were introduced into strain PJ69-4A, a reporter strain which allows testing for possible interactions by its growth on different drop-out media

(James *et al*., 1996). Transformants were spotted onto selective media for plasmid maintenance and also onto media additionally lacking histidine or adenine, which indicate either weak or strong interactions between the two proteins, respectively. A strong interaction between Inn1 and Hof1 could be deduced from the good growth on all media (Fig. 3.7A).

In order to delimit the regions of interaction between the two proteins, several gene fragments were again cloned into the two-hybrid vectors. Inn1 contains three proline-rich motifs, which in other proteins have been shown to interact with SH3 domains (Ren *et al*., 2005). Since Hof1 contains a SH3 domain at its carboxy-terminal end, these regions were the most likely candidates responsible for the observed interaction. In fact, truncations lacking the SH3 domain of Hof1 failed to interact with Inn1, in contrast to the SH3 domain itself, which showed strong interaction. Accordingly, Inn1 truncations lacking the carboxy-terminal part with the proline-rich motifs did not interact with full length Hof1, whereas the carboxy-terminal part did (Fig. 3.7A).

The next question was, whether all three proline-rich motifs are required for the interaction with Hof1. To this end, additional carboxy-terminal truncations of Inn1 were tested in a yeast two-hybrid assay, using the specific β-galactosidase activities as a quantitative readout (Fig. 3.7B). Full length Inn1 showed the strongest interaction with Hof1, with β-galactosidase activities gradually decreasing with the consecutive removal of the proline-rich motifs. This indicates that all of these motifs additively contribute to the interaction with Hof1.

3.3.2 Inn1 physically interacts with Hof1

In the yeast two-hybrid assay, overproduction of the proteins of interest and their artificial redirection into the nucleus occasionally give rise false-positive interactions. Therefore a co-immunoprecipitation approach was used as an additional method to confirm the interaction between Inn1 and Hof1. In this technique, all proteins are produced at physiological levels as epitope fusions expressed from their native chromosomal loci and under the control of their native promoters. Inn1-GST is then precipitated from yeast crude extracts with GST-specific antibodies coupled to magnetic beads, and, in case of an interaction with Hof1-3HA, this protein should also be detectable in a Western blot with the precipitate probed with HA-specific antibodies. *Vice versa*, when Hof1-GST is precipitated from a cell extract, Inn1-3HA

should also be present in the precipitate. This was indeed observed (Fig. 3.7C), consistent with the results from the two-hybrid assays reported above. In summary, these observations provide strong evidence that Inn1 and Hof1 also interact *in vivo*.

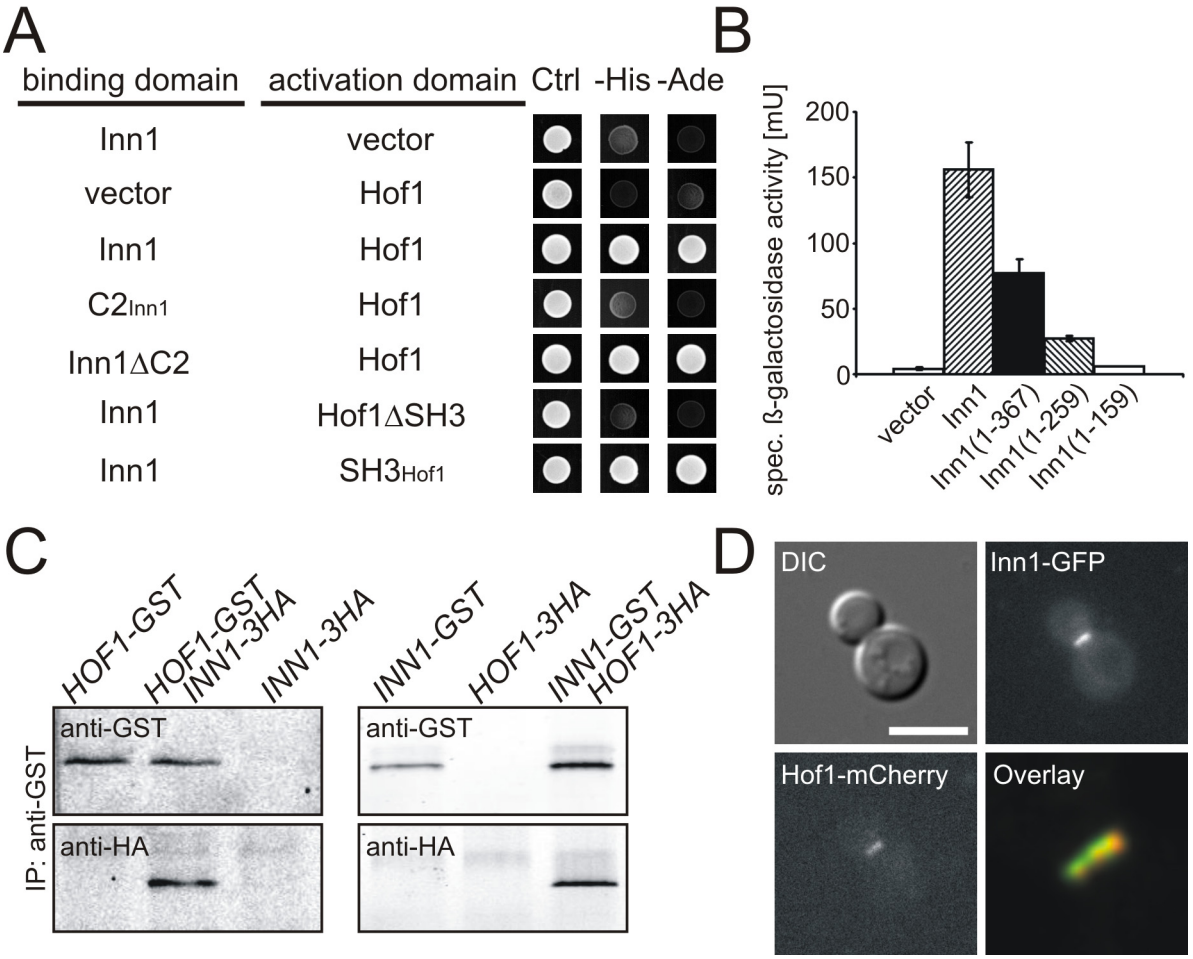

Fig. 3.7: Inn1 directly interacts with Hof1. A. The yeast two-hybrid strain PJ69-4A was used as a recipient for different combinations of plasmids encoding Gal4 DNA binding domain or Gal4 activation domain fusions (pAJ025 (Inn1), pAJ030 ($C2_{Inn1}$), pAJ063 (Inn1ΔC2) in conjunction with pAJ015 (Hof1), pAJ016 ($SH3_{Hof1}$), or pAJ009 (Hof1ΔSH3)). Double transformants were grown in selective media for plasmid maintenance over night and 6 µl each were spotted onto media lacking leucine and tryptophane (Ctrl) or additionally lacking histidine (-His) or adenine (-Ade). **B.** Strain PJ69-4A was transformed with truncated versions of the *INN1* construct as described in A. in conjunction with a plasmid carrying the SH3 domain of Hof1 fused to the Gal4 transcription activation domain. Specific β-galactosidase activities were determined from three independent double transformants, each, as described in 2.2.6.2. Combinations tested were (pAJ016 ($SH3_{Hof1}$) together with the empty vector pGBD-C2, and either pAJ025 (Inn1), pAJ027 (1-367), pAJ030 (1-259) or pAJ030 (1-159)) **C.** Strains HAJ46-B, HAJ52-A and HAJ22-A carrying gene fusions with the indicated tags were grown to early logarithmic phase and crude extracts prepared for co-immunoprecipitation as described in 2.2.6.3. Epitope-tagged proteins were precipitated with anti-GST magnetic beads and the precipitates were probed with anti-GST and anti-HA antisera (left panels). Strains HAJ23-B, HAJ41-A and HAJ27-B were also tested for co-immunoprecipitation as described above (right panels). **D.** Strain HAJ56-A was grown to early logarithmic phase in synthetic complete medium and investigated by fluorescence microscopy. Pictures of a single large-budded cell are shown acquired with DIC optics and the corresponding fluorescence pictures with the FITC/GFP and the DsRed filter detecting Inn1-GFP and Hof1-mCherry, respectively. An overlay of the two fluorescence images scaled up to 400% is shown to underline the co-localization of the two proteins. The scale bar represents 5 µm.

3.3.3 Inn1 co-localizes with Hof1

Further hints for a functional interaction of proteins *in vivo* can be obtained from their coincident spatial and temporal cellular localization. Therefore, strain HAJ56-A expressing both Inn1-GFP and Hof1-mCherry fusion proteins was obtained. Hof1 has previously been shown to localize in a ring-like structure at the bud neck during cytokinesis (Kamei *et al*., 1998; Lippincott and Li, 1998a). As evident from Fig. 3.7D, Inn1-GFP shows a similar localization during this stage of the cell cycle. Thus, the two proteins co-localize, supporting the notion that Inn1 and Hof1 physically interact with each other during yeast cytokinesis.

3.3.4 Identification of novel interaction partners for Inn1 by a yeast two-hybrid approach

Whereas Inn1 has been shown to be an essential protein, Hof1 is only essential for growth at an elevated temperature of 37°C. At 30°C, a *hof1* deletion displays only moderate defects in cytokinesis (Lippincott and Li, 1998a). Thus, Inn1 must also act on other effectors than Hof1 to account for the lack of viability upon its depletion. Given that Inn1 interacts with the SH3 domain of Hof1, one can assume that other interacting proteins would also contain such a domain. In *Saccharomyces cerevisiae*, 25 proteins with SH3 domains have been described, 11 of which have been related either to cytokinesis and/or to the organization of the actin cytoskeleton, which should be the most likely interaction partners of a cytokinesis regulator. Apart from Hof1 itself, these are Boi1, Boi2, Bem1, Bud14, Cdc25, Cyk3, Lsb3, Rvs167, Sla1 and Ysc84. DNA fragments encoding the SH3 domains of all these proteins were cloned into a yeast two-hybrid vector, to yield fusion proteins with the Gal4-activation domain. They were tested in combination with the full length Inn1 protein fused to the Gal4-DNA-binding domain. As shown in Fig. 3.8A, besides the SH3 domain of Hof1 used as a positive control, only the SH3 domain of Cyk3 mediated growth on medium lacking histidine. Among the tested candidate proteins, this indicates an interaction of Inn1 exclusively with Hof1 and Cyk3.

3.3.5 Inn1 interacts with Cyk3 in a yeast two-hybrid assay

To confirm this novel interaction of Inn1 with Cyk3, different truncations of both proteins were tested with the two-hybrid method. As expected, both full length

proteins interacted weakly, as deduced from growth of the respective transformants on medium lacking histidine. In contrast to the strong interaction of Inn1 with Hof1, no growth on adenine-free medium was observed. The interacting regions could be delimited to the SH3 domain of Cyk3 with the carboxy-terminal proline-rich motifs of Inn1 (Fig. 3.8B). All attempts to co-immunoprecipitate Inn1 with Cyk3, as exemplified for Hof1 in chapter 3.3.2, failed so far.

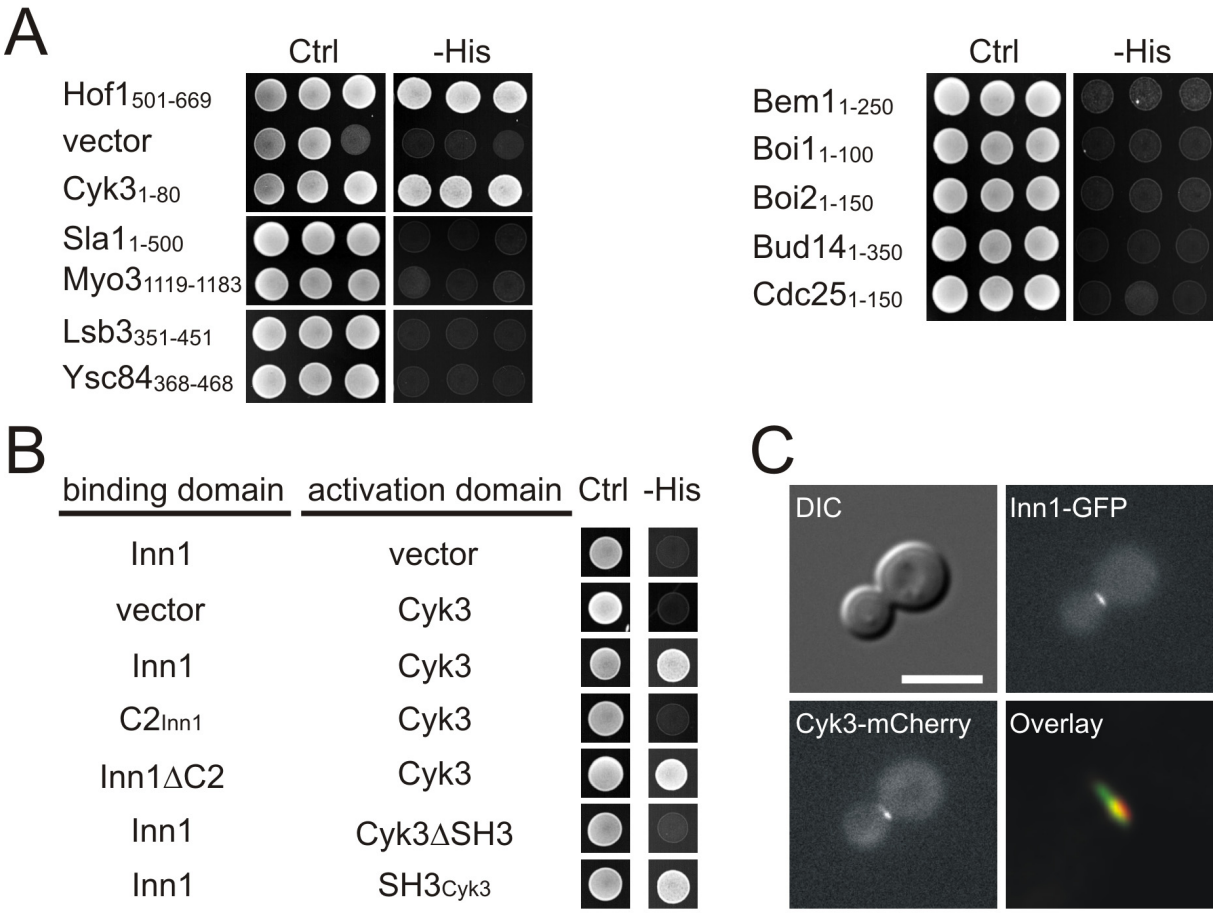

Fig. 3.8: Inn1 directly interacts with Cyk3. A. The yeast two-hybrid strain PJ69-4A was transformed with pAJ025 encoding Inn1 fused to the Gal4 DNA-binding domain together with different plasmids encoding SH3 domains of the proteins indicated fused to the Gal4 transcription activation domain. Plasmids used were the positive control pAJ016 (Hof1), the negative control pGAD424B (vector) or pAJ010 (Cyk3), pAJ005 (Sla1), pAJ007 (Myo3), pAJ061 (Lsb3), pAJ062 (Ysc84), pAJ014 (Bem1), pAJ011 (Boi1), pAJ012 (Boi2), pAJ008 (Bud14) and pAJ013 (Cdc25). Three independent double transformants of each combination were grown in selective media for plasmid maintenance over night before 6 µl each were spotted on media lacking leucine and tryptophane (Ctrl) or additionally lacking histidine (-His) **B.** Strain PJ69-4A was transformed with different combinations of plasmids encoding Gal4 DNA-binding domain or activation domain fusions and one double transformant each was spotted onto the indicated media as described in A. (pAJ025 (Inn1), pAJ030 ($C2_{Inn1}$) or pAJ063 (Inn1ΔC2) together with pAJ017 (Cyk3), pAJ010 ($SH3_{Cyk3}$) or pAJ018 (Cyk3ΔSH3)). **C.** Strain HAJ119-A was grown to early logarithmic phase in SCD and investigated by fluorescence microscopy. Pictures of a single large-budded cell are shown acquired with DIC optics and the corresponding fluorescence pictures with the FITC/GFP and the DsRed filter representing Inn1-GFP and Cyk3-mCherry, respectively. Additionally, an overlay of the two fluorescence images scaled up to 400% is shown to underline the co-localization of the two proteins. The scale bar represents 5 µm.

3.3.6 Inn1 co-localizes with Cyk3

To obtain further experimental evidence for an interaction of Inn1 and Cyk3, co-localization studies were performed. Cyk3 has previously been described as a cytokinetic regulator. It was shown to localize to the bud neck at the beginning of mitotic telophase and to persist until the start of the next cell cycle (Korinek *et al*., 2000). Here, a mCherry-tag was introduced at the carboxy-terminal end of Cyk3, again by *in vivo*-recombination of the encoding sequence at the 3'-end of the chromosomal *CYK3* gene, in a strain also expressing Inn1-GFP (HAJ119-A). The observed fluorescence signals co-localize at the site of cell division (Fig. 3.8C), which would allow for an interaction of the proteins *in vivo*.

3.3.7 Inn1, Hof1 and Cyk3 are recruited to the bud neck in a specific temporal order

The co-localization of Inn1, Hof1 and Cyk3 and the observed interaction of Inn1 with the latter two proteins, raises the interesting question of the temporal order of their appearance at the bud-neck. Moreover, a possible recruitment of one component by the other should be investigated. In order to obtain a timing device, a strain expressing a Myo1-mCherry fusion protein was crossed with strains expressing C-terminal GFP fusions of Inn1, Hof1 or Cyk3. After sporulation and tetrad analysis, segregants showing both fluorescence signals were chosen from each cross and subjected to live-cell imaging to generate a time-lapse movie of dividing cells. Pictures were taken every 2 minutes, a frame sufficiently long to monitor the state of cytokinesis, without running too much risk of bleaching the fluorophor. Their appearance relative to the known dynamics of Myo1-mCherry allowed the temporal alignment of the three different GFP-fusion proteins.

As already described in section 3.2.2, Inn1-GFP appears at the bud neck at the onset of cytokinesis, and as a single ring, which completely overlaps with the Myo1 localization. Later on, Inn1 also mimics the localization of Myo1: It follows the constriction of the CAR and disappears from the bud neck, when the cytokinesis apparatus is disassembled. Accordingly, Inn1-GFP signals can only be detected for eight to ten minutes within a complete cell cycle, which in this case lasts approximately 2h (Fig. 3.9A).

Hof1-GFP localization has been extensively studied before (Kamei *et al*., 1998; Lippincott and Li, 1998a), and is consistent with the findings described here. Thus, Hof1 re-localizes from the double-ringed septin collar to the single ring of the CAR at the onset of cytokinesis and co-localizes with Myo1 for about seven minutes during ring constriction. After the latter is completed, the Hof1-GFP signal splits to join again with the septins, and then vanishes. This strongly suggests that both, Inn1 and Hof1, are components of the CAR during its constriction.

Cyk3-GFP has also been described to form a ring at the bud neck during late anaphase. The ring-like structure constricts and then splits into two, coincident with the completion of cell separation. Furthermore, Cyk3-GFP was found to persist at the bud scar of the mother and the birth scar of the daughter cell (Korinek *et al*., 2000). Interestingly, a slightly different behaviour of Cyk3-GFP could be observed in the studies reported here. Consistent with previous reports, Cyk3-GFP appeared as a ring at the bud neck around three minutes after the onset of cytokinesis. However, this ring started to constrict only after completion of CAR constriction and disappeared right after that, coincident with the depletion of Hof1 from the bud neck.

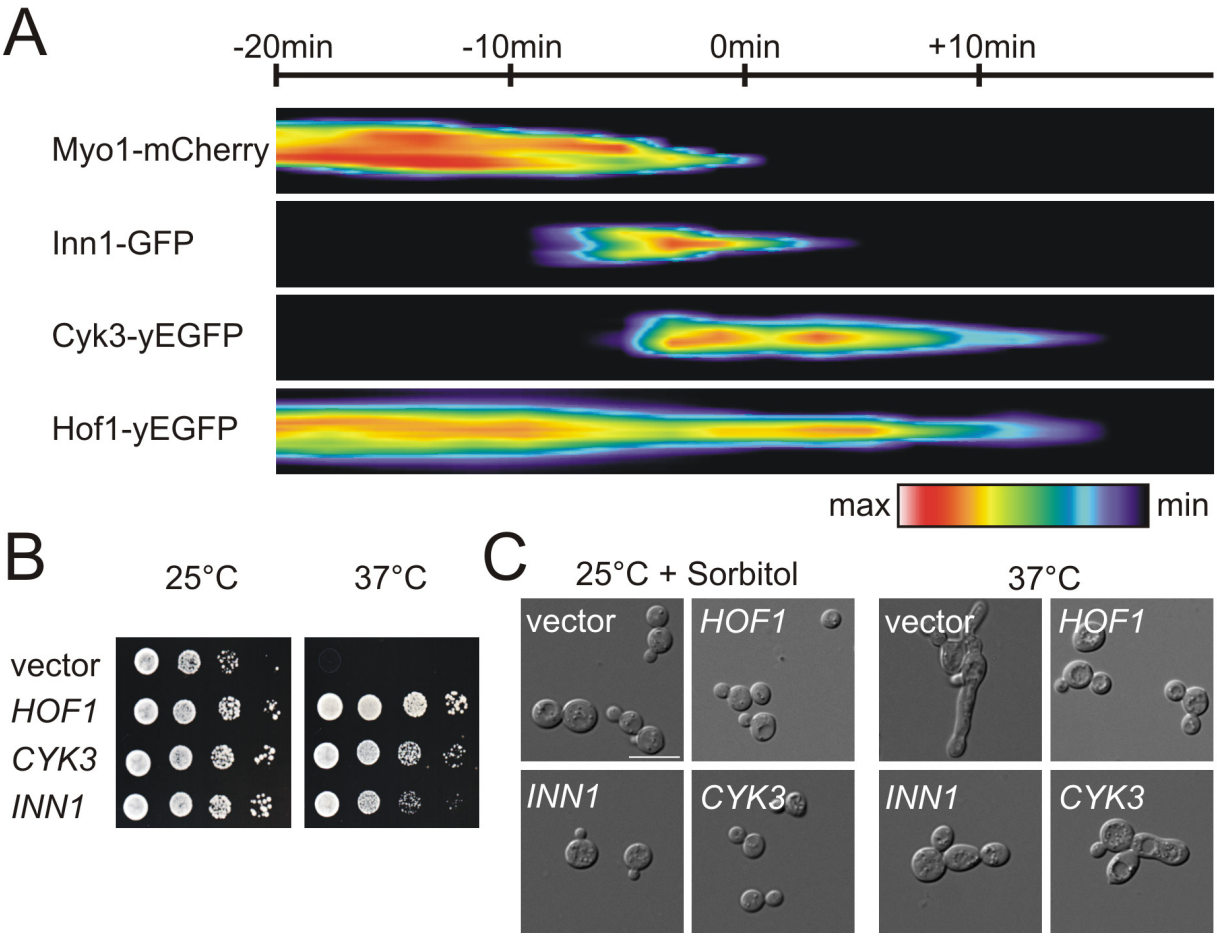

Fig. 3.9: Order of action of Inn1, Hof1, and Cyk3. A. Strains HAJ96-B, HAJ50-B and HAJ48-B were grown to early logarithmic phase in SCD and kymographs of the different fluorescence signals were created as described in 2.2.7.3. The three different GFP-kymographs were aligned according to the Myo1-mCherry kymograph. Colour intensities reflect the concentration of the respective fusion proteins as indicated and the width corresponds to the diameter at the bud neck. The kymographs were scaled up to 400% in diameter and additionally stretched. **B.** A haploid *hof1* deletion strain was transformed with multicopy plasmids encoding the indicated cytokinetic regulators (the negative control YEp352 (vector), pAJ023 (*HOF1*), pAJ022 (*INN1*) or pAJ024 (*CYK3*)). Transformants were tested in a serial drop dilution assay as described in 2.2.3. Cells were spotted onto SCD lacking uracil for plasmid maintenance and incubated as indicated. **C.** Cells from the strains as indicated in B were resuspended in SCD and microscopically examined. All DIC images presented were acquired at the same magnification and the scale bar represents 10 µm.

3.4 Genetic interactions of *INN1*, *HOF1* and *CYK3*

As shown above, the deletion of *INN1* is lethal, as is a double deletion of *HOF1* and *CYK3*, i.e. they are synthetically lethal (Korinek *et al.*, 2000). Since little is known about the function of Inn1 and the relation to its two interaction partners Hof1 and Cyk3, an epistasis analysis of the encoding genes could give valuable hints about the order of events during cytokinesis.

3.4.1 *INN1* and *CYK3* are multicopy suppressors of a *hof1* deletion

The complete loss of the cytokinesis regulator Hof1 causes a temperature-sensitive growth defect at 37°C, with no prominent cytokinesis defects displayed at the permissive growth temperature of 25°C (Lippincott and Li, 1998a). To test whether *INN1* or *CYK3* functionally act downstream of *HOF1*, a multicopy suppression analysis was performed. For this purpose, the complete open reading frames of *HOF1*, *INN1* and *CYK3*, including their promoter and terminator regions, were each cloned into the yeast multicopy vector YEp352 and introduced into a *hof1* deletion strain. The recipient vector without any insertion was used as a control. Transformants carrying the different plasmids were spotted in serial dilutions onto plates selective for plasmid maintenance, and incubated either at 25°C or at 37°C for three days. As apparent from Fig. 3.9B, strains carrying either *INN1* or *CYK3* on multicopy plasmids are able to grow at the restrictive temperature, indicating that both are multicopy suppressors of *hof1*. Representative pictures of single cells of the repressed *hof1* deletion are shown in Fig. 3.9C. Thus, overexpression of either *INN1* or *CYK3* weakens the cytokinesis defects of the *hof1* deletion, but can not restore wild-type cell morphology.

Next, *HOF1* and *CYK3* were tested for their ability to suppress the lethal phenotype of an *inn1* deletion. To this end, a heterozygous diploid strain with an *inn1::SpHIS5/INN1* genotype was transformed with the respective multicopy plasmids carrying either *HOF1* or *CYK3*, sporulated and subjected to tetrad analysis. None of the combinations gave rise to visible colonies bearing the *inn1* deletion, indicating that both genes are incapable of multicopy suppression. It should be noted that a *cyk3* deletion does not exhibit a pronounced growth defect and thus could not be tested in a similar fashion. Nevertheless, these genetic analyses suggest that *INN1* acts downstream of *HOF1* and probably also of *CYK3*.

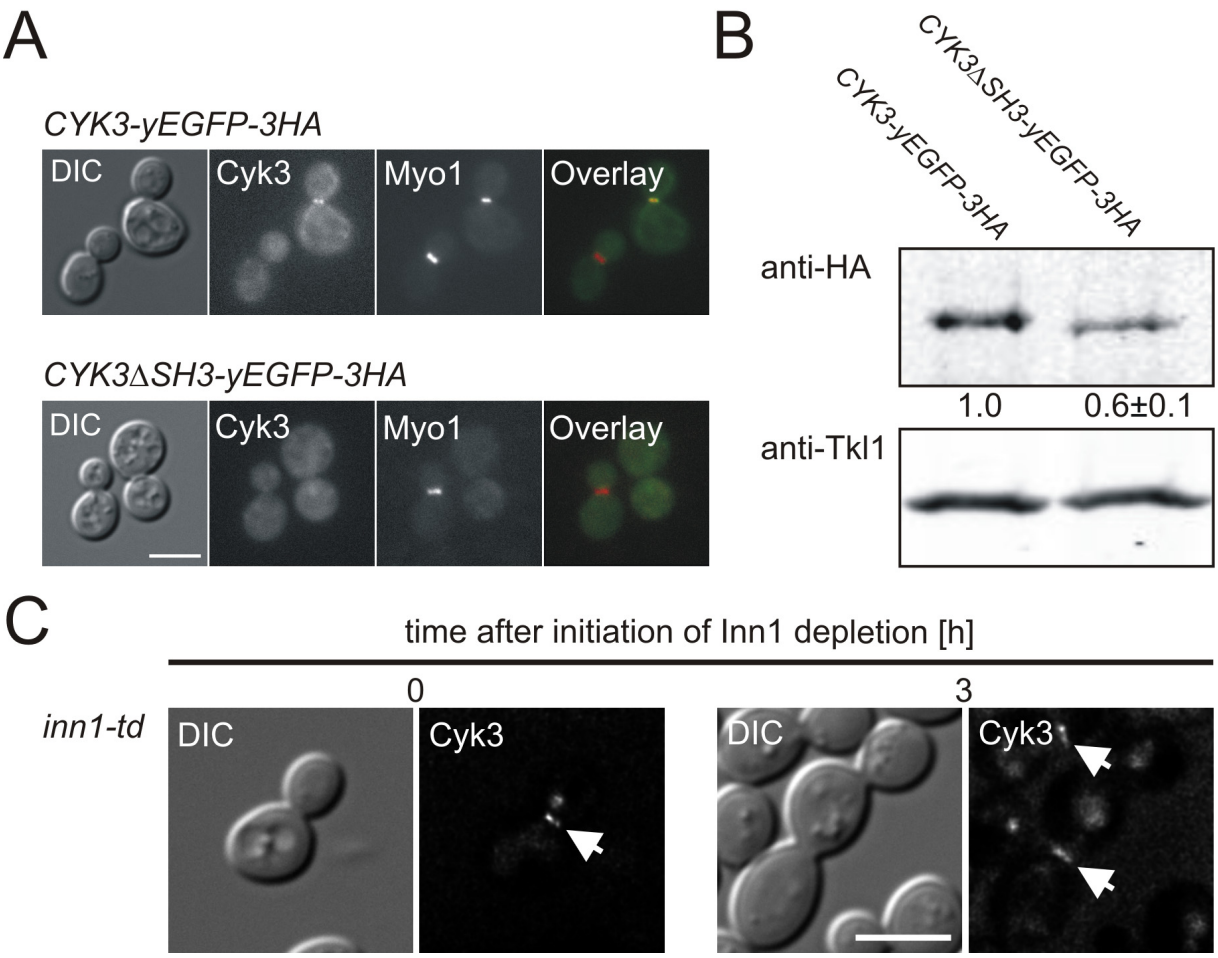

Fig. 3.10: Cyk3 requires its SH3 domain but not Inn1 for proper localization to the bud neck. A. Strains HAJ138-A and HAJ140-A, carrying the indicated yEGFP-3HA fusions of *CYK3* and additionally expressing Myo1-mCherry, were grown to early logarithmic phase in SCD and investigated by fluorescence microscopy. Pictures of cells from the same stage of the cell cycle were acquired with DIC optics and the corresponding fluorescence pictures with the FITC/GFP and the DsRed filter representing Cyk3-yEGFP and Myo1-mCherry, respectively. Additionally, an overlay of the two fluorescence images is shown to underline the co-localization of the two proteins. More than 200 cells each were observed, but no signal for Cyk3-yEGFP lacking the SH3 domain could be detected. The scale bar represents 5 µm. **B.** Crude extracts of 2 OD_{600} units of cells described in A were prepared and probed with an anti-HA antiserum. The relative amount of HA-fusion proteins was normalized against the anti-Tkl1 loading control. **C.** Cells from strain HAJ64-B were incubated to initiate the depletion of Inn1 (see text for details) and investigated for the localization of Cyk3-yEGFP by fluorescence microscopy. Micrographs of representative cells taken at the initiation of Inn1 depletion (upper panels) and 3 h later (bottom panels) are displayed. DIC images are shown in the left panels and the corresponding fluorescence pictures obtained with the FITC/GFP filter representing Cyk3-yEGFP are shown in the right panels. The arrows point to Cyk3-yEGFP localizing to the bud neck even after depletion of Inn1. The scale bar represents 5 µm.

3.4.2 The SH3 domains of either Cyk3 or Hof1 are required for viability

The epistasis analyses reported above suggest a functional relation of *INN1* with *HOF1* and *CYK3*. Since Inn1 interacts with the latter two exclusively through their SH3 domains, a strain lacking those should not be viable, since *hof1 cyk3* double deletions are synthetically lethal. To test this assumption, strains lacking either of the two SH3 domains were first obtained by one-step gene replacements. In order to

monitor the expression of the respective SH3-less proteins, C-terminal GFP fusions were employed in Western analyses of strains carrying either one of the SH3 deletions. A GFP-fusion protein of Hof1 lacking its SH3 domain showed an intracellular localization similar to the wild-type Hof1-GFP and lacked any pronounced phenotype (e.g. it grew normally at 37°C). In contrast, Cyk3-yEGFP lacking its SH3 domain misslocalized and failed to appear at the bud neck in the appropriate stage of the cell cycle (Fig. 3.10A). Yet, the total intracellular amount of the truncated protein was only slightly reduced as compared to the full length protein (Fig. 3.10B).

Next, the localization of full-length Cyk3-yEGFP (i.e. including its SH3 domain) was tested in a strain depleted for Inn1 by induced protein degradation (*inn1-td*). Under these conditions, Cyk3-yEGFP was still observed at the sites of cell division, although the latter appeared dramatically deformed due to the lack of Inn1 (Fig. 3.10C). This indicates that Cyk3 requires its SH3 domain, but surprisingly not Inn1, for its proper localization to the bud neck.

Taken together, deletion of the SH3 domain of either of the two interaction partners of Inn1 does not affect cell growth. Therefore, the SH3 domain single deletion strains were crossed to give a heterozygous diploid strain, which was sporulated and subjected to tetrad analysis. From 32 tetrads analysed, only one viable colony appeared with the genetic markers indicating the presence of a double deletion in the SH3 domain sequences of *CYK3* and *HOF1* (Fig. 3.11A). This strain showed severe morphological defects (Fig. 3.11B, tetrad 2A) and was presumed to carry a genomic suppressor mutation. All other segregants lacking the two SH3 domains were non-viable with a terminal phenotype reminiscent of an *inn1* deletion (Fig. 3.11B, tetrad 1B; compare with Fig. 3.1C).

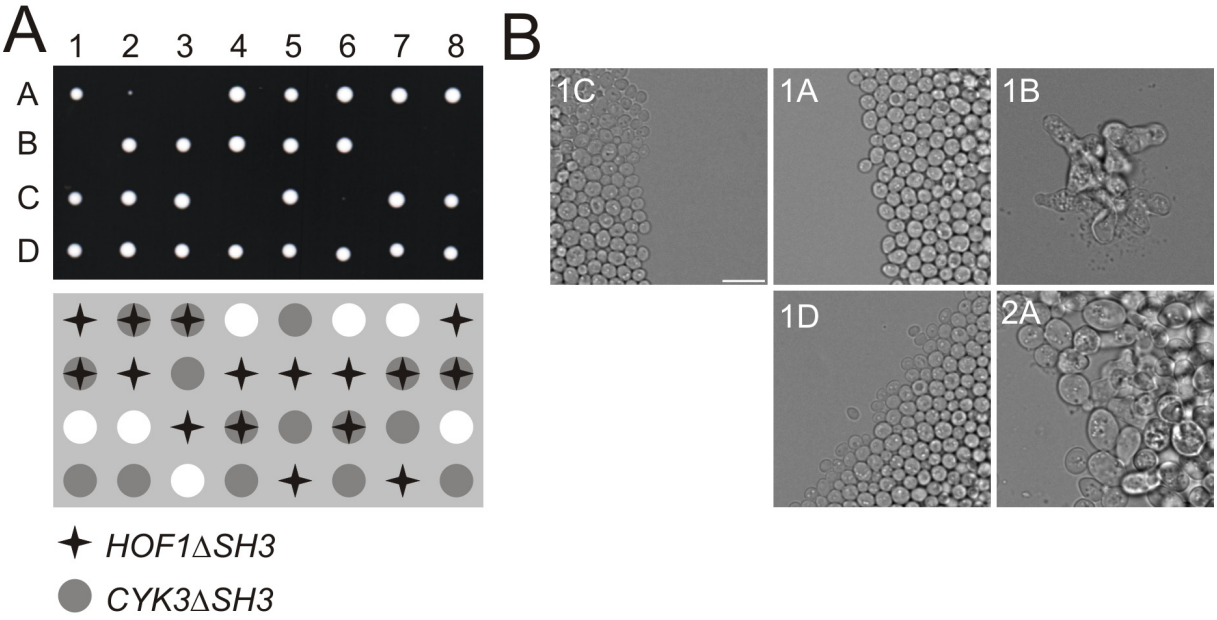

Fig. 3.11: The SH3 domains of either Cyk3 or Hof1 are required for viability. A. Tetrads of strain DAJ34 heterozygous for *CYK3ΔSH3-3HA* and *HOF1ΔSH3-3HA* were dissected on YEPD (upper panel). The cartoon in the lower panel indicates the genotypes of the segregants. Stars represent *HOF1ΔSH3-3HA* and grey circles represent *CYK3ΔSH3-3HA*. Note that all double deletions fail to grow except for segregant 2A. **B.** Micrographs of segregants from strain DAJ24 representing the different combinations of alleles obtained from the tetrad analysis in A are shown. All micrographs were obtained with the same magnification and the scale bar represents 10 µm.

3.5 Regulation of Inn1 recruitment to the bud neck

The genetic evidence presented so far suggests that *INN1* is acting downstream of *HOF1* and *CYK3*. Thus, Hof1 and Cyk3 could recruit Inn1 to the bud neck at the time of cytokinesis. This hypothesis was further investigated.

3.5.1 Deletion of either *HOF1* or *CYK3* does not prevent Inn1 recruitment to the bud neck

First, the localization of Inn1-GFP in the background of single *hof1* and *cyk3* deletion mutants was investigated. As expected from the localization of the remaining cytokinesis regulator in each strain and the presence of its SH3 domain, no significant changes in Inn1 localization could be detected in these strains. Although showing highly abnormal bud neck morphology in a *hof1* deletion strain, Inn1-GFP still appeared in a ring-like structure. The *cyk3* deletion strain did not display any difference in Inn1-GFP localization compared to the respective isogenic wild-type strain (Fig. 3.12A), as expected from its lack of growth defects.

3.5.2 Overproduction of either Hof1 or Cyk3 provokes an aberrant localization of Inn1

A strong overproduction of *HOF1* has been reported to be lethal (Lippincott and Li, 1998a). Thus, Inn1-GFP and Myo1-mCherry were studied in a strain expressing *HOF1* at its chromosomal locus under the control of the conditional *GAL1* promoter. Only slight morphological defects could be observed when cells were grown in media with glucose as a carbon source and in the presence of osmotic stabilization (i.e. under repressing conditions). Consequently, Inn1 and the CAR displayed no pronounced differences in their localization and dynamics as compared to wild-type cells. To follow up this observation, cells from the early logarithmic phase were harvested and transferred to medium with galactose as a sole carbon source, thus inducing the overexpression of *HOF1*. After four hours of incubation, cells were examined by fluorescence microscopy. Whereas CAR localization was hardly affected in comparison to the wild-type control, Inn1-GFP localization was dramatically altered. Upon overproduction of Hof1, Inn1-GFP formed double ring structures at the bud neck, which were never observed in the wild-type background (Fig. 3.12B, cell 1). Moreover, Inn1-GFP was frequently retained, even after CAR disassembly (Fig. 3.12B, cell 2).

Until now, no phenotypes have been assigned to the overexpression of *CYK3.* To test, whether *CYK3* overexpression affects the subcellular localization of Inn1, the native *CYK3* promoter at its chromosomal locus was also replaced by the *GAL1* promoter. As expected from the results reported above, the localization of Inn1-GFP and the CAR was not affected under repressing conditions for *CYK3* expression (i.e. on glucose medium). After induction of *CYK3* overexpression by a shift to galactose medium for four hours, CAR localization remained unaltered. However, in contrast to a wild-type control, Inn1-GFP signals were still frequently observed in cells with a disassembled CAR (Fig. 3.12C). The cultures were also quantified for the relative number of cells which displayed an overlapping localization of Inn1-GFP with the CAR, represented by Myo1-mCherry. Upon overexpression of *CYK3* about half of the Inn1-GFP signals did not co-localize with the CAR anymore. When shifted back to glucose medium (i.e. upon repression of *CYK3* expression), the percentage of cells co-localizing Inn1-GFP with Myo1-mCherry was restored to wild-type levels (Fig. 3.12D). Taken together, these results demonstrate that overexpression of either

HOF1 or *CYK3* can alter the localization of Inn1-GFP without significantly affecting the CAR.

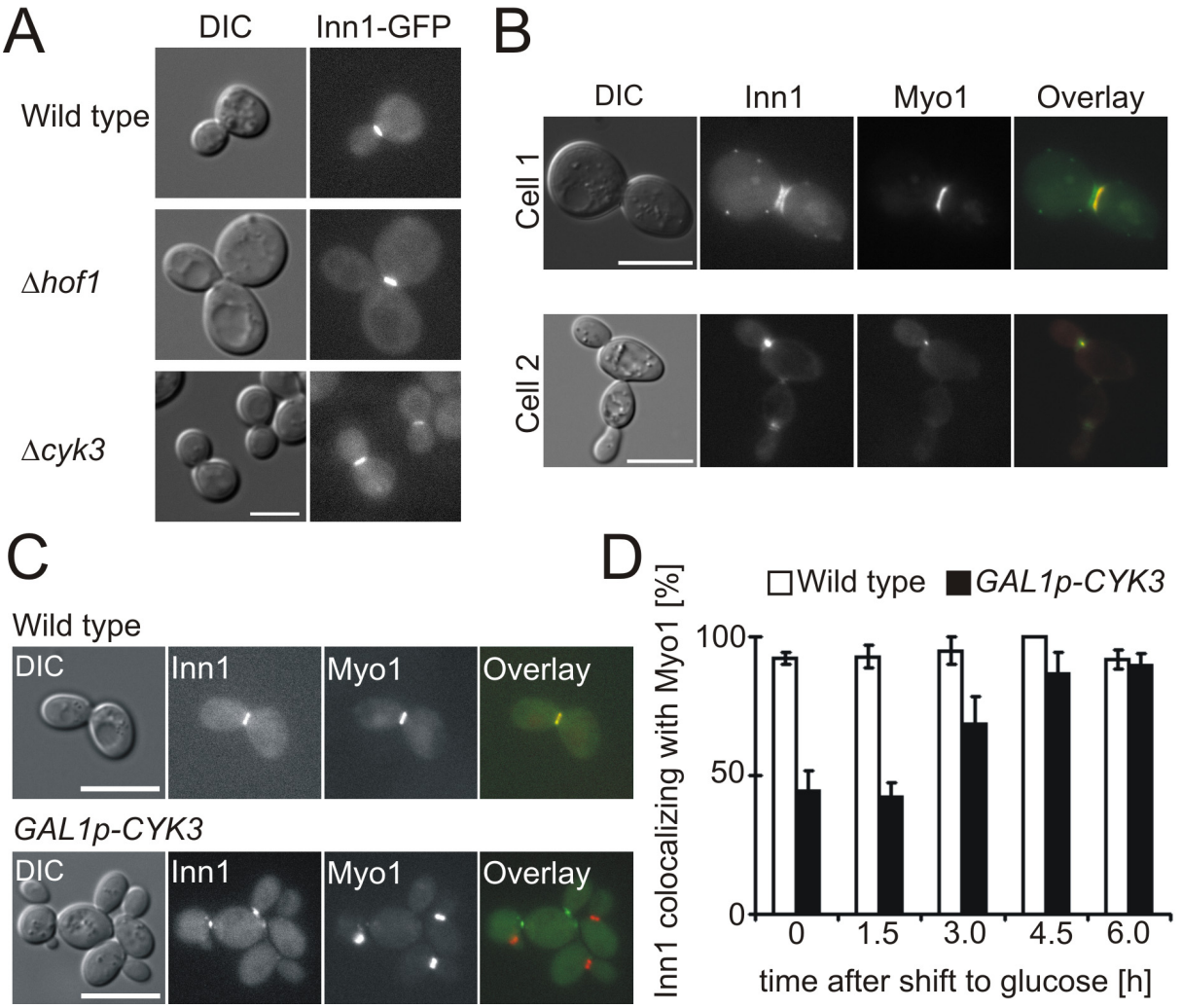

Fig. 3.12: Overproduction of Hof1 or Cyk3 alters Inn1 localization. A. Cells from strains HAJ93-B (*Δcyk3*) and HAJ94-B (*Δhof1*) together with the wild-type control (HAJ28-B) were examined by fluorescence microscopy for the localization of Inn1-GFP. The scale bar represents 5 µm. **B.** Strain HAJ93-B was incubated in rich medium with galactose for 4 h to induce overexpression of *HOF1* and investigated by fluorescence microscopy for the localization of Inn1-GFP and Myo1-mCherry. Micrographs of two different cells representing the different localization pattern of Inn1-GFP are shown. The scale bar represents 10 µm. **C.** Strain HAJ106-B (*GAL1p-CYK3*) and the appropriate wild-type control (HAJ96-B) were incubated in rich medium with galactose for 12 h and investigated by fluorescence microscopy for the localization of Inn1-GFP and Myo1-mCherry. The scale bar represents 10 µm. **D.** Cells from C were shifted from galactose to glucose medium and quantified for the localization of Inn1-GFP and Myo1-mCherry at the indicated time points after the shift to glucose. More than 200 cells each were examined and the percentage of Inn1-GFP signals that co-localize with Myo1-mCherry is given.

3.5.3 Inn1 redistributes upon simultaneous depletion of *HOF1* and *CYK3*

In order to support the hypothesis that Cyk3 and Hof1 can recruit Inn1 to the bud neck during cytokinesis, a strain expressing both *CYK3* and *HOF1* under *GAL1* promoter control was obtained by crossing, sporulation and tetrad analysis from the

single conditional mutants described above. Tetrads from such a heterozygous diploid strain were dissected on media containing either glucose with osmotic stabilization or galactose. As expected, segregants overexpressing *HOF1* formed only very small or no colonies at all (Fig. 3.13A). Segregants overexpressing *CYK3* did not show any growth defects. Interestingly, segregants simultaneously overexpressing both genes were viable and grew to colonies with an only slightly decreased size compared to wild-type segregants. Under repressing conditions with osmotic stabilization neither *GAL1p-HOF1* nor *GAL1p-CYK3* segregants showed significant growth defects. Only if both gene expressions were shut down, colony formation was inhibited, as expected from the synthetic lethality of the respective double deletions (Fig. 3.13A).

The different segregants were also employed to investigate the subcellular localization and dynamics of Inn1-GFP and the CAR (represented by the Myo1-mCherry fusion) under the different growth conditions. When both *CYK3* and *HOF1* were overexpressed in the same strain, Inn1-GFP appeared in double ring structures and was retained even after CAR disassembly, in addition to the normal localization (Fig. 3.13C). Upon a subsequent shift to glucose (i.e. repressing conditions for *HOF1* and *CYK3* expression) Inn1-GFP was not recruited to the bud neck anymore. The latter behaviour was quantified by determining the frequency of specific Inn1-GFP signals at the bud necks of approximately 200 cells at each time point. In wild-type cells (*CYK3* and *HOF1* under control of their native promoters), approximately 8% of the bud necks displayed an Inn1-GFP signal, which did not change significantly upon the shift from galactose to glucose. In contrast, the simultaneous repression of *HOF1* and *CYK3* led to an almost complete lack of Inn1-GFP signals at the bud necks (Fig. 3.13B). Representative cells photographed 6 hours after the shift to the repressing conditions are shown in Fig. 3.13C, as compared to cells grown with galactose.

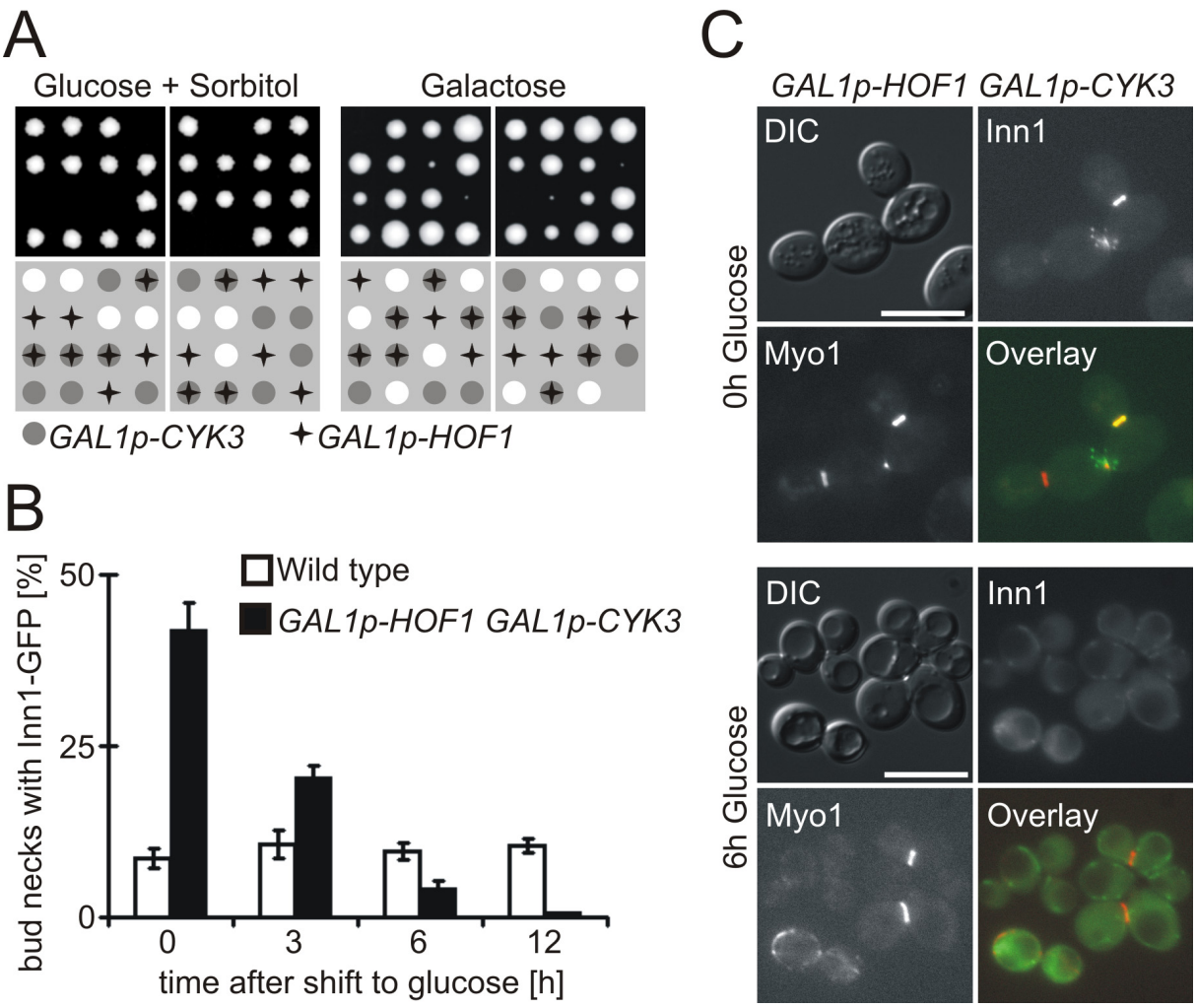

Fig. 3.13: Inn1 is not recruited to the bud neck in cells repressed for HOF1 and CYK3 expression. A. Tetrads of strain DAJ25 heterozygous for *GAL1p-CYK3* and *GAL1p-HOF1* were dissected on YEPD supplemented with 1M sorbitol (upper left panel) and on YEPG (upper right panel). The cartoons in the lower panels designate the genotypes of the single segregants. Stars represent *GAL1p-HOF1* and grey circles represent *GAL1p-CYK3*. **B.** Strain HAJ95-A (*GAL1p-CYK3 GAL1p-HOF1*) and the appropriate wild-type control (HAJ96-A) were incubated in rich medium with galactose for 12 h and then shifted to glucose and examined by fluorescence microscopy for the localization of Inn1-GFP. More than 100 cells were quantified at the indicated time points after the shift to glucose medium and the percentage of bud necks decorated with Inn1-GFP was determined. **C.** Micrographs of representative cells from strain HAJ95-A incubated as described in B are depicted. The scale bar represents 10 µm.

3.5.4 Overproduction of *CYK3* bypasses the requirement for a functional CAR

Sanchez-Diaz *et al*. (2008) reported that a functional CAR is required to localize Inn1 to the bud neck. Thus, upon depletion of either Myo1 or Iqg1, Inn1-GFP does not accumulate at the division site, anymore. As shown in section 3.5.2, cells overexpressing *CYK3* recruited Inn1-GFP to the bud neck independent of the CAR. Therefore it was investigated, whether the function of Myo1 can be bypassed by overexpression of either of the regulatory components investigated here. First, the genetic interactions were determined. Interestingly, *CYK3* as well as *HOF1, INN1*

and *IQG1* are efficient multicopy suppressors of a *myo1* deletion (Fig. 3.14A), but not of an *iqg1* deletion (i.e. no viable segregants of an *iqg1* deletion were obtained upon transformation with the respective multicopy plasmids, except for *IQG1* itself). Moreover, overexpression of *CYK3* from the *GAL1* promoter almost restores wild-type growth in a *myo1* deletion and re-establishes Inn1-GFP localization to the bud neck, which is lost in the *myo1* deletion background. Interestingly, both viability and bud neck localization of Inn1-GFP were also restored in an *iqg1* deletion by the overexpression of *CYK3*, albeit with a very low efficiency (see Fig. 3.14B and the representative cells in C and D).

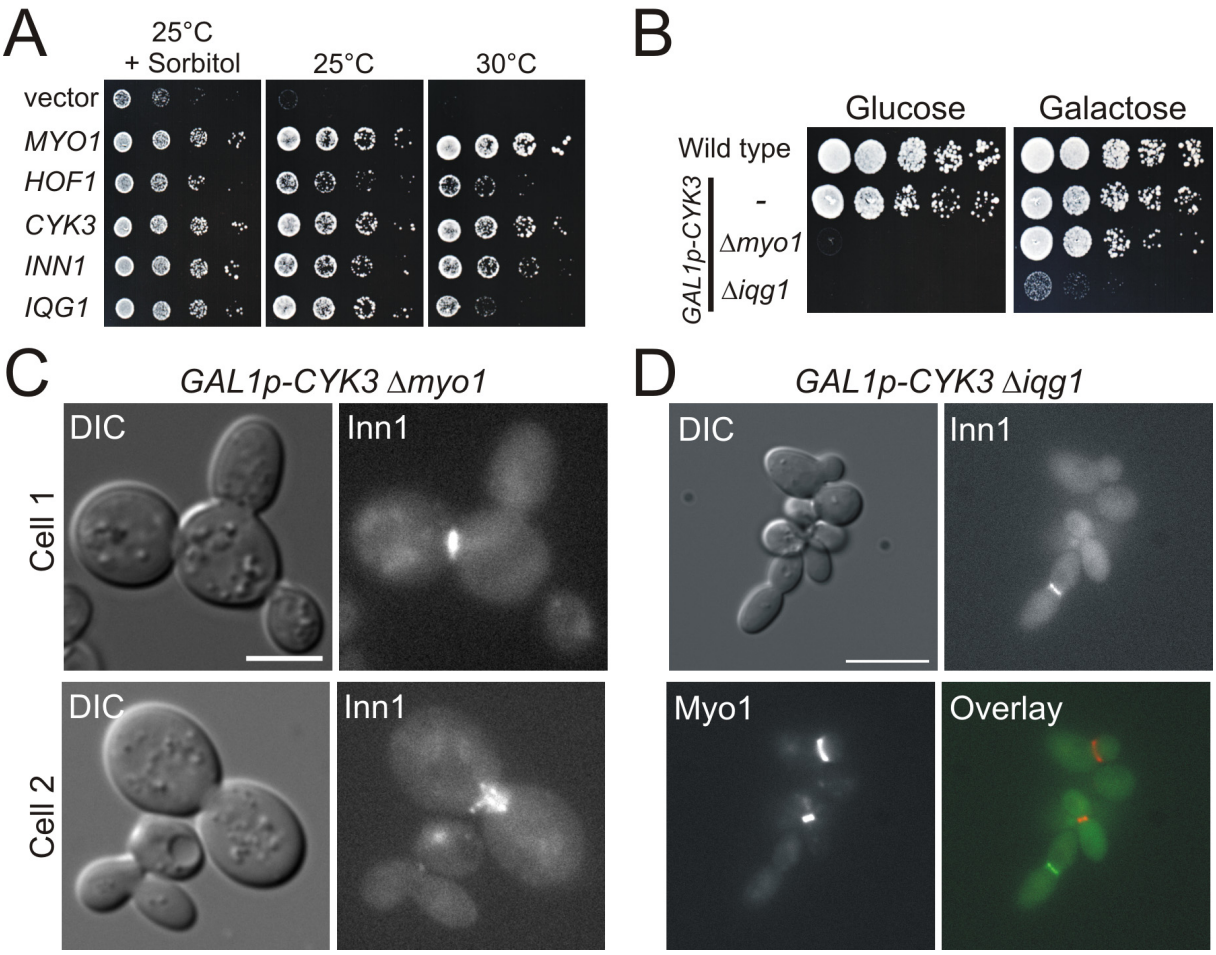

Fig. 3.14: CYK3 overexpression bypasses the requirement for a functional CAR by recruiting Inn1. A. Haploid *myo1* deletion strains transformed with multicopy plasmids encoding the cytokinetic regulators (the negative control YEp352 (vector), pAJ055 (*MYO1*), pAJ023 (*HOF1*), pAJ022 (*INN1*) or pAJ024 (*CYK3*) and pAJ044 (*IQG1*)) were tested in a serial drop dilution assay as described in 2.2.3. Cells were spotted onto SCD lacking uracil for plasmid maintenance and incubated for 3 days under the conditions indicated. **B.** Strains HAJ139-B (*Δmyo1*), HAJ129-B (*Δiqg1*), and the control HAJ106-B (-) were tested together with the wild-type control HAJ96-B in a serial drop dilution assay as described in 2.2.3. All strains were pregrown in rich medium with galactose and then spotted onto plates with the indicated carbon sources. Plates were incubated for 3 days at 25°C. **C.** Strain HAJ139-B was incubated in rich medium with galactose and investigated by fluorescence microscopy for the localization of Inn1-GFP. Micrographs of two different cells representing the different localization patterns of Inn1-GFP are shown. The scale bar represents 5 µm. **D.** Strain HAJ129-B was incubated and examined as in C for the localization of Inn1-GFP and Myo1-mCherry, as indicated. The scale bar represents 10 µm.

3.6 Function of Vrp1 in cytokinesis

Another factor sharing interesting genetic and physical interactions with *HOF1* is encoded by *VRP1*. A *vrp1* deletion is temperature-sensitive and displays a prominent block in cytokinesis. Both phenotypes are reminiscent of those observed in a *hof1* deletion (Naqvi *et al*., 2001). Hof1 and Vrp1 directly interact with each other, mediated by the SH3 domain of Hof1 and the so-called HOT (**Ho**f1 **t**rap) domain of Vrp1, which consists of proline-rich stretches. Interestingly, the removal of the SH3 domain of Hof1 can partially rescue the lethality of a *vrp1* deletion at 37°C (Ren *et al*., 2005). The authors propose that cytokinesis is blocked in wild-type cells until a yet to be identified inhibitor of Hof1 is removed by the interaction of its SH3 domain with Vrp1. Therefore, a possible role of Vrp1 for Inn1 recruitment to and maintenance at the bud neck was addressed.

3.6.1 Genetic interactions of *VRP1* with other cytokinesis regulators

In a first step the influence of a *VPR1* overproduction on the growth defects of a *hof1* deletion was investigated. As evident from Fig. 3.15A, no effect could be observed. *Vice versa*, expression of *HOF1* from a multicopy vector did not affect the growth and temperature-sensitivity of a *vrp1* deletion, either. In fact, all of the other cytokinesis regulators described above did neither enhance nor suppress the phenotypes of a *vrp1* deletion (Fig. 3.15B).

3.6.2 Kinetics of Vrp1 appearance at the bud neck

Vrp1 has been suggested to not only exert its effect on cytokinesis through Hof1, but also influences the formation of the CAR (Naqvi *et al*., 2001; Thanabalu and Munn, 2001). To gain further insight into these functions of Vrp1, an mCherry fusion was constructed and studied for its localization throughout the cell cycle. Vrp1 is a component of actin patches and probably accumulates at the bud neck shortly after completion of CAR constriction. Since this time point coincides with the splitting of the Hof1 rings (see also 3.3.7 and the introduction, section 1.2.4), the Vrp1-mCherry localization was examined together with that of Hof1-yEGFP. As expected, a co-localization of the two proteins could be detected exactly and only at this time point during the cell cycle (Fig. 3.15C).

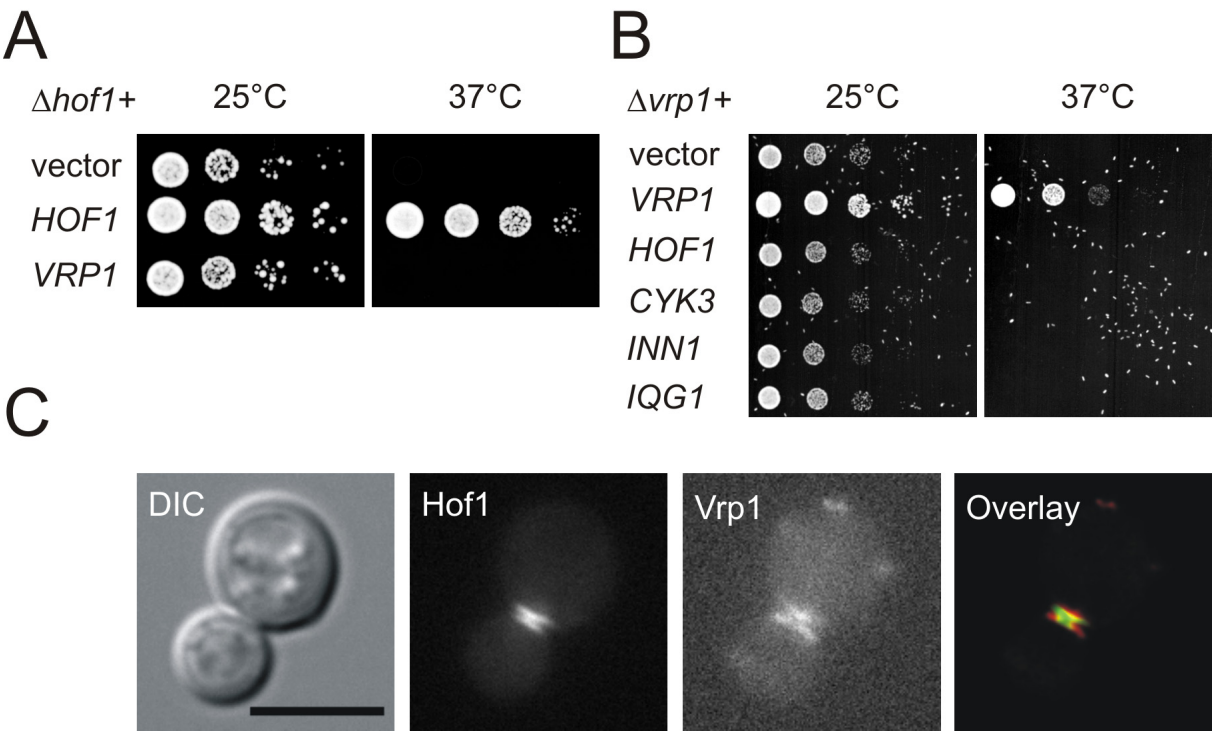

Fig. 3.15: Interactions of *VRP1* and *HOF1*. A. A haploid *hof1* deletion strain was used as a recipient for multicopy plasmids encoding different cytokinetic regulators (the negative control YEp352 (vector), pAJ023 (*HOF1*) or pAJ047 (*VRP1*)), and tested in a serial drop dilution assay as described in 2.2.3. Cells were spotted onto SCD lacking uracil for plasmid maintenance and incubated for 3 days at the indicated temperatures. **B.** Haploid *vrp1* deletion cells transformed with multicopy plasmids encoding the cytokinetic regulators (the negative control YEp352 (vector), pAJ047 (*VRP1*), pAJ023 (*HOF1*), pAJ022 (*INN1*) or pAJ024 (*CYK3*) and pAJ044 (*IQG1*)) were tested in a serial drop dilution assay as in A. **C.** Strain HAJ103-A expressing functional fusion proteins of Hof1-yEGFP and Vrp1-mCherry at physiological levels was grown to early logarithmic phase in SCD and investigated by fluorescence microscopy. Pictures of a single large-budded cell are shown acquired with DIC optics, as are the corresponding fluorescence pictures with the FITC/GFP and the DsRed filter representing Hof1-yEGFP and Vrp1-mCherry, respectively. An overlay of the two fluorescence images is also shown. The scale bar represents 5 µm.

3.6.3 Effect of Vrp1 on Inn1 dynamics

Since Vrp1 and Hof1 were shown to directly interact with each other at a time point shortly after CAR disassembly, i.e. when Inn1 has been removed from the bud neck (Ren *et al.*, 2005) and this study), the effect of a *vrp1* deletion on the localization of Inn1 was investigated. The localization of the Inn1-GFP fusion protein described in 3.2.2 together with Myo1-mCherry as a marker for the completion of cytokinesis was studied in a strain deleted for *vrp1*. Interestingly, a prominent signal of Inn1-GFP could still be detected in cells that already completed cytokinesis. Thus, the concomitant kinetics of the Inn1-GFP signals with those of Myo1-mCherry observed in wild-type cells is decreased to 60% in *vrp1* cells (Fig. 3.16A). The dynamics of the two fluorescence signals were also followed by time-lapse microscopy. Whereas the CAR (represented by Myo1-mCherry) was not affected in the *vpr1* deletion, an

altered dynamic was observed for the Inn1-GFP fusion: the protein is recruited at the beginning of CAR constriction and mimics its dynamics, but persists at the bud neck for approximately five more minutes after its completion. Approximately ten percent of the cells also show a splitting of the Inn1-GFP signal, which is strongly reminiscent of the behaviour of Hof1 during this stage of the cell cycle (Fig. 3.16B).

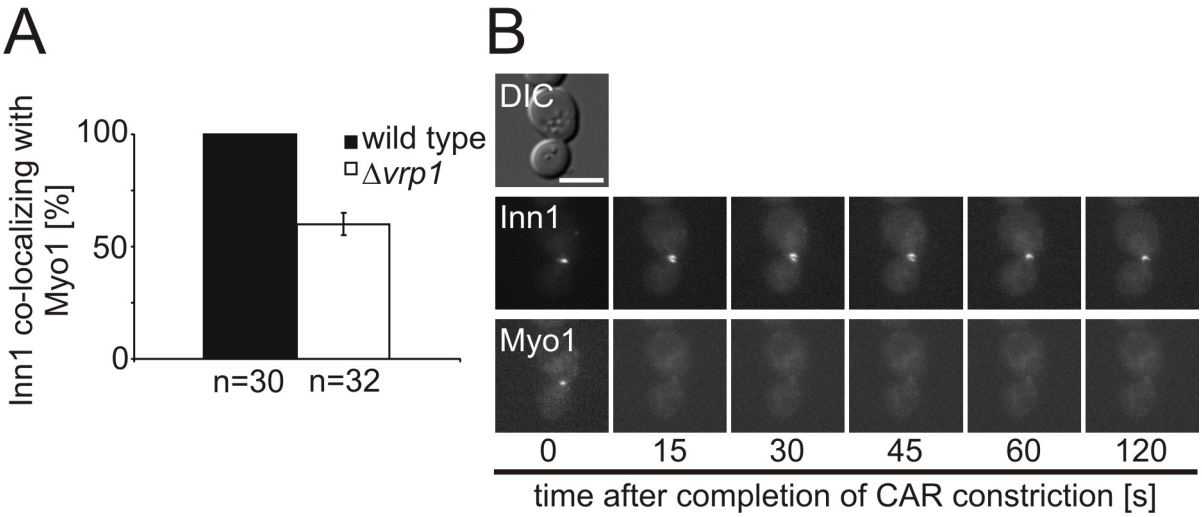

Fig. 3.16: Effects of vrp1 deletion on Inn1 dynamics. A. Cells from strain HAJ104-A (*Δvrp1*) and the appropriate control HAJ96-A (wild type) were grown in SCD at 25°C to early logarithmic phase and quantified for the percentage of Inn1-GFP signals that co-localize with Myo1-mCherry. More than 200 cells were counted. **B.** Single cells from strain HAJ104-A were incubated as described in A and the dynamics of Inn1-GFP and Myo1-mCherry were followed by live cell imaging as described in 2.2.7.3. The series of fluorescence pictures were acquired every 15 seconds. The scale bar represents 5 µm.

3.7 Investigation of the role of the Inn1-C2 domain in lipid binding

3.7.1 Purification of GST-tagged Inn1 from *E. coli*

Heterologous gene expression in *E. coli* can be used to produce large amounts of a protein of interest. For this purpose, an *INN1-GST* fusion gene was obtained in a bacterial expression plasmid (pAJ032) and expressed under control of the inducible *T7* promoter. Total protein extracts from *E. coli* cells induced for up to 4 hours were analyzed by SDS-PAGE.

The fusion protein was purified from extracts by affinity chromatography and the different fractions were tested for the presence of Inn1-GST by Western blot analysis. A prominent band could be detected in a silver-stained gel, migrating at the expected molecular weight of 73 kDa (Fig. 3.17A). Additional lower molecular weight bands were also present and are probably caused by degradation products, since they also reacted with an anti-GST antiserum in a subsequent immunoblot.

In addition to the full length protein, a truncation of Inn1 lacking the C2 domain was purified, employing a similar expression plasmid (pAJ036; see material and methods). As observed for the full length protein, additional lower molecular weight degradation products were detected besides the main 55 kDa band representing Inn1ΔC2-GST (Fig. 3.17A).

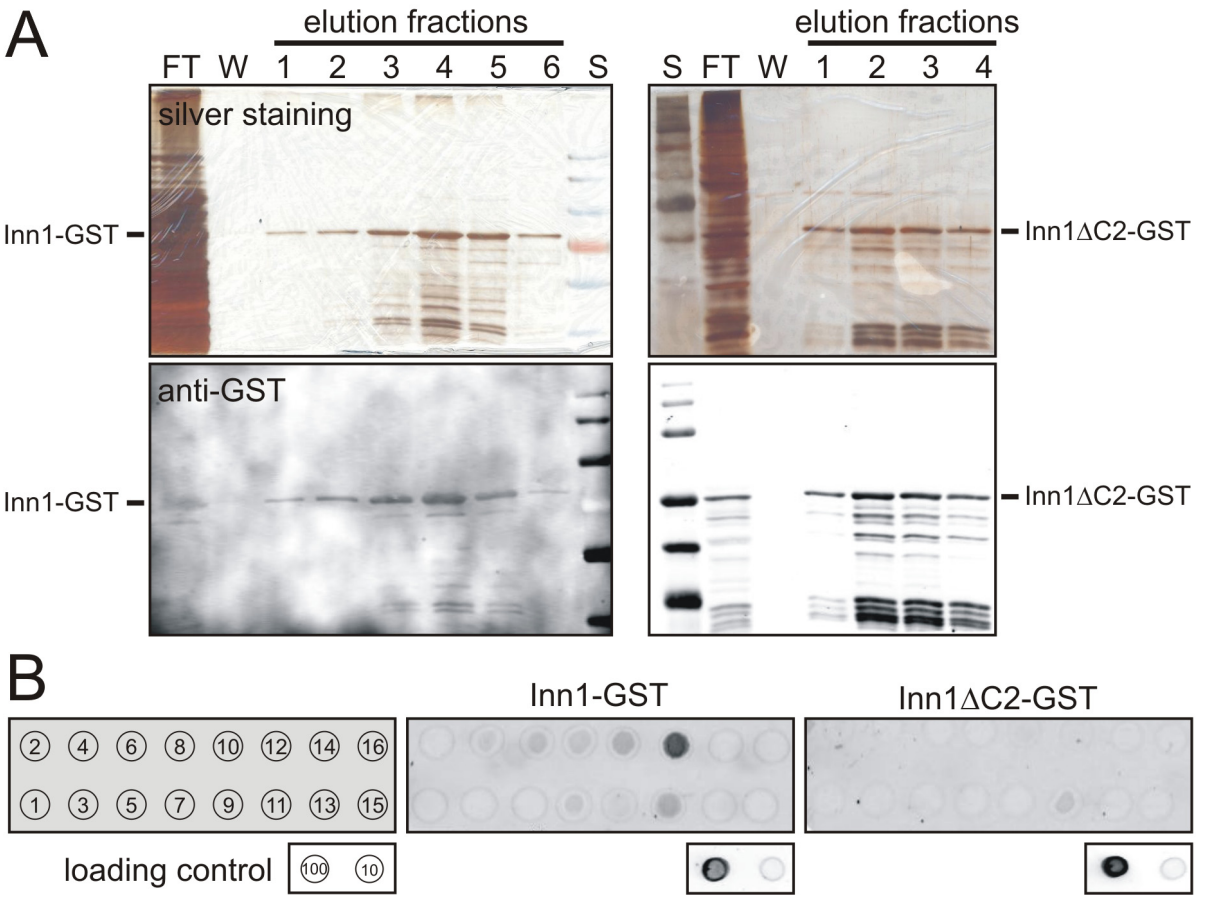

Fig. 3.17: Heterologously expressed Inn1 binds to phosphatidic acid via the C2 domain. A. Inn1-GST and Inn1ΔC2-GST were expressed in *E. coli* BL21-DE3 and purified as described in 2.2.6.9 and 10. Different fractions from the affinity-chromatography were separated in 10% agarose gels and either detected by silver staining or immunoblotted with an anti-GST antiserum. FT (flow through; unbound protein during the loading process), W (flow through from washing step), S (size marker Fermentas PageRuler prestained) and elution fractions are displayed. **B.** PIP strips were incubated with the purified proteins as described in 2.2.6.11. 100 and 10 ng of protein was spotted directly onto a nitrocellulose membrane as a loading control. Proteins were visualized by immune-detection as described in 2.2.6.8. Spots contained: 1 Lysophosphatidic acid, 2 Lysophosphatidyl-choline, 3 Phosphatidylinositol, 4 PtdIns(3)P, 5 PtdIns(4)P, 6 PtdIns(5)P, 7 Phosphatidylethanolamine, 8 Phosphatidyl-choline, 9 Sphingosine 1-Phosphate, 10 PtdIns(3,4)P2, 11 PtdIns(3,5)P2, 12 PtdIns(4,5)P2, 13 PtdIns(3,4,5)P3, 14 Phosphatidic acid, 15 Phosphatidylserine, 16 Blank.

3.7.2 Inn1 binds to phosphatidic acid

To test the lipid-binding properties of Inn1, commercially available PIP strips were incubated with the purified Inn1 peptides. A strong binding of Inn1-GST could be detected at the phosphatidic acid (PA) spot. Some weaker signals also appeared with

phosphatidyl-inositol-phosphates (PIPs). Interestingly, the strong signal for PA could not be detected, when the membrane was incubated with the truncated form of Inn1-GST lacking the C2 domain (Fig. 3.17B). This result suggests that Inn1 binds to phosphatidic acid via its C2 domain.

4 Discussion

The aim of this thesis was the characterization of the open reading frame *YNL152w* from the baker's yeast *Saccharomyces cerevisiae*, with some preliminary studies performed previously in this laboratory. Thus, a transposon mutant expressing a modified protein with the eight carboxy-terminal amino acids exchanged to GLTLSGTKTHVKGFWS displayed an increased activity in a reporter system, designed to measure the activity of cell integrity signalling (Schmitz, 2001). As it was one of many genes found in that genetic screen, the molecular function of Ynl152w was not specifically addressed in that thesis. From genome-wide screens on protein function and interaction performed in the meantime in *Saccharomyces cerevisiae*, first hints indicating a putative function of Ynl152w were obtained. It was shown to be an essential protein (Giaever *et al*., 2002) erroneously localized to the cytoplasm. A possible role in binding of phospholipids was suggested by the presence of an amino-terminal C2 domain (Hazbun *et al*., 2003). Further studies addressing the yeast interactome identified Hof1 as an interaction partner of Ynl152, a protein required for cytokinesis (Ito *et al*., 2001).

Although it was isolated in a genetic screen by its effects on the cell wall integrity (CWI) pathway as described above, a direct role of Ynl152w in that pathway could not be confirmed in another work performed in this laboratory (Ciklic, 2007). Rather, evidence for a role of Ynl152w in cell division kept accumulating. Using carboxy-terminal truncations, it turned out that more than half of the protein (270 out of the total 409 amino acids in the primary sequence) can be deleted without a loss of cell viability (Ciklic, 2007). However, growth and sporulation defects became more severe the shorter the protein became, and the average DNA content of mitotic cells also became affected. These cumulative phenotypes were attributed to the number of proline-rich motifs in the remaining parts of Ynl152w, which were proposed to mediate the binding to the SH3 domain of Hof1, as the sole known interaction partner at the time. In fact, the truncation mutants apparently affected Hof1 localization, since Hof1-GFP fusions appeared to persist longer at the bud neck than in wild-type cells (Ciklic, 2007).

While work on the thesis presented here was carried out, two other groups published their data on Ynl152w. In the first work, the systematic name of the open reading frame was substituted for *INN1*, due to its proposed role in plasma membrane

ingressio**n** (Sanchez-Diaz *et al*., 2008). The authors claimed that Inn1 couples the constriction of the actomyosin ring to the ingression of the plasma membrane during cytokinesis, and present data and conclusions largely overlapping with the results presented here. In 2009, another work on Inn1 function was published with some contradicatory findings, as discussed below in further detail in the appropriate context (Nishihama *et al*., 2009).

4.1 *INN1* is an essential gene encoding a novel regulator of cytokinesis

In a first step of this thesis, the most relevant results from the preceding works in our group, regarding a putative role of Inn1 in cell division, had to be confirmed. The complete open reading frame of one of the *INN1* alleles was therefore replaced by the *SpHIS5* marker in a diploid strain. Tetrad analysis showed a clear failure of segregants with an *inn1* deletion to form visible colonies, confirming previous claims that *INN1* is an essential gene (Giaever *et al*., 2002; Sanchez-Diaz *et al*., 2008). It should be noted that viability is not restored by osmotic stabilization of the medium with 1 M sorbitol. Additionally, the *Δinn1* microcolonies were microscopically examined and showed severe morphological disorders and a pronounced failure in cell separation.

These phenotypes were substantiated by conditional expression and depletion experiments. To this end, the native *INN1* promoter of a single allele was replaced by the regulable *GAL1* promoter in a diploid strain. Tetrad analysis was performed on different plates containing either glucose or galactose as carbon sources to render the *GAL1* promoter either in the repressed or induced state, respectively. The 2:0 segregation on glucose medium in conjunction with the histidine-auxotrophy of all viable segregants further confirmed the essential function of the encoded protein, which is not produced under such repressing conditions. In contrast, under inducing conditions (i.e. on galactose medium) all segregants were viable and did not show a significant difference in cell morphology, despite the presumed overproduction of Inn1. On the other hand, a shut-off experiment of the *GAL1p-INN1* construct, performed by shifting cells from galactose to glucose medium, revealed severe morphological disorders at the mother-bud neck 8 hours after the shift to the repressing conditions. After prolonged incubation, a clear failure to separate the daughter from the mother cell became obvious. This delay in the appearance of

phenotypes could be explained by a large surplus of mRNA and Inn1 protein produced while cells were growing under inducing conditions, with *INN1* expression driven from the strong *GAL1* promoter. It is likely that sufficient amounts of Inn1 accumulate in such cells to allow for a number of cell divisions, before the depletion effect becomes apparent. Since it was also observed that the amount of Inn1 in the cell is not down-regulated by cell-cycle dependent proteolysis (see data on the APC complex discussed below), it is likely that Inn1 could fulfill its function in successive rounds of cell divisions.

To ensure a faster protein depletion, the heat-inducible degron system, which allows the depletion of a protein of interest within 20 min, was employed (Sanchez-Diaz *et al*., 2004; see also Fig. 3.3A and explanations in the text). That the constructed DHFR-Inn1 fusion protein functions *in vivo* (a pre-requisite for further studies) was shown by the growth of the strain with the inn1-td construct under non-inducing conditions. The morphological defects observed after induction of the degron system further supported a role of Inn1 in promoting cytokinesis. However, the cell separation defect caused by a loss of Inn1 could have multiple reasons: Inn1 could be involved in the formation of a protein complex necessary for cell division (e.g. the septin collar or the cytokinetic actin ring). Alternatively, Inn1 could be required to couple the cell-cycle regulatory network to cytokinesis in order to initiate CAR constriction. Moreover, Inn1 could simply regulate chitin synthase activity or localization. These different possibilities were initially addressed by the visualization of morphological defects associated with a loss of Inn1. Cells depleted of Inn1 revealed no defect in the actin cytoskeleton which would support an eminent role of this structure. Actin patches and cables showed normal cell-cycle dependent localization and the actin ring could still be formed after Inn1 was depleted. This also indicates that Inn1 is not involved in the assembly of the septin collar, since no actin ring can be formed in cells lacking this structure. Thus, Inn1 has to affect subsequent events in the yeast cell cycle, such as cytokinesis or septum formation. The staining with Calcoflour white revealed that Inn1 is required for the formation of the chitinous primary septum. Upon Inn1 depletion, chitin distributed normally within the cell walls, but was not deposited in the cleavage furrow. Normal septum formation is dependent on precedent cytokinetic actin ring constriction and cleavage furrow ingression, so that the behaviour of the CAR (represented by a Myo1-mCherry fusion) was to be subsequently investigated. These became obsolete, when Sanchez-Diaz *et al*.

(2008) published their work on Inn1, demonstrating that CAR constricts as usual in Inn1 depleted cells. However, the plasma membrane does not follow this ingression upon Inn1 depletion, explaining the lack of a primary septum formation in the experiments presented here.

4.2 Inn1 is not a target of the anaphase-promoting complex

Carboxy-terminal GFP fusions of Inn1 co-localize with Myo1-mCherry at the mother-bud neck during constriction of the cytokinetic actin ring. After completion of CAR constriction, Inn1 disappears from the bud neck in wild-type cells. CAR disassembly is thought to be regulated by the anaphase-promoting complex (APC). Cells lacking Cdh1, the major activator of the APC during cytokinesis, fail to disassemble the CAR and are thus also deficient in the final stage of primary septum formation (Tully *et al*., 2009). Iqg1 has been identified as a direct target of the APC and the expression of a mutant Iqg1 resistant to degradation shows defects in septum formation similar to those displayed by a *cdh1* deletion (Ko *et al*., 2007; Tully *et al*., 2009).

A closer inspection revealed that the amino acids 142 to 150 of Inn1 perfectly match the recognition sequence of a destruction box recognized by the APC complex, prompting the investigation of Inn1 as a possible target. Interestingly, a mutant allele of *INN1* lacking the sequence for the putative destruction box failed to complement the *inn1* deletion when expressed at physiological levels. Concomitantly, GFP fusions of the mutant protein could never be detected at the bud neck. However, when expressed from an episomal multicopy plasmid, an *inn1* deletion was complemented by the construct lacking the destruction box and Inn1ΔDB-GFP appeared at the bud neck, although with a decreased fluorescence intensity. If the destruction box in Inn1 was indeed a target of the APC complex, one would have expected the protein lacking this sequence to be stabilized. Instead, the data discussed above indicate, that the intracellular concentration of Inn1ΔDB is decreased. By increasing the gene dosage, this effect can be counteracted, demonstrating that the protein's function in cytokinesis is not impaired. Moreover, the results on the overexpression of *CDH1* or *CDC20*, which should lead to an increased activity of the APC complex towards its target proteins, did not affect the amount of HA-tagged Inn1 in logarithmically growing cells. In addition, the concentration of Inn1 does not fluctuate in the course of the cell cycle, as demonstrated in section 3.2.4 and further discussed below. Together, these

findings suggest that Inn1 is not a target of the APC and that the deletion of the destruction box merely effects the general stability of the Inn1 protein. In fact, the sequence which forms the putative destruction box of Inn1 is not conserved among the homologous proteins in other yeast species (e.g. *Kluyveromyces lactis*, *Aspergillus nidulans*, *Ashbya gosypii*, and *Schizosaccharomyces pombe*). In the investigation of Inn1 stability throughout the cell cycle, cells arrested in the G1-phase contained the same amount of protein as logarithmically growing cells or those arrested in mitosis. However, additional higher molecular weight bands could be observed for Inn1-3HA during mitotic arrest. This indicated that Inn1 function is posttranslationally regulated, a notion supported by the work of (Nishihama *et al*., 2009), who showed that these higher molecular weight bands are the result of phosphorylation, proposed to be driven by the mitotic exit network. The exact phosphorylation sites in Inn1 and the kinases responsible still remain to be identified.

4.3 Inn1 interacts with the cytokinetic regulators Hof1 and Cyk3

The functional relationship between Inn1 and Hof1 reported in Ciklic (2007), as well as data from a genome-wide two-hybrid screen, suggested a direct interaction between the two proteins (Ito *et al*., 2001). These results were first confirmed by a yeast two-hybrid approach. As expected, the interacting regions of the two proteins could be delimited to the SH3 domain of Hof1 and the carboxy-terminal part including the proline-rich motifs (PRM) of Inn1. PRMs have previously been shown to be able to interact with SH3 domains, including that of Hof1 (Kamei *et al*., 1998; Ren *et al*., 2005; Ren *et al*., 1993). In the thesis of Ciklic (2007), it was demonstrated that carboxy-terminal truncation mutants of Inn1 caused an increased retention time of Hof1 at the bud neck. Therefore, Inn1 proteins with gradually decreasing numbers of PRMs, were tested here for interaction with Hof1 in the yeast two-hybrid system. Interestingly, the interaction strength, reflected by the β-galactosidase reporter activity, decreased with the sequential removal of each PRM from the carboxy-terminal end. This suggests that all three motifs are involved in the binding of Hof1 and act in concert. A similar result was reported for the interaction between Hof1 and the proline-rich protein Vrp1, in which multiple PRMs were shown to form a so-called **Ho**f1 **t**rap (HOT) domain (RenMunn 2005). The yeast two-hybrid data indicating an interaction between Hof1 and Inn1 were further substantiated by the observed

co-immunoprecipitation of the two proteins and by their co-localization at the bud neck during cytokinesis (see section 3.3).

Since *INN1* is an essential gene but *HOF1* is not, it was expected that Inn1 should have other effectors. The yeast two-hybrid method seemed to be a valuable approach to search for additional interaction partners of Inn1. The logical candidates were proteins which also contain a SH3 domain and are involved either in the organization of the actin cytoskeleton, in the establishment of cell polarity, or in the regulation of cytokinesis. Of the ten different proteins tested here which fulfill these criteria, only Cyk3 interacted with Inn1. Again as expected, the interacting regions were delimited to the SH3 domain of Cyk3 and the proline-rich carboxy-terminal part of Inn1. All attempts on a co-immunoprecipitation of Inn1 and Cyk3 (including the use of synchronized cell cultures) failed so far. This could be due to a very weak, transient interaction of the two proteins, which is also indicated by the failure of the two-hybrid constructs to promote growth on adenine-free medium. The latter is believed to indicate strong interaction, whereas the *lacZ*- and the *HIS3*-reporters are already induced by weaker interactions (James *et al*., 1996). Nevertheless, the co-localization of Inn1-GFP and Cyk3-mCherry fusions at the bud neck during cytokinesis (section 3.a.b; and Jendretzki *et al*., 2009) provides further evidence for an interaction of the two proteins.

A two-hybrid interaction between Inn1 and Cyk3 was also found by Nishihama *et al*. (2009), where *CYK3* was identified as a multicopy suppressor of a viable *inn1* deletion mutant. It should be noted that these authors use a *S. cerevisiae* strain with a quite peculiar genetic background, which differs significantly in phenotypes to the strain used here or the one employed by Sanchez-Diaz *et al.* (2008), who also found *INN1* to be an essential gene. Nevertheless, Nishihama *et al*. (2009)not only found that Inn1 and Cyk3 interact in the yeast two-hybrid assay, but also demonstrated an interaction between the two proteins purified from *E. coli*, in which the first proline-rich motif (PIPPLP) of Inn1 was required and sufficient for the binding of the SH3 domain of Cyk3.

4.4 Inn1 is recruited to the bud neck by the concerted action of Hof1 and Cyk3

Remarkably, the interaction between Inn1 and Cyk3 in the two-hybrid assay was weaker than the one between Inn1 and Hof1. This coincides with the severity of the deletion phenotypes. Whereas the deletion of *CYK3* only causes mild defects with abnormally shaped bud necks (Korinek *et al*., 2000), a *hof1* deletion displays severe morphological disorders and cytokinesis defects, and is even lethal at 37 C (Kamei *et al*., 1998; Lippincott and Li, 1998a). Interestingly, the *hof1 cyk3* double deletion is also lethal, presumably caused by the cumulative defects of the respective single deletions (Korinek *et al*., 2000). The next question to be addressed was whether any of the proteins were required for the recruitment of another to the bud neck.

The order of appearance at the division site was determined by time-lapse microscopy with cells expressing GFP-labelled fusion proteins of Inn1, Hof1, and Cyk3 together with Myo1 fused to the red-fluorescent mCherry protein. The latter was used as a marker for the onset and completion of cytokinesis and allowed the alignment of the three different GFP signals according to the state of CAR constriction. Clearly, Hof1-GFP was the first of the three proteins at the bud neck and appeared as a double ring structure. With the onset of CAR constriction and the merging of the Hof1 rings, Inn1-GFP could be detected as a single ring that constricts together with the contractile ring and Hof1. During the constriction process, Cyk3-GFP assembled to a ring at the bud neck and started to contract immediately. Constriction of the Cyk3 ring was completed 12 min after CAR disassembly at a time point coinciding with the degradation of Hof1. In contrast to former studies, no splitting of the Cyk3 ring could be observed at the end of cytokinesis in our strains. Moreover, Cyk3-GFP was not retained at the bud neck after completion of constriction as previously reported (Korinek *et al*., 2000). There may be two reasons for the differences observed. On the one hand, a homozygous diploid instead of a haploid strain was used in the cited studies, and, on the other hand, a different GFP fusion was employed. Different linker regions between the protein of interest and the label can interfere with protein function and/or localization. For example, functional GFP fusions of the chitin synthase Chs2 require the additional insertion of 8 glycin residues into the linker region. Otherwise GFP-fusions show the same localization, but are not catalytically active (Schmidt *et al*., 2002). The functionality of the fusion protein used in this study was confirmed by the creation of a haploid strain deleted for

hof1 with the *CYK3-GFP* fusion gene as the only copy of *CYK3*. Since this strain was viable, the Cyk3-GFP fusion must be able to fulfil the essential functions of the wild-type protein.

The genetic interactions of *INN1*, *CYK3* and *HOF1* gave additional hints to their order of action during cytokinesis. Whereas *INN1* and *CYK3* were shown to be multicopy suppressors of a *hof1* deletion, the *inn1* deletion could not be suppressed by high-copy introduction of any of the genes which encode the cytokinetic regulators investigated in this work. This indicates that Inn1 acts downstream of these components leading to cytokinesis. In contrast to the data presented here, Nishihama *et al*. (2009) were able to identify *CYK3* as a multicopy suppressor of a viable *inn1* deletion mutant. These differences can only be explained by the use of different genetic backgrounds in the yeast strains employed. Whereas the depletion of essential cytokinetic regulators like Myo1, Iqg1, and Inn1 is lethal in most wild-type yeast strains (e.g. W303, BY4717 and the strain DHD5 used in this work) (Giaever *et al*., 2002; Jendretzki *et al*., 2009; Sanchez-Diaz *et al*., 2008), some strains can compensate for the loss of these proteins (Bi *et al*., 1998). These strains have most likely accumulated a set of suppressor mutations eleviating lethality. The creation of a viable haploid *inn1* deletion mutant as employed by Nishihama *et al*. (2009) can be taken as an example. A haploid *inn1* deletion carrying the wild-type *INN1* gene on a plasmid with the *URA3* marker was grown on synthetic minimal media in the presence of 5-FOA. Since 5-FOA is toxic to cells carrying the plasmid, the strong selective pressure applied by this method might have favoured the appearance of secondary mutations which suppress the *inn1* lethality. Consequently, the results obtained with such strains should be considered with care, since they cannot be unequivocally attributed to the mutations introduced into the genes of interest.

The results discussed so far could have been explained by the recruitment of Inn1 to the bud neck by the concerted action of Hof1 and Cyk3. Thus, deletion of neither *HOF1* nor that of *CYK3* prevented Inn1-GFP accumulating at the bud neck, but the overexpression of either gene causes an aberrant localization of Inn1-GFP. In the case of *HOF1*, the overexpression resulted in different phenotypes regarding Inn1 localization. On the one hand, Inn1-GFP was found in a double ring structure, mimicking the localization of Hof1 prior to cytokinesis. On the other hand, the Inn1-GFP signal was retained at the bud neck even after CAR constriction. Both phenotypes were never observed in wild-type cells. With the altered localization

possibly interfering with Inn1 function, these results also offer an explanation for the lethality of cells overexpressing *HOF1* (Lippincott and Li, 1998a). Thus, if Inn1 indeed provides a link between the contractile ring and the membrane, its aberrant localization in a double ring could cause misguided plasma membrane invaginations, which could interfere with nuclear division or polarized secretion.

Similar to its deletion, the overexpression of *CYK3* only caused mild phenotypes that did not culminate in a pronounced growth defect. Nevertheless, the localization of Inn1-GFP was remarkably altered in the cells. Upon *CYK3* overexpression, Inn1-GFP was retained at the bud neck long after CAR constriction, this time mimicking the behaviour of Cyk3, consistent with the notion that Cyk3 recruits Inn1 to the bud neck.

The fact that simultaneous overexpression of *CYK3* rescued the lethality of an *HOF1* overexpression further supports this hypothesis: One would assume that the two anchors, Hof1 and Cyk3, need to be balanced against each other to guarantee correct Inn1 recruitment and function during cell division. As would be expected, a simultaneous depletion of Hof1 and Cyk3 resulted in a complete loss of Inn1 recruitment to the bud neck. Consistent with this model, the concomitant deletion of the SH3 domains of both Hof1 and Cyk3, the regions shown to interact with Inn1, is also lethal, while the respective single truncations did not show any growth defects. This result again stands in contradiction to the work of Nishihama *et al*. (2009). They constructed a viable *hof1 cyk3* double deletion mutant in which Inn1 is still recruited. As explained above, this could be a secondary effect of a suppressor mutation, such as one enabling another protein with an SH3 domain to recruit Inn1 to the bud neck. Indeed, we were also able to obtain a single viable segregant lacking the SH3 domains of both Hof1 and Cyk3. Segregant 2A from the tetrad analysis presented in Fig. 3.11A could also be such a suppressor mutant. Time did not permit to follow up this line of investigation.

4.5 Cyk3 acts in CAR-independent cytokinesis by recruiting Inn1

Sanchez-Diaz *et al*. (2008) have shown that a functional CAR is required for the recruitment of Inn1. Thus, mutants depleted for either Myo1 or Iqg1, which lack a CAR, did not show accumulation of Inn1 at the bud neck. *CYK3* has originally been identified as a multicopy suppressor of an *iqg1* deletion, which does not restore CAR formation (Korinek *et al*., 2000). Furthermore, overexpression of *CYK3* causes Inn1 to concentrate at the bud neck independent of the CAR represented by Myo1-

mCherry (Jendretzki *et al*., 2009). These results supported a role for the mainly uncharacterized protein Cyk3 in the process of CAR-independent cytokinesis. This is further supported by the observation that *CYK3* is also a multicopy suppressor of a *myo1* deletion (section 3.5.4), as also found in studies on the role of Iqg1 as a target of the APC complex (Ko *et al*., 2007).

To further investigate these relations, the role of Inn1 in this CAR-independent function of Cyk3 was tested in this thesis: First, it was shown that *CYK3* overexpressed from the *GAL1* promoter could suppress the lethality caused by a lack of *myo1* or *iqg1*. In a drop dilution assay, the growth of the *myo1* deletion could be restored to that of the wild-type, whereas suppression of *iqg1* was less efficient. Nevertheless, Inn1-GFP signals could be observed frequently at the bud necks of both strains when grown in media containing galactose and thus overexpressing *CYK3*. Remarkably, Inn1-GFP did not localize as a sharp ring to the bud necks of *myo1* cells, but in a more diffuse spreading. In fact, Nishihama *et al*. (2009) made similar observation on the Inn1 localization in their viable *myo1* deletion background. There, Inn1-GFP appeared either as a faint band or as two asymmetrically moving dots that never clearly contracted during cytokinesis. A possible explanation for their difference in localization is again the use of different yeast strains. The presence of a suppressor mutation (which could for instance lead to a slight overexpression of *CYK3*) could explain the observed localization of Inn1-GFP in cells lacking *myo1* as reported by Nishihama *et al*. (2009). Interestingly, *HOF1* and *INN1* also act as efficient multicopy suppressors of a *myo1* deletion, which further supports the role of Inn1 in CAR-independent cytokinesis.

4.6 The molecular function of Inn1

It is undisputed that the function of the proline-rich carboxy-terminal part of Inn1 is the recruitment of the protein to the division site. This is mainly mediated by the interaction with the SH3 domain of Hof1 and that of Cyk3. Yet, the molecular function of Inn1 still remains unclear, but seems to be carried out by the amino-terminal 130 amino acids, which form a C2 domain. These domains have been shown to be either involved in phospholipid-binding (Cho and Stahelin, 2006; Rizo and Sudhof, 1998) or they can form interfaces for the interaction with other proteins (Benes *et al*., 2005; Dai *et al*., 2007). Therefore, an Inn1 protein purified from *E. coli* as well as a truncated version lacking the C2 domain were tested for their lipid-binding properties

in an overlay assay. Interestingly, the full length protein displayed binding to phosphatidic acid, which was not observed for the protein lacking the C2 domain.

Phosphatidic acid (PA) is mainly produced by the hydrolysis of phosphatidylcholine catalyzed by phospholipase D and has been shown to be a second messenger regulating actin dynamics in mammalian cells. For example, changing levels of PA in the plasma membrane was demonstrated to control the actin-myosin contractility during changes in cell shape (reviewed in Rudge and Wakelam, 2009). An alternative function for phosphatidic acid is suggested by the cone-shaped structure of the molecule. The small negatively-charged head group of PA has been shown to induce negative membrane curvature as a prerequisite for membrane fission (Kooijman *et al*., 2005; Kozlovsky and Kozlov, 2003). Such a role for phosphatidic acid (PA) in cytokinesis has been suggested mainly from experiments with mammalian cell lines.

In *Saccharomyces cerevisiae*, phosphatidic acid has been demonstrated to be important for sporulation. Mutations in the gene encoding yeast phospholipase D, *SPO14*, caused an accumulation of Golgi-derived vesicles at the spindle pole bodies (SPB). These vesicles deliver material to form the prospore membrane and failed to fuse due to the lack of PA in their membranes (Rudge *et al*., 1998; Rudge *et al*., 2004). The role of phospholipase D during mitotic growth is still not fully understood, but seems to predominantly affect secretion (reviewed in Mendonsa and Engebrecht, 2009). Nevertheless, PA could have a function in cytokinesis, since it is a central intermediate in phospholipid biosynthesis and can be generated by pathways other than phospholipase D- mediated hydrolysis (Carman and Henry, 2007). Indeed, a role for phosphatidic acid in yeast cytokinesis and cell morphology has been suggested: Disruption of the putative phosphatidic acid phosphatase Dpp1 causes an unusual aggregation of cells which fail to separate (Katagiri and Shinozaki, 1998). It is tempting to speculate that disturbances in PA metabolism might also affect actin and/or membrane dynamics during cytokinesis in *Saccharomyces cerevisiae* and that this effect could be mediated at least partially by its interaction with Inn1.

The intracellular localization of PA in yeast cells during mitotic growth could be visualized by the expression of the PA-binding domain from mammalian protein phosphatase 1 fused to GFP. Unfortunately, the respective experiments yielded no specific GFP fluorescence and hence PA could not be detected. Additional methods are thus required to follow the distribution of PA during yeast cytokinesis. For example, the amino-terminal PA-binding domain of Spo20 fused to GFP has been

used as PA sensor in mammalian cells (Zeniou-Meyer *et al*., 2007), but it was not tested if it works in yeast, yet. PA-binding might also suggest an additional role for Inn1 during the process of sporulation. Interestingly, some of the carboxy-terminal truncation mutants of *INN1* mentioned above were shown to be defective in sporulation (Ciklic, 2007).

Taken together, the molecular function of Inn1 still remains to be fully understood. The protein is thought to be responsible for the coupling of cleavage furrow ingression to cytokinetic actin ring constriction (Sanchez-Diaz *et al*., 2008). It might further be required for the abscission process at the end of cytokinesis as suggested from its interaction with phosphatidic acid. Another possibility is presented in the work of Nishihama *et al*. (2009). The authors dispute a phospholipid-binding function by the C2 domain of Inn1, but suggest that it modulates Chs2 activity during septum formation.

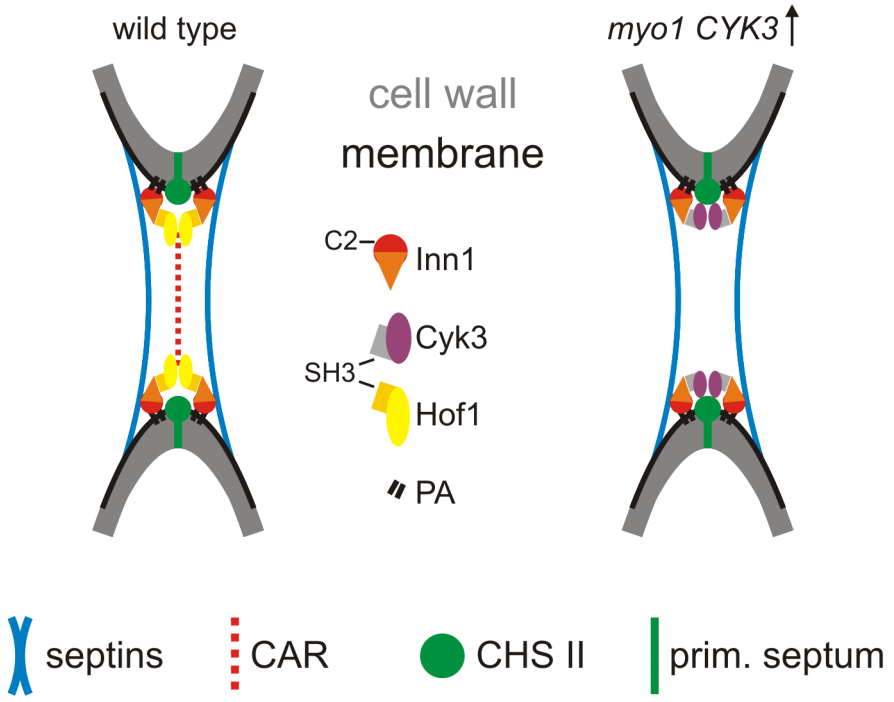

Fig. 4.1: Hypothetical model on Inn1 function. Cytokinesis in wild-type cells (left picture) and CAR-independent cytokinesis in *myo1* deletion cells overproducing Cyk3 (right picture). **Left picture.** In the wild type, Inn1 is recruited to the bud neck by the interaction with the SH3 domain of Hof1. The C2 domain of Inn1 binds phosphatidic acid and causes the accumulation of the lipid at the bud neck to facilitate plasma membrane ingression during CAR constriction. Membrane ingression is accompanied by the directed chitin deposition into the cleavage furrow to build the primary septum. **Right picture.** The overproduction of Cyk3 bypasses the requirement for a functional CAR. Cyk3 locates to the bud neck by an undefined mechanism and recruits Inn1 to the division site. Primary septum formation by chitin synthase II drives the constriction of the Cyk3-Inn1 complex. The Inn1-mediated phosphatidic acid accumulation facilitates membrane ingression and subsequent cytokinesis.

4.7 The role of Vrp1 in cytokinesis

Vrp1 is a protein that has been identified in *S. cerevisiae* in a screen for mutants deficient in the internalization step of endocytosis (Munn *et al*., 1995). It was shown that its role in endocytosis is distinct from an additional function in cytokinesis (Naqvi *et al*., 2001; Thanabalu and Munn, 2001). Some controversial results complicated the characterization of the role of Vrp1 in cytokinesis. On the one hand, functional Vrp1-GFP fusions localize to actin patches that accumulate at the bud neck at the end of CAR constriction, but on the other hand, the protein has been shown to be required for the recruitment of Hof1 to the bud neck early in the cell cycle. To address this, the timing of interaction of Vrp1 and Hof1 was investigated first. With the help of fluorescently-labelled fusion proteins, the co-localization of the two proteins at the bud neck could be demonstrated. Right after completion of CAR-constriction, the Hof1 signal divided and actin patches accumulated together with Vrp1 at the bud neck, overlapping with the Hof1-GFP signals. This co-localization can be seen as an indirect evidence for the interaction of Vrp1 with Hof1 at this stage. A co-localization of the two proteins at an earlier stage, which would support a Vpr1-mediated recruitment of Hof1 to the bud neck, could not be observed in this experiment.

To further support a concerted action, the genetic interactions of *HOF1* and *VRP1* were investigated. However, none of the genes acted as a multicopy suppressor of the growth phenotypes associated with the deletion of the other. An interesting genetic interaction has been reported in that the deletion of the SH3 domain of Hof1 can rescue the lethality of a *vrp1* deletion (Ren *et al*., 2005). Since the SH3 domain mediates the interaction of the two proteins, it was proposed that the domain is somehow involved in the inhibition of cytokinesis. To exert this function, Vrp1 would displace a not yet identified hypothetical inhibitor of cytokinesis from Hof1 upon binding itself to its SH3 domain (Ren *et al*., 2005). As stated above, the overproduction of Hof1 is lethal and retains Inn1 longer than usual at the prospective division site. Since cytokinesis does not occur under these conditions, Inn1 could well serve as the putative negative regulator. The experiments described in the last part of the results section were performed to test this hypothesis.

The localization of Inn1-GFP was investigated in *vrp1* deletion cells. Interestingly, about 40% of the Inn1-GFP signals did not show a co-localization with Myo1-mCherry, anymore; a behaviour which could never be observed in wild-type cells. Time-lapse video microscopy revealed that Inn1-GFP is retained at the bud neck

after completion of CAR constriction in such a *vrp1* deletion. In about 10% of the cells, a splitting of the Inn1-GFP signal could be observed directly after the disassembly of the actomyosin ring, reminiscent of the ring-splitting observed for Hof1 at exactly the same stage of the cell cycle. This further supports the hypothesis that Vrp1 interacts with the SH3 domain of Hof1 to displace Inn1, leading to the removal of the latter from the bud neck. Only then would cytokinesis be allowed to go through its final stages and complete the separation of the daughter from the mother cell.

5 Summary

The essential open reading frame *YNL152w* (now called *INN1*) of *Saccharomyces cerevisiae* was previously identified in a screen for negative regulators of cell integrity signaling. Subsequent studies and data from genome-wide functional analyses suggested, that the encoded protein plays a role in cell division. This was further addressed in the thesis presented here. Functional Inn1-GFP fusions were shown to co-localize with the contractile actomyosin ring component Myo1 during cytokinesis. Mutants depleted for Inn1 failed to form a primary septum, but did not affect the dynamics of the cytokinetic actin ring (CAR). This has been attributed to the inability to couple plasma membrane **in**gressio**n** (hence Inn1) to CAR constriction, a phenomenon also found by Sanchez-Diaz *et al*. (2008).

Further investigations focused on the question of how Inn1 is recruited to the bud neck and identified the cytokinetic regulators Hof1 and Cyk3, which act in concert for this purpose. Each of them contains a SH3 domain, which interacts with the proline-rich carboxy-terminal part of Inn1. Localization studies and genetic analyses indicate that Inn1 acts downstream of Hof1 and Cyk3. Either the simultaneous repression of *HOF1* and *CYK3* gene expression or the deletion of their SH3 domains was lethal, with a concomitant failure to localize Inn1-GFP to the division site. Overproduction of either, Hof1 or Cyk3 perturbed the dynamics of Inn1-GFP distribution, which followed that of the overproduced proteins. This atypical CAR-independent localization of Inn1 supports a presumed role of Hof1 and Cyk3 in an alternative cytokinesis pathway to form a primary septum. Since *INN1* is also a multicopy suppressor of a *myo1* deletion, this further supports the notion that Inn1 may be required for plasma membrane ingression, also in CAR-independent cytokinesis. Preliminary data suggest, that the protein Vrp1 is responsible for the required removal of Inn1 from the bud neck after completion of cytokinesis.

The essential amino-terminal C2 domain of Inn1 may mediate plasma membrane ingression by interaction with the membrane lipid phosphatidic acid, observed in biochemical studies. Alternatively, the C2 domain has been suggested to modulate chitin synthesis in the primary septum by modulating Chs2 activity (Nishihama *et al*., 2009).

6 References

Adams, A. E. and Pringle, J. R. (1984). Relationship of actin and tubulin distribution to bud growth in wild-type and morphogenetic-mutant *Saccharomyces cerevisiae*. *J Cell Biol* **98**, 934-45.

Baladron, V., Ufano, S., Duenas, E., Martin-Cuadrado, A. B., del Rey, F. and Vazquez de Aldana, C. R. (2002). Eng1p, an endo-1,3-beta-glucanase localized at the daughter side of the septum, is involved in cell separation in *Saccharomyces cerevisiae*. *Eukaryot Cell* **1**, 774-86.

Balasubramanian, M. K., McCollum, D., Chang, L., Wong, K. C., Naqvi, N. I., He, X., Sazer, S. and Gould, K. L. (1998). Isolation and characterization of new fission yeast cytokinesis mutants. *Genetics* **149**, 1265-75.

Bardin, A. J., Visintin, R. and Amon, A. (2000). A mechanism for coupling exit from mitosis to partitioning of the nucleus. *Cell* **102**, 21-31.

Benes, C. H., Wu, N., Elia, A. E., Dharia, T., Cantley, L. C. and Soltoff, S. P. (2005). The C2 domain of PKCdelta is a phosphotyrosine binding domain. *Cell* **121**, 271-80.

Bi, E. (2001). Cytokinesis in budding yeast: the relationship between actomyosin ring function and septum formation. *Cell Struct Funct* **26**, 529-37.

Bi, E., Maddox, P., Lew, D. J., Salmon, E. D., McMillan, J. N., Yeh, E. and Pringle, J. R. (1998). Involvement of an actomyosin contractile ring in *Saccharomyces cerevisiae* cytokinesis. *J Cell Biol* **142**, 1301-12.

Bradford, M. M. (1976). A rapid and sensitive method for the quantitation of microgram quantities of protein utilizing the principle of protein-dye binding. *Anal Biochem* **72**, 248-54.

Bretscher, A. (2003). Polarized growth and organelle segregation in yeast: the tracks, motors, and receptors. *J Cell Biol* **160**, 811-6.

Burton, J. L. and Solomon, M. J. (2000). Hsl1p, a Swe1p inhibitor, is degraded via the anaphase-promoting complex. *Mol Cell Biol* **20**, 4614-25.

Carman, G. M. and Henry, S. A. (2007). Phosphatidic acid plays a central role in the transcriptional regulation of glycerophospholipid synthesis in *Saccharomyces cerevisiae*. *J Biol Chem* **282**, 37293-7.

Chant, J., Mischke, M., Mitchell, E., Herskowitz, I. and Pringle, J. R. (1995). Role of Bud3p in producing the axial budding pattern of yeast. *J Cell Biol* **129**, 767-78.

Cho, W. and Stahelin, R. V. (2006). Membrane binding and subcellular targeting of C2 domains. *Biochim Biophys Acta* **1761**, 838-49.

Chuang, J. S. and Schekman, R. W. (1996). Differential trafficking and timed localization of two chitin synthase proteins, Chs2p and Chs3p. *J Cell Biol* **135**, 597-610.

Ciklic, I. F. (2007). Studies on the essential *YNL152w* open reading frame in *Saccharomyces cerevisiae. PhD thesis*.

Colman-Lerner, A., Chin, T. E. and Brent, R. (2001). Yeast Cbk1 and Mob2 activate daughter-specific genetic programs to induce asymmetric cell fates. *Cell* **107**, 739-50.

Corbett, M., Xiong, Y., Boyne, J. R., Wright, D. J., Munro, E. and Price, C. (2006). IQGAP and mitotic exit network (MEN) proteins are required for cytokinesis and re-polarization of the actin cytoskeleton in the budding yeast, *Saccharomyces cerevisiae*. *Eur J Cell Biol* **85**, 1201-15.

Dai, H., Shen, N., Arac, D. and Rizo, J. (2007). A quaternary SNARE-synaptotagmin-Ca2+-phospholipid complex in neurotransmitter release. *J Mol Biol* **367**, 848-63.

DeMarini, D. J., Adams, A. E., Fares, H., De Virgilio, C., Valle, G., Chuang, J. S. and Pringle, J. R. (1997). A septin-based hierarchy of proteins required for localized deposition of chitin in the *Saccharomyces cerevisiae* cell wall. *J Cell Biol* **139**, 75-93.

Dobbelaere, J. and Barral, Y. (2004). Spatial coordination of cytokinetic events by compartmentalization of the cell cortex. *Science* **305**, 393-6.

Dong, Y., Pruyne, D. and Bretscher, A. (2003). Formin-dependent actin assembly is regulated by distinct modes of Rho signaling in yeast. *J Cell Biol* **161**, 1081-92.

Epp, J. A. and Chant, J. (1997). An IQGAP-related protein controls actin-ring formation and cytokinesis in yeast. *Curr Biol* **7**, 921-9.

Fankhauser, C., Reymond, A., Cerutti, L., Utzig, S., Hofmann, K. and Simanis, V. (1995). The *S. pombe cdc15* gene is a key element in the reorganization of F-actin at mitosis. *Cell* **82**, 435-44.

Field, C. M. and Kellogg, D. (1999). Septins: cytoskeletal polymers or signalling GTPases? *Trends Cell Biol* **9**, 387-94.

Frenz, L. M., Lee, S. E., Fesquet, D. and Johnston, L. H. (2000). The budding yeast Dbf2 protein kinase localises to the centrosome and moves to the bud neck in late mitosis. *J Cell Sci* **113 Pt 19**, 3399-408.

Fukata, M., Kuroda, S., Fujii, K., Nakamura, T., Shoji, I., Matsuura, Y., Okawa, K., Iwamatsu, A., Kikuchi, A. and Kaibuchi, K. (1997). Regulation of cross-linking of actin filament by IQGAP1, a target for Cdc42. *J Biol Chem* **272**, 29579-83.

Geymonat, M., Spanos, A., de Bettignies, G. and Sedgwick, S. G. (2009). Lte1 contributes to Bfa1 localization rather than stimulating nucleotide exchange by Tem1. *J Cell Biol* **187**, 497-511.

Giaever, G., Chu, A. M., Ni, L., Connelly, C., Riles, L., Veronneau, S., Dow, S., Lucau-Danila, A., Anderson, K., Andre, B. *et al*. (2002). Functional profiling of the *Saccharomyces cerevisiae* genome. *Nature* **418**, 387-91.

Gietz, R. D., Schiestl, R. H., Willems, A. R. and Woods, R. A. (1995). Studies on the transformation of intact yeast cells by the LiAc/SS-DNA/PEG procedure. *Yeast* **11**, 355-60.

Gietz, R. D. and Sugino, A. (1988). New yeast-*Escherichia coli* shuttle vectors constructed with in vitro mutagenized yeast genes lacking six-base pair restriction sites. *Gene* **74**, 527-34.

Gordon, C. N. (1977). Chromatin behaviour during the mitotic cell cycle of *Saccharomyces cerevisiae*. *J Cell Sci* **24**, 81-93.

Gueldener, U., Heinisch, J., Koehler, G. J., Voss, D. and Hegemann, J. H. (2002). A second set of *loxP* marker cassettes for Cre-mediated multiple gene knockouts in budding yeast. *Nucleic Acids Res* **30**, e23.

Hanahan, D. (1983). Studies on transformation of *Escherichia coli* with plasmids. *J Mol Biol* **166**, 557-80.

Hawker, L. E. (1965). Fine Structure Of Fungi As Revealed By Electron Microscopy. *Biol Rev Camb Philos Soc* **40**, 52-92.

Hazbun, T. R., Malmstrom, L., Anderson, S., Graczyk, B. J., Fox, B., Riffle, M., Sundin, B. A., Aranda, J. D., McDonald, W. H., Chiu, C. H. *et al*. (2003). Assigning function to yeast proteins by integration of technologies. *Mol Cell* **12**, 1353-65.

Heinisch, J. J., Buchwald, U., Gottschlich, A., Heppeler, N. and Rodicio, R. (2010) A tool kit for molecular genetics of *Kluyveromyces lactis* comprising a congenic strain series and a set of versatile vectors. *FEMS Yeast Res*.

Hill, J. E., Myers, A. M., Koerner, T. J. and Tzagoloff, A. (1986). Yeast/*E. coli* shuttle vectors with multiple unique restriction sites. *Yeast* **2**, 163-7.

Huckaba, T. M., Lipkin, T. and Pon, L. A. (2006). Roles of type II myosin and a tropomyosin isoform in retrograde actin flow in budding yeast. *J Cell Biol* **175**, 957-69.

Igual, J. C., Johnson, A. L. and Johnston, L. H. (1996). Coordinated regulation of gene expression by the cell cycle transcription factor Swi4 and the protein kinase C MAP kinase pathway for yeast cell integrity. *Embo J* **15**, 5001-13.

Imamura, H., Tanaka, K., Hihara, T., Umikawa, M., Kamei, T., Takahashi, K., Sasaki, T. and Takai, Y. (1997). Bni1p and Bnr1p: downstream targets of the Rho family small G-proteins which interact with profilin and regulate actin cytoskeleton in *Saccharomyces cerevisiae*. *Embo J* **16**, 2745-55.

Ito, T., Chiba, T., Ozawa, R., Yoshida, M., Hattori, M. and Sakaki, Y. (2001). A comprehensive two-hybrid analysis to explore the yeast protein interactome. *Proc Natl Acad Sci U S A* **98**, 4569-74.

James, P., Halladay, J. and Craig, E. A. (1996). Genomic libraries and a host strain designed for highly efficient two-hybrid selection in yeast. *Genetics* **144**, 1425-36.

Janke, C., Magiera, M. M., Rathfelder, N., Taxis, C., Reber, S., Maekawa, H., Moreno-Borchart, A., Doenges, G., Schwob, E., Schiebel, E. *et al*. (2004). A versatile toolbox for PCR-based tagging of yeast genes: new fluorescent proteins, more markers and promoter substitution cassettes. *Yeast* **21**, 947-62.

Jaquenoud, M., van Drogen, F. and Peter, M. (2002). Cell cycle-dependent nuclear export of Cdh1p may contribute to the inactivation of APC/C(Cdh1). *Embo J* **21**, 6515-26.

Jaspersen, S. L., Charles, J. F. and Morgan, D. O. (1999). Inhibitory phosphorylation of the APC regulator Hct1 is controlled by the kinase Cdc28 and the phosphatase Cdc14. *Curr Biol* **9**, 227-36.

Jendretzki, A., Ciklic, I., Rodicio, R., Schmitz, H. P. and Heinisch, J. J. (2009). Cyk3 acts in actomyosin ring independent cytokinesis by recruiting Inn1 to the yeast bud neck. *Mol Genet Genomics* **282**, 437-51.

Johnston, G. C., Pringle, J. R. and Hartwell, L. H. (1977). Coordination of growth with cell division in the yeast *Saccharomyces cerevisiae*. *Exp Cell Res* **105**, 79-98.

Kamei, T., Tanaka, K., Hihara, T., Umikawa, M., Imamura, H., Kikyo, M., Ozaki, K. and Takai, Y. (1998). Interaction of Bnr1p with a novel Src homology 3 domain-containing Hof1p. Implication in cytokinesis in *Saccharomyces cerevisiae*. *J Biol Chem* **273**, 28341-5.

Katagiri, T. and Shinozaki, K. (1998). Disruption of a gene encoding phosphatidic acid phosphatase causes abnormal phenotypes in cell growth and abnormal cytokinesis in *Saccharomyces cerevisiae*. *Biochem Biophys Res Commun* **248**, 87-92.

Kaufmann, A. and Philippsen, P. (2009). Of bars and rings: Hof1-dependent cytokinesis in multiseptated hyphae of *Ashbya gossypii*. *Mol Cell Biol* **29**, 771-83.

Kilmartin, J. V. and Adams, A. E. (1984). Structural rearrangements of tubulin and actin during the cell cycle of the yeast *Saccharomyces*. *J Cell Biol* **98**, 922-33.

Kinoshita, M. (2006). Diversity of septin scaffolds. *Curr Opin Cell Biol* **18**, 54-60.

Kirchrath, L., Lorberg, A., Schmitz, H. P., Gengenbacher, U. and Heinisch, J. J. (2000). Comparative genetic and physiological studies of the MAP kinase Mpk1p from *Kluyveromyces lactis* and *Saccharomyces cerevisiae*. *J Mol Biol* **300**, 743-58.

Klebe, R. J., Harriss, J. V., Sharp, Z. D. and Douglas, M. G. (1983). A general method for polyethylene-glycol-induced genetic transformation of bacteria and yeast. *Gene* **25**, 333-41.

Ko, N., Nishihama, R., Tully, G. H., Ostapenko, D., Solomon, M. J., Morgan, D. O. and Pringle, J. R. (2007). Identification of yeast IQGAP (Iqg1p) as an anaphase-promoting-complex substrate and its role in actomyosin-ring-independent cytokinesis. *Mol Biol Cell* **18**, 5139-53.

Kooijman, E. E., Chupin, V., Fuller, N. L., Kozlov, M. M., de Kruijff, B., Burger, K. N. and Rand, P. R. (2005). Spontaneous curvature of phosphatidic acid and lysophosphatidic acid. *Biochemistry* **44**, 2097-102.

Korinek, W. S., Bi, E., Epp, J. A., Wang, L., Ho, J. and Chant, J. (2000). Cyk3, a novel SH3-domain protein, affects cytokinesis in yeast. *Curr Biol* **10**, 947-50.

Kozlovsky, Y. and Kozlov, M. M. (2003). Membrane fission: model for intermediate structures. *Biophys J* **85**, 85-96.

Kozubowski, L., Panek, H., Rosenthal, A., Bloecher, A., DeMarini, D. J. and Tatchell, K. (2003). A Bni4-Glc7 phosphatase complex that recruits chitin synthase to the site of bud emergence. *Mol Biol Cell* **14**, 26-39.

Kumar, A., Agarwal, S., Heyman, J. A., Matson, S., Heidtman, M., Piccirillo, S., Umansky, L., Drawid, A., Jansen, R., Liu, Y. *et al*. (2002). Subcellular localization of the yeast proteome. *Genes Dev* **16**, 707-19.

Kuranda, M. J. and Robbins, P. W. (1991). Chitinase is required for cell separation during growth of *Saccharomyces cerevisiae*. *J Biol Chem* **266**, 19758-67.

Lee, S. E., Frenz, L. M., Wells, N. J., Johnson, A. L. and Johnston, L. H. (2001). Order of function of the budding-yeast mitotic exit-network proteins Tem1, Cdc15, Mob1, Dbf2, and Cdc5. *Curr Biol* **11**, 784-8.

Lim, H. H. and Surana, U. (2003). Tome-1, wee1, and the onset of mitosis: coupled destruction for timely entry. *Mol Cell* **11**, 845-6.

Lippincott, J. and Li, R. (1998a). Dual function of Cyk2, a cdc15/PSTPIP family protein, in regulating actomyosin ring dynamics and septin distribution. *J Cell Biol* **143**, 1947-60.

Lippincott, J. and Li, R. (1998b). Sequential assembly of myosin II, an IQGAP-like protein, and filamentous actin to a ring structure involved in budding yeast cytokinesis. *J Cell Biol* **140**, 355-66.

Longtine, M. S. and Bi, E. (2003). Regulation of septin organization and function in yeast. *Trends Cell Biol* **13**, 403-9.

Longtine, M. S., McKenzie, A., 3rd, Demarini, D. J., Shah, N. G., Wach, A., Brachat, A., Philippsen, P. and Pringle, J. R. (1998). Additional modules for versatile and

economical PCR-based gene deletion and modification in *Saccharomyces cerevisiae*. *Yeast* **14**, 953-61.

Lord, M., Laves, E. and Pollard, T. D. (2005). Cytokinesis depends on the motor domains of myosin-II in fission yeast but not in budding yeast. *Mol Biol Cell* **16**, 5346-55.

Luo, J., Vallen, E. A., Dravis, C., Tcheperegine, S. E., Drees, B. and Bi, E. (2004). Identification and functional analysis of the essential and regulatory light chains of the only type II myosin Myo1p in *Saccharomyces cerevisiae*. *J Cell Biol* **165**, 843-55.

Martinez, E., Bartolome, B. and de la Cruz, F. (1988). pACYC184-derived cloning vectors containing the multiple cloning site and *lacZ alpha* reporter gene of pUC8/9 and pUC18/19 plasmids. *Gene* **68**, 159-62.

Mendonsa, R. and Engebrecht, J. (2009). Phospholipase D function in *Saccharomyces cerevisiae*. *Biochim Biophys Acta* **1791**, 970-4.

Mohl, D. A., Huddleston, M. J., Collingwood, T. S., Annan, R. S. and Deshaies, R. J. (2009). Dbf2-Mob1 drives relocalization of protein phosphatase Cdc14 to the cytoplasm during exit from mitosis. *J Cell Biol* **184**, 527-39.

Morrison, T. B. and Parkinson, J. S. (1994). Liberation of an interaction domain from the phosphotransfer region of CheA, a signaling kinase of *Escherichia coli*. *Proc Natl Acad Sci U S A* **91**, 5485-9.

Munn, A. L., Stevenson, B. J., Geli, M. I. and Riezman, H. (1995). end5, end6, and end7: mutations that cause actin delocalization and block the internalization step of endocytosis in *Saccharomyces cerevisiae*. *Mol Biol Cell* **6**, 1721-42.

Naqvi, S. N., Feng, Q., Boulton, V. J., Zahn, R. and Munn, A. L. (2001). Vrp1p functions in both actomyosin ring-dependent and Hof1p-dependent pathways of cytokinesis. *Traffic* **2**, 189-201.

Nishihama, R., Schreiter, J. H., Onishi, M., Vallen, E. A., Hanna, J., Moravcevic, K., Lippincott, M. F., Han, H., Lemmon, M. A., Pringle, J. R. *et al*. (2009). Role of Inn1 and its interactions with Hof1 and Cyk3 in promoting cleavage furrow and septum formation in S. *cerevisiae*. *J Cell Biol* **185**, 995-1012.

O'Conallain, C., Doolin, M. T., Taggart, C., Thornton, F. and Butler, G. (1999). Regulated nuclear localisation of the yeast transcription factor Ace2p controls expression of chitinase (*CTS1*) in *Saccharomyces cerevisiae*. *Mol Gen Genet* **262**, 275-82.

Pfleger, C. M. and Kirschner, M. W. (2000). The KEN box: an APC recognition signal distinct from the D box targeted by Cdh1. *Genes Dev* **14**, 655-65.

Pfleger, C. M., Lee, E. and Kirschner, M. W. (2001). Substrate recognition by the Cdc20 and Cdh1 components of the anaphase-promoting complex. *Genes Dev* **15**, 2396-407.

Rabilloud, T., Carpentier, G. and Tarroux, P. (1988). Improvement and simplification of low-background silver staining of proteins by using sodium dithionite. *Electrophoresis* **9**, 288-91.

Ren, G., Wang, J., Brinkworth, R., Winsor, B., Kobe, B. and Munn, A. L. (2005). Verprolin cytokinesis function mediated by the Hof one trap domain. *Traffic* **6**, 575-93.

Ren, R., Mayer, B. J., Cicchetti, P. and Baltimore, D. (1993). Identification of a ten-amino acid proline-rich SH3 binding site. *Science* **259**, 1157-61.

Rizo, J. and Sudhof, T. C. (1998). C2-domains, structure and function of a universal Ca^{2+}-binding domain. *J Biol Chem* **273**, 15879-82.

Rudge, S. A., Morris, A. J. and Engebrecht, J. (1998). Relocalization of phospholipase D activity mediates membrane formation during meiosis. *J Cell Biol* **140**, 81-90.

Rudge, S. A., Sciorra, V. A., Iwamoto, M., Zhou, C., Strahl, T., Morris, A. J., Thorner, J. and Engebrecht, J. (2004). Roles of phosphoinositides and of Spo14p (phospholipase D)-generated phosphatidic acid during yeast sporulation. *Mol Biol Cell* **15**, 207-18.

Rudge, S. A. and Wakelam, M. J. (2009). Inter-regulatory dynamics of phospholipase D and the actin cytoskeleton. *Biochim Biophys Acta* **1791**, 856-61.

Sambrook, J., Fritsch, E. F., und Maniatis, T. (1989). 'Molecular Cloning - A Laboratory Manual.' 2nd Edn. (Cold Spring Habor Laboratory Press: New York.)

Sanchez-Diaz, A., Kanemaki, M., Marchesi, V. and Labib, K. (2004). Rapid depletion of budding yeast proteins by fusion to a heat-inducible degron. *Sci STKE* **2004**, PL8.

Sanchez-Diaz, A., Marchesi, V., Murray, S., Jones, R., Pereira, G., Edmondson, R., Allen, T. and Labib, K. (2008). Inn1 couples contraction of the actomyosin ring to membrane ingression during cytokinesis in budding yeast. *Nat Cell Biol* **10**, 395-406.

Sanders, S. L. and Field, C. M. (1994). Cell division. Septins in common? *Curr Biol* **4**, 907-10.

Santos, B. and Snyder, M. (1997). Targeting of chitin synthase 3 to polarized growth sites in yeast requires Chs5p and Myo2p. *J Cell Biol* **136**, 95-110.

Schmidt, M., Bowers, B., Varma, A., Roh, D. H. and Cabib, E. (2002). In budding yeast, contraction of the actomyosin ring and formation of the primary septum at cytokinesis depend on each other. *J Cell Sci* **115**, 293-302.

Schmitz, H. P. (2001). Physiologische und genetische Untersuchungen zur Funktion regulatorischer Proteindomänen in der Signaltransduktion am Beispiel der Proteinkinase C von *Saccharomyces cerevisiae. PhD thesis.*

Shannon, K. B. and Li, R. (1999). The multiple roles of Cyk1p in the assembly and function of the actomyosin ring in budding yeast. *Mol Biol Cell* **10**, 283-96.

Shannon, K. B. and Li, R. (2000). A myosin light chain mediates the localization of the budding yeast IQGAP-like protein during contractile ring formation. *Curr Biol* **10**, 727-30.

Shapiro, A. L., Vinuela, E. and Maizel, J. V., Jr. (1967). Molecular weight estimation of polypeptide chains by electrophoresis in SDS-polyacrylamide gels. *Biochem Biophys Res Commun* **28**, 815-20.

Sheff, M. A. and Thorn, K. S. (2004). Optimized cassettes for fluorescent protein tagging in *Saccharomyces cerevisiae*. *Yeast* **21**, 661-70.

Shou, W., Seol, J. H., Shevchenko, A., Baskerville, C., Moazed, D., Chen, Z. W., Jang, J., Shevchenko, A., Charbonneau, H. and Deshaies, R. J. (1999). Exit from mitosis is triggered by Tem1-dependent release of the protein phosphatase Cdc14 from nucleolar RENT complex. *Cell* **97**, 233-44.

Stevens, R. C. and Davis, T. N. (1998). Mlc1p is a light chain for the unconventional myosin Myo2p in *Saccharomyces cerevisiae*. *J Cell Biol* **142**, 711-22.

Takeda, T., Kawate, T. and Chang, F. (2004). Organization of a sterol-rich membrane domain by cdc15p during cytokinesis in fission yeast. *Nat Cell Biol* **6**, 1142-4.

Thanabalu, T. and Munn, A. L. (2001). Functions of Vrp1p in cytokinesis and actin patches are distinct and neither requires a WH2/V domain. *Embo J* **20**, 6979-89.

Tolliday, N., VerPlank, L. and Li, R. (2002). Rho1 directs formin-mediated actin ring assembly during budding yeast cytokinesis. *Curr Biol* **12**, 1864-70.

Trilla, J. A., Duran, A. and Roncero, C. (1999). Chs7p, a new protein involved in the control of protein export from the endoplasmic reticulum that is specifically engaged in the regulation of chitin synthesis in *Saccharomyces cerevisiae*. *J Cell Biol* **145**, 1153-63.

Tully, G. H., Nishihama, R., Pringle, J. R. and Morgan, D. O. (2009). The anaphase-promoting complex promotes actomyosin-ring disassembly during cytokinesis in yeast. *Mol Biol Cell* **20**, 1201-12.

Vallen, E. A., Caviston, J. and Bi, E. (2000). Roles of Hof1p, Bni1p, Bnr1p, and Myo1p in cytokinesis in *Saccharomyces cerevisiae*. *Mol Biol Cell* **11**, 593-611.

Vas, A. C., Andrews, C. A., Kirkland Matesky, K. and Clarke, D. J. (2007). *In vivo* analysis of chromosome condensation in *Saccharomyces cerevisiae*. *Mol Biol Cell* **18**, 557-68.

VerPlank, L. and Li, R. (2005). Cell cycle-regulated trafficking of Chs2 controls actomyosin ring stability during cytokinesis. *Mol Biol Cell* **16**, 2529-43.

Wagner, W., Bielli, P., Wacha, S. and Ragnini-Wilson, A. (2002). Mlc1p promotes septum closure during cytokinesis via the IQ motifs of the vesicle motor Myo2p. *Embo J* **21**, 6397-408.

Wallar, B. J. and Alberts, A. S. (2003). The formins: active scaffolds that remodel the cytoskeleton. *Trends Cell Biol* **13**, 435-46.

Wilk, S., Wittland, J., Thywissen, A., Schmitz, H. P. and Heinisch, J. J. (2010). Endocytosis of the yeast cell wall integrity sensors Wsc1 and Wsc2 provides a selective advantage. *Mol Genet Genomics.* In preparation.

Yoshida, S., Bartolini, S. and Pellman, D. (2009). Mechanisms for concentrating Rho1 during cytokinesis. *Genes Dev* **23**, 810-23.

Zachariae, W. and Nasmyth, K. (1999). Whose end is destruction: cell division and the anaphase-promoting complex. *Genes Dev* **13**, 2039-58.

Zeniou-Meyer, M., Zabari, N., Ashery, U., Chasserot-Golaz, S., Haeberle, A. M., Demais, V., Bailly, Y., Gottfried, I., Nakanishi, H., Neiman, A. M. *et al*. (2007). Phospholipase D1 production of phosphatidic acid at the plasma membrane promotes exocytosis of large dense-core granules at a late stage. *J Biol Chem* **282**, 21746-57.

Zhang, G., Kashimshetty, R., Ng, K. E., Tan, H. B. and Yeong, F. M. (2006). Exit from mitosis triggers Chs2p transport from the endoplasmic reticulum to mother-daughter neck via the secretory pathway in budding yeast. *J Cell Biol* **174**, 207-20.

Zheng, Y., Bender, A. and Cerione, R. A. (1995). Interactions among proteins involved in bud-site selection and bud-site assembly in *Saccharomyces cerevisiae*. *J Biol Chem* **270**, 626-30.

Ziman, M., Chuang, J. S., Tsung, M., Hamamoto, S. and Schekman, R. (1998). Chs6p-dependent anterograde transport of Chs3p from the chitosome to the plasma membrane in *Saccharomyces cerevisiae*. *Mol Biol Cell* **9**, 1565-76.

Ziman, M., Preuss, D., Mulholland, J., O'Brien, J. M., Botstein, D. and Johnson, D. I. (1993). Subcellular localization of Cdc42p, a *Saccharomyces cerevisiae* GTP-binding protein involved in the control of cell polarity. *Mol Biol Cell* **4**, 1307-16.

Zimmermann, F. K. (1975). Procedures used in the induction of mitotic recombination and mutation in the yeast *Saccharomyces cerevisiae*. *Mutat Res* **31**, 71-86.

7 List of abbreviations

APC	Anaphase promoting complex
CAR	Cytokinetic actin ring
CWI	Cell wall integrity
DB	Destruction box
DIC	Differential interference contrast (microscopy)
DNA	Desoxyribonucleic acid
e.g.	For example (from latin *exempli gratia*)
G1	Gap one phase (cell cycle)
G2	Gap two phase (cell cycle)
GFP	Green fluorescent protein
M	Mitosis phase (cell cycle)
OD_{600}	Optical density at a wavelength of 600 nm
PA	Phosphatidic acid
PCR	Polymerase chain reaction
pH	negative logarithm (log_{10}) of the hydroxonium concentration
PRM	Proline rich motif
RNA	Ribonucleic acid
SC	Synthetic complete medium
S	Synthesis phase (cell cycle)
SPB	Spindle pole body
UV	Ultraviolet radiation
yEGFP	Yeast enhanced green fluorescent protein
YEPD	Yeast extract peptone dextrose (rich medium)
YNB	Yeast nitrogen base

Nucleotides and amino acids are represented with the single letter code (IUPAC-IUB Commission on Biochemical Nomenclature).

8 Acknowledgements

Zuerst möchte ich mich bei Herrn Prof. Dr. Jürgen J. Heinisch für das Überlassen dieses spannenden Themas und die Freiräume während meiner Promotion, aber auch für die Unterstützung und Diskussionsbereitschaft bedanken.

Herrn apl. Prof. Dr. Hans Merzendorfer danke ich für die Betreuung während der Zeit im Graduiertenkolleg und der damit verbundenen Übernahme des Zweitgutachtens.

Herrn Prof. Dr. Christian Ungermann möchte ich für die anregenden Diskussionen und die bereitwillige Teilnahme an der Prüfungskommission danken.

Besonderer Dank gilt Dr. Hans-Peter Schmitz in erster Linie für die kompetente Hilfe bei allen Mikroskop- und Computerfragen.

Ausserdem bedanke ich mich bei der kompletten Arbeitsgruppe Genetik, insbesondere der Nordseite für das angenehm freundliche Arbeitsklima und auch für das kühlere Klima an sich. Besonders hervorheben möchte ich Janina und Nele für entspannende Urlaube und das Korrekturlesen meiner Arbeit, sowie Ulf für drei schöne Jahre in der Hasestraße. Auch Franzi und Conny danke ich für biochemische Unterstützung während der Arbeit.

Ich bedanke mich auch bei meinen Sportsfreunden, besonders Pavel und Isabel, für die beste Zerstreuung nach einem stressigen Arbeitstag.

Vor allem aber bedanke ich mich bei Franzi und meinen Eltern für die uneingeschränkte Unterstützung über die ganzen Jahre auch in nicht so einfachen Lebensabschnitten.

9 Statutory declaration

Erklärung über die Eigenständigkeit der erbrachten wissenschaftlichen Leistung

Ich erkläre hiermit, dass ich die vorliegende Arbeit ohne unzulässige Hilfe Dritter und ohne Benutzung anderer als der angegebenen Hilfsmittel angefertigt habe. Die aus anderen Quellen direkt oder indirekt übernommenen Daten und Konzepte sind unter Angabe der Quelle gekennzeichnet.
Bei der Auswahl und Auswertung folgenden Materials haben mir die nachstehend aufgeführten Personen in der jeweils beschriebenen Weise unentgeltlich geholfen.

1. Im Rahmen von Abschlußarbeiten wurde ein Teil der Laborarbeiten gemeinsam mit Studenten durchgeführt. Dabei ist die Abbildung 3.2C in Zusammenarbeit mit Cornelia Broecker und die Abbildung 3.5C in Zusammenarbeit mit Lilli Schröder entstanden. Janina Wittland war an der Enstehung von Abbildung 3.8A beteiligt.

Weitere Personen waren an der inhaltlichen materiellen Erstellung der vorliegenden Arbeit nicht beteiligt. Insbesondere habe ich hierfür nicht die entgeltliche Hilfe von Vermittlungs- bzw. Beratungsdiensten (Promotionsberater oder andere Personen) in Anspruch genommen. Niemand hat von mir unmittelbar oder mittelbar geldwerte Leistungen für Arbeiten erhalten, die im Zusammenhang mit dem Inhalt der vorgelegten Dissertation stehen.

Die Arbeit wurde bisher weder im In- noch im Ausland in gleicher oder ähnlicher Form einer anderen Prüfungsbehörde vorgelegt.

_____ _____

(Ort, Datum) (Unterschrift)